The effect of CO_2 enrichment on the photochemical efficiency of the scleractinian Coral *Acropora millepora* (Ehrenberg, 1834).

Ashleigh Claire McNie

Department of Environmental Science
2022

A thesis Submitted to Auckland University of Technology
in partial fulfilment of the requirements for the
degree of Master of Science (Research)

Supervised by Associate Professor Kay C. Vopel and Dr. Daniel Breen

Table of Contents

Attestation of Authorship

I hereby declare that this submission is my own work and that, to the best of my knowledge and belief, it contains no material previously published or written by another person (except where explicitly defined in the acknowledgements), nor material that, to a substantial extent, has been submitted for the award of any other degree or diploma from a university or institute of higher learning.

Ashleigh McNie

Abstract

Global trends of increasing atmospheric CO_2, warming, and eutrophication enrich seawater with CO_2, either directly, through gas absorption, or indirectly, through microbial processes. This enrichment alters the speciation of inorganic carbon, increasing seawater [H^+] and [HCO_3^-], and decreasing the seawater carbonate saturation state and buffering capacity. Because corals use [HCO_3^-] as carbon source, CO_2 enrichment may increase coral photosynthesis. The CO_2 induced increase in [H^+] on the other hand, may increase the energy required for the upregulation of the calcifying fluid pH resulting in a decrease in photosynthesis. Here, I tested the effects of CO_2 enrichment on the photochemical efficiency of the reef building coral *Acropora millepora (*Ehrenberg, 1834) at an ambient temperature of ~25 ℃ using pulse-amplitude modulated fluorometry. Nine coral fragments were acclimated to a daily light cycle increasing to ~70 µmol m^{-2} s^{-1} at midday and then exposed to increasing seawater pCO_2 during the following 16 days. A saturation pulse analysis was conducted every thirty minutes to assess the photochemical efficiency of the coral fragments. This time series was interrupted daily between 0200 and 0230 hours to conduct a fast sequence of saturation pulse analyses during the induction of photosynthesis and subsequent recovery. These measurements failed to demonstrate that CO_2 enrichment affects the maximum photochemical efficiency (F_v/F_m), the effective photochemical efficiency ($\Delta F/F_m'$), or the maximum excitation pressure over PSII (Q_m) of the coral symbiont adding to the existing evidence that CO_2 enrichment does not affect coral photosynthesis. Furthermore, the time-series measurements revealed diel variations in the F_v/F_m ratio that point to the existence of an alternate respiratory pathway, chlororespiration, and the induction of state transitioning: a nocturnal decreases in the F_v/F_m ratio followed by a sharp increase in F_v/F_m at the onset of low irradiance at the start of the day.

List of Tables

List of Figures

Acknowledgements

I would like to extend my deepest gratitude to my supervisor Dr. Kay Vopel for whom without this thesis would not have been possible. I am grateful for the endless hours of teaching, support, guidance, and patience. I have learnt an immeasurable amount about the scientific world and writing and could not have hoped for a better mentor. I am glad that you have enjoyed working with me on this topic.

I must also thank the undergraduate students; Courtney Johnson, Daneka Cronje, and Laurence Quilter, who helped me in the lab to keep my coral alive and the experiments running. I would like to acknowledge Dr. Armagan Sabetian who first allowed me to study corals in the Solomon Islands, and Dr. Daniel Breen who first taught me about coral species and identification. Both igniting a passion to take my study further.

I'd also like to express my gratitude to Nick Garret and Irene Zeng for their help with the statistical analysis for this project. This is further extended to my brother Pierce McNie who also aided in my understanding of the statistical analysis and for answering my questions at all times of the day. I want to also thank you Pierce for inspiring me to go to university to study science.
I would like to thank my good friend Samantha Patterson who studied with me and kept me focused and motivated, the endless hours of writing would not have been possible without you. In addition, I would like to thank my Mum Desiree McNie and Thomas Watson for helping me through the hard times last year.

Introduction

Coral reefs are of great ecological importance supplying habitat, structure, and food, supporting an estimated 25% of marine species as well as providing services important to humans and coastal communities[1,2,3]. Each year approximately 10^4 g $CaCO_3$ m^{-2} is produced through calcification on coral reefs[4] with corals contributing the greatest amount[4]. The future of coral reefs is affected by the effects of ocean acidification and ocean warming. Bleaching events are caused by the expulsion of the coral symbionts, or the loss of photosynthetic pigments associated with the symbionts, most commonly due to warming and high irradiance levels[5]. Zooxanthellae, from the phylum dinoflagellata are in an obligate symbiotic relationship with the coral polyp providing photosynthetically fixed carbon, supporting calcification, metabolism, and reproduction[6,7]. In return the zooxanthellae receive waste products and protection from the coral. As the water surrounding coral reefs are oligotrophic this relationship is beneficial for both organisms to get enough nutrients[8]. The occurrence of bleaching breaks down this relationship, resulting in the death of the coral host if all symbionts are lost[9]. The exact mechanism that triggers expulsion is not well known. It has been shown that the symbiont maintains photosynthetic ability after expulsion indicating that this breakdown in relationship is not due to symbiont deterioration[9].

Greater density of zooxanthellae has been shown to increase coral tolerance to stressors due to greater levels of self-shading and UV absorption concentrations[10]. Species have also shown differing levels of expulsion of zooxanthellae, while not correlated with the initial density of zooxanthellae, species who can hold onto their zooxanthellae better exhibit lower mortality rates[10]. A decline in coral reefs leads to the dominance of macroalgae species resulting in a change in the community structures and a reduction in the high biodiversity of fish associated with coral reefs[11,12].

This review first discusses the complex effects of ocean acidification on the calcification processes of scleractinian corals. The effects of acidification on calcification have been widely discussed and debated using research on the different mechanisms causing reduced rates of calcification. Photosynthesis provides necessary metabolites and energy requirements for calcification, therefore, damage to the photosynthetic apparatus may be deleterious. Therefore, the mechanisms involved in photoprotection are important in understanding how coral will react to various stressors in the future and how this will influence calcification and productivity. Damage to the photosynthetic apparatus is discussed in the following review in detail describing photoprotective mechanisms working under several stressors including light, heat, and pCO_2. Coral symbiont genotypes vary between coral species, which will influence their response to pCO_2, temperature, light, and the combination of these. Likewise, studies have used different exposure times and the acclimation ability of corals may impact these studies results. For this reason, many responses of coral and their symbionts to these stressors can vary greatly. This must, therefore, be considered when discussing this subject.

Effects of ocean acidification on calcification

Seawater omega and coral growth

The ocean is a major sink for anthropogenic carbon dioxide; it has absorbed around a third of the atmospheric CO_2 produced over the last 200 years[13]. Between 1800 and 1994, the ocean has absorbed 118 ± 19 Pg C from the atmosphere lowering the seawater pH from 8.2 to 8.1[13,14]. This change in pH, which is known as ocean acidification, reflects a change in the carbonate chemistry equilibria affecting calcifying organisms. Such organisms rely on carbonate as a substrate for calcification and the secretion of calcium carbonate[15]. The series of chemical reactions that have control over the carbonate chemistry in the seawater is as follows;

$$CO_{2(atm)} \leftrightarrow CO_{2(aq)} + H_2O \leftrightarrow H_2CO_3 \leftrightarrow H^+ + HCO_3^- \leftrightarrow 2H^+ + CO_3^{2-}\text{[15]} \quad \text{[Eq. 1]}$$

The four main components of the seawater carbonate system are the dissolved inorganic carbon (DIC) species carbon dioxide (CO_2), bicarbonate (HCO_3^-), carbonic acid (H_2CO_3), and carbonate (CO_3^{2-}). Of these, HCO_3^- makes up the largest component of DIC at 91%, CO_3^{2-} makes up 8%, and CO_2 and H_2CO_3 create the remaining 1%. Following the series of reactions shown in Eq. 1, the addition of CO_2 to seawater will cause an increase in $[H^+]$ and $[HCO_3^-]$ ions, while $[CO_3^{2-}]$ decreases. This reduction in $[CO_3^{2-}]$ reduces the calcium carbonate ($CaCO_3$) saturation state known as omega (Ω).

Omega is defined as: $\Omega = [Ca^{2+}]\,[CO_3^{2-}]/K_{sp}$[16] [Eq. 2]

Where the K_{sp} is the solubility product of either aragonite or calcite at a given temperature, salinity, or pressure.

Calcium carbonate has two mineral phases, aragonite and calcite, each of which have different solubility constants[17]. The main difference in these polymorphs is in the crystal formation of the calcium ions and the carbonate ions[18]. Aragonite is more soluble than the more stable calcite, however aragonite is precipitated more rapidly than calcite and is the preferred polymorph due to magnesium in seawater inhibiting calcite crystallisation[17,19]. Corals precipitate the calcium carbonate polymorph aragonite, so Ω will be referred to in this work as the aragonite saturation state.

Dissolution of coral calcium carbonate skeleton occurs when Ω is <1, that is the seawater is undersaturated in regard to aragonite. Formation of coral skeletons occur when Ω is >1, that is, the seawater is supersaturated in aragonite[20,21]. The surface oceans are super-saturated and the deep sea is always under-saturated[20,21]. The saturation depth, when $\Omega = 1$, is defined as the depth at which formation calcium carbonate ceases and dissolution begins[22,23,24]. For aragonite this occurs between on average 300 and 3000 m, and for calcite this occurs between 500 and 5000 m[25,20]. The saturation depth is dependent upon location as the Pacific Ocean and Indian Ocean have a shallower saturation depth than the Atlantic Ocean[25,23]. This is a result of a significant increase in dissolved inorganic carbon (DIC) in the Pacific and Indian Oceans[23]. For some regions in the Pacific Ocean, this low

saturation depth may be attributed to upwelling of deep water which is enriched in CO_2[26]. The pattern of Ω distribution across the world's oceans is like that of the surface temperature. As temperature increases the aragonite saturation state decreases[20]. Ocean acidification (OA) causes the saturation depth to become shallower due to an increase in DIC causing dissolution of calcium carbonate at shallower depths.

Lowered Ω has been linked with many adverse effects on coral growth such as reduced linear extension rate and skeletal calcium carbonate density. Cooper et al.[27] have shown a reduction in skeletal growth of the stony coral genus *Porites* over a 16-year period in the Great Barrier Reef. Their results indicate a reduction in skeletal length and overall calcification rates trending with an increase in sea surface temperatures. Skeletal density, however, while declining, was unrelated to temperature change suggesting another factor may be causing a reduction in growth. A decrease in pH from 8.0 to 7.2 reduced growth by a factor of 0.5[28]. When the pH returned to 8.0, the growth rates recovered. This indicates that corals are somewhat resilient to short-term decreases in pH.

World-wide $CaCO_3$ precipitation is optimal when Ω is >3.5[29,30,31]. This occurs when [CO_3^{2-}] decreases below 220 μmol kg^{-1} and atmospheric [CO_2] rises towards 480 ppm[1]. Coral reefs are, therefore, restricted to areas which do not exceed these limitations and the Ω saturation levels remain in a supersaturated state above 3.5. Using two models which predict the surface seawater Ω, Kleypas et al.[29] determined that optimal calcification growth occurred when Ω > 4.0. According to these models the average tropical Ω is currently 4.0 ± 0.2 and is predicted to drop to 2.8 ± 0.2 by the year 2100. With the rising saturation depth, Zheng and Cao[31] suggest that less than 1% of corals by 2100 will remain in aragonite supersaturated waters. The remaining areas with Ω > 4.0 are predicted to be in areas such as the Red Sea, which is currently around 6.0 ± 0.2[32]. The Ω in these areas are predicted to drop at a greater rate than less saturated areas, however, may remain around 4.0 ± 0.2 by the year 2100[32]. This model uses the projected Ω to predict the future calcification rates of coral reefs.

The link between Ω and calcification rates is due to Ca^{2+} and CO_3^{2-} being the required substrates for calcification. As the [Ca^{2+}] is constant in the ocean, then changing Ω is therefore a function of changing [CO_3^{2-}]. Previous studies have shown a linear relationship between Ω and net calcification allowing us to predict when $CaCO_3$ dissolution should occur[e.g., 33,34,35]. As stated earlier, this will occur when Ω levels decrease below 3.5[29,30,31]. In short term studies and in mesocosm studies, however, diel hysteresis of Ω may cause inaccurate linear relationships between Ω and calcification to be made[36]. A stronger relationship between Ω and calcification is seen in mesocosm experiments, for instance, as other naturally occurring factors which may influence calcification, such as nutrients, are missing[36]. This may cause inaccurate estimations on the level of Ω where a coral will shift into dissolution. Conducting long term in situ experiments may remedy this issue. For example, the cold-

water coral *Lophelia pertusa* (Linnaeus, 1758) showed a reduction in calcification rates by 26–29% when subjected to a lowered pH level from 8.0 to 7.9 over one week[37]. When exposed for a longer period of six months calcification rates appeared to increase indicating that *L. pertusa* was able to adapt to the decreased pH[37].

Adaptations may also be increased through their symbionts specific genotypes allowing greater thermal tolerance[38,39]. Species living in areas which are highly variable in temperature and CO_2 enriched conditions, such as inshore reefs, may tolerate diel and seasonal variation. These communities, however, often live at their stress tolerance limiting their capabilities to overcome further or increased pressure[38]. Dissolution may be delayed by an organisms' capacity to regulate the Ω internally at the site of calcification due to the changes of calcifying fluid Ω being far greater than the seawater Ω. Therefore, the link between seawater Ω and calcification rates is a flawed concept and other factors must be considered.

Biological control of the calcifying fluid Ω and transportation of ions

Corals are capable of regulating the ionic composition of the calcifying fluid at the site of calcification. The ability to regulate the $[H^+]$ of the calcifying fluid and actively exchange DIC, Ca^{2+}, and H^+, through mechanisms such as the Ca-ATPase pump, allow the coral to control Ω in the calcifying fluid[1,17]. This ability would suggest that the seawater Ω has little effect on coral calcification. The extent of this control, however, may be dependent on the life stage of an organism, and seawater Ω may be a greater influence on the more susceptible early developmental stages as shown in other species as they are not yet able to control internal Ω[40].

Knowing how the required substrates (Ca^{2+} and CO_3^{2-}) are transported for use in calcification is necessary in understanding how corals can control the calcifying fluid Ω. Corals possess the ability to transport seawater directly to the site of calcification[41,42,43]. Ca^{2+} has been demonstrated to be transported transcellularly to the site of calcification using L-type voltage-dependent Ca^{2+} channels such as the Ca-ATPase pump[44,43,45]. Calcein labelling has been used to show paracellular pathways, movement of ions between cells due to a concentration gradient, may also be taken by Ca^{2+} from the seawater to the site of calcification[42]. To date no CO_3^{2-} transporter has been described in corals. HCO_3^- transporters have been described[46], however, and as HCO_3^- is abundant in acidified oceans it has been proposed to be the greatest source of carbon used for calcification[46]. HCO_3^- is also used for photosynthesis, and so is already being transported for photosynthesis, whereas CO_3^{2-} is not used in photosynthesis[47]. Therefore, the assumptions that HCO_3^- is the main DIC substrate transported for $CaCO_3$ precipitation is reasonable.

Once transported to the site of calcification the coral will actively alter the chemistry in the calcifying fluid to raise the pH (upregulation) creating a shift in the DIC species promoting an increase in $[CO_3^{2-}]$[48,49]. This will create a thermodynamically favourable condition for $CaCO_3$

precipitation to occur. The removal of H^+ through the calcification process will cause the calcifying fluid pH to increase and further facilitate calcification. Therefore, for the surrounding seawater Ω to have an effect on the calcifying fluid Ω, the ability to alter the calcifying fluid chemistry will need to be inhibited. Testing corals under extreme conditions, a reduction in Ω from 2.6 to 1.6, Ries et al.[50] revealed a non-linear response between Ω and calcification rates which could be indicative of a threshold at which point the corals was unable to maintain control over the calcifying fluid Ω. To ensure this response was from lack of $CaCO_3$ deposition and not dissolution, measurements were taken in areas which had living tissue as the skeleton in these areas would not be readily dissolving. Stress may negatively affect the ability of the coral to control the chemical conditions in the calcifying fluid.

Geochemical analyses through measuring boron isotopic concentrations ($\delta^{11}B$) in coral skeletons has allowed a better insight into this topic[e.g.,51,52,53,54]. Boron isotopes are not radioactive, unlike carbon isotopes, and therefore do not decay, allowing historical observation into the changes in seawater composition. BOH_4^- increases with increasing pH resulting in more deposition of this heavier boron isotope composition[55,56]. Using a free ocean CO_2 enrichment experiment, Georgiou et al.[52] demonstrate the ability of the coral *Porites cylindrica* (Dana, 1846) to mediate pH within the calcifying fluid. Despite large changes in pH in the surrounding water the $\delta^{11}B$ values in the new apical growth of the coral remained constant across all pH treatments and the control. The pH within the calcifying fluid in these experiments remained stable within 8.4–8.6 while the surrounding seawater pH seasonally shifted between 7.7 to 8.3[52]. This small pH range was also shown by Wall et al.[57] in the coral massive *Porites* and by Allison and Finch[58] in the coral *Porites lobata* (Dana, 1846). When testing the effects of OA on the coral *Stylophora pistillata* (Esper, 1792), Holcomb et al.[53] reported a decrease in $\delta^{11}B$ with decreasing pH across all treatments. The pH of the calcifying fluid, however, remained higher than the surrounding seawater and precipitation occurred across all treatments suggesting a limited control over the calcifying fluid Ω. The results from this study also indicate that different areas of the coral may be more susceptible to the changing seawater pH than other areas as apical growth was greater than lateral growth[53]. In a similar study, the coral *S. pistillata* showed no significant decline in lateral growth in pH treatments of 8, 7.8, and 7.4[59]. In the pH treatment of 7.2, however, growth significantly reduced[59].

Studies exposing coral to elevated pCO_2 may show different responses depending on the time of exposure. The coral *Pocillopora damicornis* (Linnaeus, 1758) showed a positive response of calcification to increased pCO_2 during the first 17 days of exposure, however, after this time the coral was unable to maintain increased calcification rates[60]. Long term exposure to increased pCO_2 reduces the positive effects of the increased HCO_3^- as upregulation of the calcifying fluid pH becomes energetically demanding. Likewise, for calcification to occur, the H^+ generated within the calcifying fluid must be removed. With a decrease in seawater pH, the energy required to remove protons needs

to remain high to keep the pH and Ω of the calcifying fluid stable, and therefore, keep calcification rates constant. This is described in a model by Venn et al.[59]. With lowered pH in the surrounding seawater the energy required for proton removal will not need to increase if calcification rates also decrease. Corals have, however, been shown to cope with lowered pH to a certain threshold. This limit was 7.2 in *S. pistillata* when tested by Venn et al.[59]. Before this point the corals were able to maintain calcifying fluid pH by compensating for energy investments to be put towards proton removal. Calcification rates remained stable in all other pH treatments until 7.2. The authors suggest that at this lowered pH the energy investment was too great, and protons were not being readily removed.

Seawater bicarbonate and coral growth

Decreasing seawater Ω and calcifying fluid Ω have often been correlated with decreased calcification. In Equation 2 Ω is a function of the changing CO_3^{2-} as Ca^{2+} is abundant and has little variation in concentration globally. The decrease in CO_3^{2-} leading to decreased calcification, however, does not confirm that Ω is the underlying factor for decreased calcification as the concentration of other dissolved inorganic carbon species also correlate with decreased calcification. Many studies have aimed to separate the effects of these different components.

Ocean acidification increases the concentration of bicarbonate which can be transported to the calcifying fluid while CO_3^{2-} cannot[46]. Jury et al.[61] therefore, suggested that [HCO_3^-] is important when determining calcification rates. Their methods allowed them to separate the effects of HCO_3^-, CO_3^{2-}, and pH on calcification rates in the stony coral *Madracis auretenra* (Locke Weil & Coates, 2007). They did this by manipulating the total alkalinity and DIC to produce variations of pH and [CO_3^{2-}]. Their results indicate that when [HCO_3^-] remained abundant pH and CO_3^{2-} did not influence calcification rates. Therefore, the Ω model does not fit these results. This response supports evidence of active transportation of HCO_3^- to the calcifying fluid. Marubini and Thake[62] discusses the importance of HCO_3^- to increased calcification in their research, however, fail to separate the DIC components. The increase of HCO_3^- in this study resulted in an increase in CO_3^{2-}, therefore HCO_3^- cannot be separated as the independent cause for the increased calcification.

Schneider and Erez[63] conducted three separate experiments where they kept the DIC constant while adjusting the pH, the pH constant while changing the DIC, and the pCO_2 kept constant while changing the DIC. Through these experiments they found that CO_3^{2-} and calcification were positively correlated in all experiments concluding that seawater Ω is the driving factor in lowered calcification rates. The method of altering seawater chemistry affects the proportions of each carbon species thereby affecting the equilibrium of the DIC. For example, when Marubini and Thake[62] added just 2 mM of HCO_3^- to their treatment, HCO_3^- tripled, CO_2 increased by a third, and CO_3^{2-} doubled. Marubini et al.[64] addressed this issue in their study which aimed to separate the effects of CO_3^{2-}, pH,

and pCO_2 on calcification. They did this by repeating the experiments at ambient HCO_3^- concentrations and again at a doubled concentration. The addition of HCO_3^- increased the growth rates of *S. pistillata* by an average of 27% regardless of the pH level. Photosynthesis also increased significantly with the addition of HCO_3^-. Marubini et al.[64] conclude that this may be due to the coral previously being carbon limited. This is supported by Herfort et al.[65] as photosynthesis and calcification rates increased in the corals *Porites porites* (Pallas, 1766) and *Acropora* sp. until HCO_3^- saturation was reached. HCO_3^- saturation for photosynthesis in both species was met with an addition of 6 mM of HCO_3^-. $CaCO_3$ production in *P. porites* saturated at 6 mM of HCO_3^-, however as *Acropora* sp. did not reach $CaCO_3$ saturation throughout all trials, the authors suggest that this species may have a greater capacity to produce $CaCO_3$ and is carbon limited in this experiment.

Testing the effects of HCO_3^- and CO_3^{2-} on calcification in new coral recruits, *Favia fragum* (Esper, 1793) and *Porites astreoides* (Lamarck, 1816), results from de Putron et al.[66] differed from the results of the above studies. As with Schneider and Erez[63], de Putron et al.[66] tested the effects of HCO_3^- and CO_3^{2-} in two experiments by increasing the pCO_2 at a constant TA, thereby increasing HCO_3^- and decreasing CO_3^{2-}, and through keeping the pCO_2 constant while adding acid, thereby decreasing $[HCO_3^-]$and $[CO_3^{2-}]$. Results from this study indicate a sensitivity of the coral species to Ω changes for both changes in pCO_2 and acid-addition. Unlike other studies[e.g.,33,34] which show a linear relationship between calcification rates and Ω, the results by were non-linear. While this shows an opposite result to other studies such as Jury et al.[61] these tests were conducted on new recruits which may be more susceptible to seawater Ω as discussed above. These studies all suggest that reduced calcification could result from changing $[CO_3^{2-}]$, $[HCO_3^-]$, and pH and that these factors often correlate with each other. While CO_3^{2-} is necessary for calcification, transportation methods of this ion have not been described for corals. If HCO_3^- is actively transported to the site of calcification and is the most abundant substrate available for calcification we would expect to see an increase in calcification with ocean acidification This, however, is not the case as reduced calcification rates continue with ocean acidification This and many discrepancies mentioned above indicate that there must be other factors which need to be taken into consideration.

Proton flux hypothesis

Studies focussing on the drivers of coral calcification have resulted in inconsistent explanations for lowered calcification[e.g.,61,63,64]. One common theme throughout the studies is the movement and production of the required DIC for calcification[67,68]. The proton flux hypothesis states that calcification is limited by the diffusion of H^+ through the animal–seawater boundary layer. Movement through this boundary layer is lowered under acidified conditions because the $[H^+]$ gradient between the surrounding seawater and the tissues is reduced[67]. This hypothesis focusses not only on the supply of substrates for calcification but on the removal of protons produced through calcification, which is required in $CaCO_3$ production. A number of authors have shown that calcification increases

as [HCO_3^-] increases[61,63,65,62]. The proton flux hypothesis helps to explain why under conditions of excess CO_2 calcification rates are continuing to decrease despite the increase in [HCO_3^-]. Doubling the preindustrial atmospheric pCO_2 will increase seawater [HCO_3^-] by 14% and seawater [H^+] by 78%[64]. The latter increase decreases the coral–seawater [H^+] gradient and so the flux of H^+ out of the coral. Consequently, calcification rates will decrease despite the increasing seawater [HCO_3^-].

To test the proton flux hypothesis, Jokiel[68] reviewed studies investigating the drivers of lowered calcification rates. The results from this review showed that many discrepancies could be explained by the proton flux hypothesis and that some correlations made in these studies may not be informative. Studies have shown a close correlation between lowered calcification rates and lowered [CO_3^{2-}] (or Ω)[e.g.,33,34]. Jokiel[68], however, demonstrated that [CO_3^{2-}] is also closely correlated with [H^+], indicating that decreased calcification rates in studies such as Schneider and Erez[63] and de Putron et al.[66], may in fact be due to the increase in [H^+] and not to the lowered [CO_3^{2-}]. Replotting data from Comeau et al.[47], Jokiel[67] demonstrates the same result of increased [H^+] affecting calcification rates. This was done using the [DIC]:[H^+] ratio to explain the importance of available substrates entering the coral and the ability to remove waste products. A significant correlation was observed between this ratio and calcification rates with increasing [HCO_3^-] and [H^+] decreasing the coral–seawater [H^+] gradient. When [DIC]:[H^+] is plotted against [CO_3^{2-}] and Ω a correlation is also shown, further demonstrating how the relationship between calcification and Ω was observed in the above mentioned studies.

Comeau et al.[69] further explores the effects of this ratio and the individual effects of [DIC], [H^+], and Ω. By testing the Ω and DIC on the coral *P. damicornis* and *Acropora yongei* (Veron & Wallace, 1984) Comeau et al.[69] was able to separate the effects of CO_3^{2-} from the other carbonate parameters as CO_3^{2-} is a proxy for Ω. The coral *A. yongei* was the only species tested to have responded to any treatment, which was a response to decreased pH. This response was found within the treatments where Ω did not change. Likewise, the [DIC] within the calcifying fluid did not change significantly with changing seawater Ω indicating the little effect surrounding seawater Ω has on calcification rates and the level of control the organism has on the Ω of the calcifying fluid. The results instead found that the change in calcification rates in the coral *A. yongei* resulted from the decreased pH and increased [DIC] in the surrounding seawater. This further shows the limitations of diffusion across the boundary layer and the strong physiological control these species have on the calcifying fluid pH[43]. These results support the proton flux hypothesis.

Metabolic processes involved in calcification

Photosynthesis and respiration

A constant supply of CO_2 is required for photosynthesis to occur. In seawater the [CO_2] is low, resulting in HCO_3^- being the primary DIC species used in photosynthesis. HCO_3^- is then converted to CO_2 through pH increase by the H^+- ATPase pump in the peri symbiotic space surrounding the zooxanthellae[45]. The hydration of metabolites in corals can be described using the following equation:

$$CO_2 + H_2O \Leftrightarrow HCO_3^- + H^+ \text{[70,71]} \quad \text{[Eq. 3]}$$

This reaction is enhanced by the enzyme carbonic anhydrase (CA) and facilitates the movement of CO_2 and HCO_3^- around the tissues[70]. Carbonic anhydrase has been reported to be within the calicodermis cells, on the outer edge of the surface epidermis, and the surface of the gastrodermis surface closest to the coelenteron[71,72]. These placements aid in the movement of DIC from the surrounding seawater into and throughout the tissues. The calicodermis controls precipitation of $CaCO_3$ and the presence of CA enhances the rate of calcification by increasing metabolism[73]. The removal of carbonic acid is also facilitated by CA and will further enhance calcification through the removal of two protons[74]. Some of the energy requirements necessary in upkeeping these mechanisms, and the origin of some of the required DIC for calcification, are facilitated by metabolic processes occurring in the coral and the symbionts.

Photosynthesis and respiration, in corals can be represented by the following equation:

$$HCO_3^- + H^+ \Leftrightarrow CH_2O + O_2 \text{[75]} \quad \text{[Eq. 4]}$$

As calcification also uses HCO_3^- as the main source of DIC we would assume that these two processes are not occurring in the same space as to not compete for resources. Photosynthesis enhances calcification (known as light enhanced calcification) through increasing the CO_2 taken up by zooxanthellae, increasing the calcifying fluid pH and therefore calcification[74]. Calcification can occur without the support from photosynthesis however and evidence suggests that the oxygen produced from photosynthesis aids in promotion of $CaCO_3$ deposition[76,77]. Most photosynthetically produced O_2 is consumed by respiration, which is approximately 12 times higher in the light than in the dark[74]. High rates of respiration increase [HCO_3^-], [H^+], and ATP available for use in calcification[73,78]. Increase in the metabolic energy available helps stimulate Ca-ATPase transportation and pH upregulation in the calcifying fluid[73,79]. Increased photosynthetic rates have been shown to be effective in mitigating the effects of increased [CO_2] and enhances calcification rates in *Acropora horrida* and *Porites cylindria*[80]. In a coral calcification model created by Galli and Solidoro[79], the energetic costs for calcification decrease as DIC increases. As ocean acidification intensifies the coral will expend more energy for both light and dark calcification[79]. Dark calcification will be affected more as the energy requirements are compensated for less without

photosynthesis occurring simultaneously. Reduction in the strength of a proton diffusion gradient with increasing seawater [H^+] will also result in greater energetic demand for calcification[75]. Species which can transport substrates and waste products throughout tissues whilst using less energy may be more resilient to ocean acidification.

As mentioned earlier, transport of DIC to the site of calcification is necessary in the biological control of the calcifying fluid Ω and for $CaCO_3$ precipitation. Carbon labelling has improved the understanding of the origins of inorganic carbon used for calcification. Using this technique Furla et al.[46] demonstrated that the major source of inorganic carbon originates from metabolic CO_2. Anion transporters are important in transportation of both Ca^{2+} and DIC[43,46,81]. The use of anion transport inhibitors has shown that the main inorganic carbon source is a product of metabolic processes[46]. Zoccola et al.[81] further showed evidence of HCO_3^- being the main carbon source as eight HCO_3^- anion transporter genes were identified in the coral *S. pistillata.* As HCO_3^- is necessary for both photosynthesis and calcification, these studies have supported the assumption that a passive diffusion of HCO_3^- into the coral is used for photosynthesis in the areas closest to the surface, and the resulting metabolically produced HCO_3^- is used in calcification[46,75,82].

Jokiel[75] proposes a model in which the area of rapid calcification sits above the area of rapid photosynthesis in the corrallum. Branch tips on the coral have very few zooxanthellae allowing rapid calcification and lengthening of branches. This is supported by increased ATP supply on the branch tips[75,83]. This area is the proposed "area of rapid calcification" and is where primary calcification and respiration occur. Below this is the "area of rapid photosynthesis" where photosynthesis and secondary calcification occur. Zooxanthellae are in high densities lower on the branch where rapid calcification is not occurring and deeper within the corrallum[75,83]. Primary calcification creates growth on the tips to lengthen the branches, whereas secondary calcification will occur over a longer timescale and will thicken the branches. Calcite formed during secondary calcification will be denser due to this. ATP production derived from respiration is enhanced with greater accessibility to O_2 diffusing across the diffusive boundary layer (DBL). The DBL at the tips of the branches where rapid calcification occurs is thinner due to increased water flow across this surface. This will further enhance O_2 diffusion[84]. Increased respiration due to increased O_2 will then create higher ATP production.

Physiological changes under stress

Zooxanthellae metabolism is important in the carbon supply for calcification. If this process is impacted by other stressors, such as heat, a less tolerable environment for upregulation of the calcifying fluid Ω could form, resulting in further negative impacts on adult corals. McCulloch et al.[54] showed that the calcifying fluid pH of a *Porites* coral species had large seasonal changes of on average 0.2 units, and pH upregulation of 0.4 units compared to the surrounding seawater. They

document a higher calcifying fluid pH in the winter and a higher calcifying fluid [DIC] in summer. The authors note that the calcifying fluid Ω is therefore less impacted by the seasons, and the surrounding seawater Ω, as the calcifying fluid Ω is raised in summer due to the increase in calcifying fluid [DIC], and in winter due to the increase in calcifying fluid pH creating a more homeostatic environment. Venti et al.[85] showed similar findings and suggest that the large seasonal change in seawater temperature and light have more impact on the calcification rates than the seasonal changes in seawater Ω. This supports the idea that metabolically derived DIC enhances calcification, likewise, it also shows that corals can maintain a higher calcifying fluid Ω all year round. Langdon and Atkinson[86] report seasonal variations in net carbon production (photosynthetic carbon fixation minus respiration) of 45 µmol C m^{-2} h^{-1} during summer months and 23 µmol C m^{-2} h^{-1} during the winter. This variation in carbon production reflects the metabolic process occurring in these months. Calcification rates, however, showed little variance with 16 µmol $CaCO_3$ m^{-2} h^{-1} being produced in summer, and 15 µmol $CaCO_3$ m^{-2} h^{-1} in winter. These results support the findings of McCulloch et al.[54] as the tight control over the calcifying fluid Ω reduces seasonal variations. pH upregulation through the Ca-ATPase pump is an energetically inexpensive process and can be maintained in winter when calcifying fluid [DIC] is lowered. However, with the added pressure from decreasing pH, the increased available energy from higher metabolism rates may no longer be able to support this upregulation. The coral *S. pistillata* under decreasing pH treatments of 8 to 7.2, showed a decreased ability to maintain a high calcifying fluid pH below a pH of 7.4. Corals may be able to mitigate the impact of ocean acidification through pH upregulation, however, after a certain point this becomes too energetically demanding for the coral to maintain long term[59].

Studying changes in gene expressions allows a look at the physiological impact of stressors. Upregulation of genes associated with enzymes which aid in the breakdown of lipids was shown by Kaniewska et al.[87]. Decreased lipids within the coral tissue have shown to be associated with seasonal variations; coral produce less lipids in winter because of less photosynthesis[88]. The symbionts in corals produce most of the energy required for metabolic activity[46], however, when needed, the coral host can enhance energy availability through heterotrophic feeding[89]. Likewise, lipids may provide an extra carbon source in times of need to help maintain metabolic processes[90]. A reserve of lipids may help dampen the effects of heat stress or acidification. Lowered lipid levels, however, may be indicative of a restriction to feed heterotrophically as shown in studies such as Towle et al.[91] and Teece et al.[92]. Towle et al.[91] found that heterotrophic feeding did not correlate with decreased symbiont concentration and instead suggest that increased heterotrophic feeding is driven by higher energy demand for pH upregulation under increased pCO_2. Therefore, while pH upregulation may be energetically inexpensive, the synergistic effects of multiple stressors may see a reallocation of limited energy resources towards processes other than calcification.

Kaniewska et al.[87] demonstrated that the coral *Acropora millepora* (Ehrenberg, 1834) reduced

photosynthesis and respiration under conditions of increased pCO_2 indicating an increase in energy demands. The increased demand in energy was reflected in the breakdown of lipids for energy use, a reduction in ATP and NADPH production, and a decrease in the number of H^+-ATPase channels resulting in higher energy demands to remove protons[87]. These results were represented in the differentially expressed gene transcripts identified to have been affected by increased pCO_2. In a similar study of the coral *A. millepora*, an increase in the seawater pCO_2 did not alter the regulation of 19 out of 20 genes unless the temperature was also modified[93]. However, the response of a gene involved in the production of ATP in the electron transport chain, Ubiquinol-Cytochrome-C Reductase Subunit 2 (QCR2), indicated an increased need in energy to maintain processes under ocean acidified conditions. Temperature stress further exacerbates this response. To remove the influence of symbiont photosynthesis and respiration on the effects of CO_2 Moya et al.[94] looked at the gene expression on the early life stage of the coral *A. millepora* before the association with symbionts. The results indicated a reduction in genes associated with metabolism and in genes associated with carbonic anhydrase. The downregulation of genes associated with carbonic anhydrase is common among many studies focusing on differential gene expression under pCO_2 and heat treatments as they are required less. DIC movement to the calcifying fluid and the conversion between HCO_3^- and CO_2 (Eq. 3) will be limited as carbonic anhydrase numbers decrease. The gene expression of two carbonic anhydrase isoforms in the coral *Acropora aspera* (Dana, 1846) did not change as a result of increased pCO_2 and heat individually however, significantly down-regulated under a combined increase in pCO_2 and heat[95]. In the azooxanthellate cold-water coral *Desmophyllum dianthus* (Esper, 1794), calcification rates and respiration rates appeared to not be affected by any of the pCO_2 treatments[96]. However, the gene expression profiles for this experiment indicated an upregulation in a protein involved in the corals heat shock response, an enzyme involved in the immune response, and the enzyme carbonic anhydrase. The common downregulation of carbonic anhydrase in zooxanthellate corals throughout the literature suggests that energy demands are too high under these conditions resulting in the reduction of metabolic processes.

Photorespiration in corals, brought on by high $[O_2]$ under increased illumination, works as a photoprotective mechanism redirecting excess excitation energy and reducing the chance of reactive oxygen species forming[97], however this process is considered wasteful and requires extra energy. Ribulose bisphosphate carboxylase/oxygenase form 2 (RuBisCo 2), a form of carbon dioxide fixing enzyme, is only found in corals and anaerobic bacteria due to its high affinity for O_2 instead of CO_2[97,98]. When photorespiration is triggered, RuBisCo fixes O_2 to ribulose biphosphate (RuBP) instead of carbon. Photorespiration results in the formation of phosphoglycolate (2PG) instead of 3-phosphoglycerate (3PG), creating an extra step as 2PG will then need to convert into 3PG to complete the Calvin-Benson cycle[99]. Increased energy is therefore required for the continuation of CO_2 fixation in the presence of high O_2 levels. Anaerobic environments are required for efficient carbon

fixation with this enzyme. It has also been shown that increased oxygen diffusion across the DBL resulted in greater efflux of O_2 out of the corrallum resulting in a decrease in RuBisCo 2 activity with O_2 despite an increase in photosynthesis, thus promoting CO_2 fixation[100]. Carbon concentrating mechanisms (CCM) further promote CO_2 fixation by increasing the availability of CO_2 around RuBisCo and thereby limiting the amount of oxygenation occurring[101]. Carbonic anhydrase is an important enzyme in the CCM because it facilitates the conversion of HCO_3^- to CO_2[101,102].

Corals have been shown to use HCO_3^- as a source of inorganic carbon in photosynthesis resulting in some studies showing a lack of negative effect of increasing pCO_2 on photosynthesis[e.g.,103,104]. In contrast, despite no reduction in chlorophyll and zooxanthellae density, under increased pCO_2 (1801–2193 μatm) the coral *Porites australiensis* (Vaughan, 1918) had a decrease in photochemical efficiency and calcification rates with a strong correlation between the parameters[105]. In the temperate coral *Cladocora caespitosa* (Linnaeus, 1767) gross photosynthesis during winter increased 72% in response to a 3 °C temperature increase despite a 40% decrease in zooxanthellae density[104]. However, an increase in pCO_2 had no effect on the photosynthesis or respiration rates over a short term experiment (one month) or a long term experiment (one year). The effect of increased pCO_2 on a reef's community metabolism demonstrates no change in dark respiration or net community production[106]. However, with an increase in light respiration and with no increase in net community production, this indicates an increase in mitochondrial respiration and not primary production. These data also show that despite an increase in available HCO_3^- net community production was not enhanced[106]. This may indicate that the mesocosm is a carbon limiting environment as demonstrated in a study by Marubini et al.[64] whereby an increase in HCO_3^- from 2 to 4 mM enhanced photosynthesis in the coral *S. pistillata* at all pH treatments. Changes in pH and pCO_2 did not have a significant effect on photosynthesis. A reduction in photosynthetic efficiency is observed in increasing [CO_2] in seawater related to a reduction in the Krebs cycle and the electron transport chain gene expression[87]. A reduction in ATP and NADPH is therefore expected to occur resulting in a reduction of metabolic processes and growth.

What governs light harvesting mechanisms

The light available for coral photosynthesis varies daily and seasonally. During optimal conditions photochemical quenching occurs rapidly promoting ATP synthesis and oxygen production[73]. When there is an excess in light, in which the ratio of photon flux density (PFD) to photosynthesis is high, the photosystems cannot utilise the energy efficiently and must dissipate it elsewhere to avoid photooxidative damage. Heat dissipation or fluorescence emissions are known as photoprotective (non-photochemical quenching, NPQ) mechanisms, increasing during the day with increased irradiance, aiding in the protection of the photosynthetic mechanisms within the zooxanthellae[107,108]. Limitations and damages to these photoprotective mechanisms may occur during periods of increased

light, heat, and salinity when the photoprotective mechanisms are no longer able to compensate, thereby resulting in photoinhibition[e.g.,109,110,105].

Light harvesting complexes (LHCs), also known as antenna complexes, of the PSII complex capture light energy. The LHCs in dinoflagellates are separated into two sections, the core LHC and the peripheral LHC[111]. The peripheral LHCs can be further divided depending on the protein binding pigments; the peridinin-chla/c (PCP) complex and the chlorophyll a-chlorophyll c_2-peridinin protein complex (acpPC)[111]. The majority of LHCs in coral symbionts are comprised of the acpPC complex, and therefore have been the focus in studies[111]. Captured light energy excites the primary electron donor, $P680^+$. Charge separation then occurs within the reaction centres. P680 can extract electrons from the water, producing one oxygen molecule and four hydrogen ions for every two H_2O molecules[112]. The thylakoid lumen will receive the hydrogen ions, while the oxygen will be released out of the organism. The excitation of $P680^+$ is dissipated through the transfer of one electron to the electron acceptor Pheophyton (Pheo). The plastoquinone Q_A rapidly accepts this electron, thereby stabilising this charge separation and forming the radical pair $P680^+$-Q_A-. The electron is then transferred to a second plastoquinone Q_B and then onto the b_6-f complex. If the electron is unable to move along this chain freely then damage to the PSII can occur.

Photoinhibition can cause temporary or permanent damage to the photosystems[113]. Damage to the Photosystem II (PSII) reduces the rate of photosynthesis, therefore organisms which photosynthesise require mechanisms to repair these damages. Temporary inhibition may be reversed within seconds (energy-dependent quenching of PSII), minutes (xanthophyll cycle conversions), or days (developmental changes)[107]. Inhibition may lead to more permanent damages to the PSII complex if the coral is unable to withstand the level of stress[113]. If photosynthetic processes are damaged less metabolites are produced thus limiting calcification[73,79]. Corals, and their symbiont algae, are exposed to varying levels of light and heat throughout the day as corals are largely intertidal species. Tidal changes further exacerbate the intensity of light, for example, if a low tide coincides with the high light intensity around midday the coral may be receiving more light than is optimal for photosynthesis. When this occurs, the coral system may experience physiological disruptions[113].

Photo-oxidative damage

Photoinhibition may be caused by damage to two separate processes, first on the acceptor side of the PSII through impairment of Q_A leading to a functional loss in Q_B as electrons cannot be transferred to Q_B if Q_A is impaired[114,115]. Secondly through oxidative damage caused by overactive oxidizing species, such as the P680+ itself, and the inability to transfer these electrons down the electron transport chain[116]. Both the inhibition of Q_A and Q_B have shown to induce photoinhibition[117]. Damage to PSII results in lowered efficiency of photosynthesis[118]. If the donation of electrons cannot keep up with the level of oxidation occurring in the PSII the chlorophyll pigments (P680) will oxidise the nearest pigments and amino acids which will damage the PSII

protein D1[119]. Charge recombination may also occur resulting in a triplet formation of P680 which in turn will react with triplet oxygen, thus creating singlet oxygen and damaging P680[112]. The evolution of photoprotective processes aid in minimizing this process and therefore reduces significant damage to the PSII.

Damage to the D1 protein

The PSII reaction centre is comprised of a heterodimer of two main proteins, D1 and D2. The D1 protein is important in the movement of the electrons through PSII, binding the electron acceptors and donors[126]. Degradation of D1 was found to be an innate process in the PSII reaction centres occurring regularly at different light intensities[120,121]. The D1 protein has a high turnover rate with rapid renewal allowing for the protein concentration to remain at an appropriate level. Degradation of D1 is caused by photoinactivation due to a decrease in electron movement through the plastoquinones under increased irradiance[122,123]. The inability for Q_A to be reduced and the electron passed to Q_B creates charge recombination in the PSII reaction centres leading to oxidative damage of D1[123]. Charge recombination occurs if the charge has not been stabilised and the electron gets redirected back to the P680 resulting in triplet P680 formation[112]. If the damage to D1 proteins exceeds its turnover rate, photoinhibition occurs[120].

For photosynthesis to continue, D1 damage needs to be repaired. For this to occur, the damaged protein is removed and replaced. This is done through proteolysis[120]. In the coral *P. damincornis*, under irradiances of 200 µmol photons m^{-2} s^{-1} the rate of D1 degradation and repair was able to prevent photoinhibition[124]. When the added stress of heat was introduced, damage to the D1 protein increased significantly, repair rates also increased however were unable to maintain the levels needed to prevent photoinhibition[124]. This has also been shown in cultured coral symbiodinium exposed to increased temperatures[125]. Host morphology and pigmentation may aid in reducing the rate of photoinhibition in their symbionts. Likewise, genetic differences in temperature and light sensitivity between symbiodinium will allow some species to be more susceptible to photoinhibition. Genes involved in proteolysis are upregulated under heat stress[126]. However, under acidified conditions, genes involved in proteolysis have been shown to down-regulate[127]. The sea urchin *Strongylocentrotus purpuratus* (Stimpson, 1857), was used to demonstrate transgenerational plasticity of phenotypic genes to different pCO_2 levels[127]. All urchin offspring down-regulated genes associated with proteolysis under increased pCO_2, however a greater response was experienced by offspring whose parents were also living under increased pCO_2. The length of exposure has also been shown to affect the number of changes in gene expressions at low pCO_2, while changes are expressed earlier under high pCO_2 as shown in the coral *Balanophyllia elegans* (Verrill, 1864)[128].

Photoprotective mechanisms

To prevent damage from an excess in excitation energy, energy will be readily dissipated in three competitive processes: fluorescence emission, non-photochemical quenching (heat dissipation), and photochemical quenching (the process driving photosynthesis through the electron transport chain). If the excitation energy becomes too great the reaction centres within the PSII will "close" as they become saturated with energy that is unable to continue down the electron transport chain[129]. This excitation energy may damage the PSII[118]. The main component of NPQ is the energy dependent quenching (qE) which is activated by a ΔpH in the thylakoid lumen with increasing irradiance[130,131]. The xanthophyll cycle describes one of the main mechanisms behind qE and works along with lowering the pH in the thylakoid membrane in increasing energy dissipation for photoprotection[132,133].

The vast combinations of coral and symbiont genotypes has made it difficult to determine the photoprotective mechanisms in corals. Damage caused by short term stressors to the PSII may be protected against through energy dependent quenching, the xanthophyll cycle, and through structural rearrangement of the light harvesting complexes. Corals possess xanthophylls associated with the diadinoxanthin cycle, however, many studies use information on the violaxanthin cycle, common in plants and algae, to discuss photoinhibitory and photoprotective mechanisms in corals due to limited studies on the diadinoxanthin cycle. This discussion will follow suit using evidence from violaxanthin and diadinoxanthin where applicable as evidence suggest the cycles to be analogous of one another[134].

Carotenoids aid in photosynthesis by acting as light-harvesting pigments during times of low light, and by aiding in the photoprotection of the organism during high light exposure[135]. Higher plants are known to have three main carotenoids; violaxanthin, antheraxanthin, and zeaxanthin which all aid in the regulation and use of light energy[136]. The xanthophyll cycle is the reversible de-epoxidation of carotenoids violaxanthin to zeaxanthin, this cycle prevents photoinhibition and the formation of reactive oxygen species under increased light stress[130,137]. Violaxanthin is converted into antheraxanthin through the removal of one oxygen atom (de-epoxidation) under high light environments when photosynthesis is saturated and is then reduced once more resulting in zeaxanthin[130,138]. This occurs within seconds to minutes, with increasing rate as the pH decreases[133]. During low light environments, when there is not enough light to saturate photosynthesis or in the dark, this is reversed[139]. The epoxidation process may take anywhere from a few minutes to hours[140]. Xanthophyll cycling in coral symbionts is different to the well-studied plant xanthophyll cycle described above, in that the xanthophyll pigments are diadinoxanthin and diatoxanthin. Known as the diadinoxanthin cycle (DD-cycle), diadinoxanthin (DD) will go through a de-epoxidation reaction in high light environments forming diatoxanthin (DT), and reverse in the dark through

epoxidation[141,134]. The DD-cycle has been shown to be analogous to the violaxanthin-cycle in their photoprotective roles[e.g.,141].

Both xanthophyll cycles have been demonstrated to some extent to be controlled by ΔpH. Ruban et al.[129] describes a scenario by which a ΔpH is the "trigger" in a series of changes leading to qE. Their results show that when a pH gradient is absent photoprotective mechanisms were not active, whereas in the presence of a pH gradient these mechanisms were functional. It is suggested that qE occurs within the light harvesting complexes of PSII (LHCII) due to its association with xanthophylls such as zeaxanthin[142,136]. In many species it has been reported that qE is dependent upon the xanthophyll cycle, particularly zeaxanthin[e.g.,143,142,144]. Tight pH control of the violaxanthin cycle helps prevent energy loss from excess zeaxanthin formation[133,145]. Violaxanthin de-epoxidation is controlled through several processes which revolve around the pH of the thylakoid membrane. For violaxanthin de-epoxidation to begin a pH < 6.5 is required to tightly bind the enzyme violaxanthin de-epoxidase (VDE) to the thylakoid membrane. Greatest efficiency is observed at a pH < 5.8[133,132]. Noctor et al.[146], have demonstrated that at a high ΔpH qE will function the same way in the presence and absence of zeaxanthin. In this case it has been suggested that another xanthophyll, lutein, may act as the quencher[147]. Others suggest that zeaxanthin acts as an amplifier for qE as the same amount of quenching will still occur after 45 minutes of high light[148]. These discrepancies have resulted in a theory of which qE occurs at two different sites: the light harvesting antennae and the reaction centres. The latter does not rely on the xanthophyll cycle as shown by Zulfugarov et al.[147] and Finazzi et al.[149]. Likewise, Olaizola and Yamamoto[141] found that not all DD in marine diatoms will go through de-epoxidation suggesting a separate pool of DD comparable to that of zeaxanthin.

The role of reaction centre qE is unclear from these studies, however qE in the antennae is well documented with the xanthophyll cycle[e.g.,150,151]. Results from Hennige et al.[150] indicate that modification of the reaction centre pigments and configuration is preferential over changes in antennae size. Although modification of the reaction centre pigments can lead to changes in antennae size. Results from Zulfugarov et al.[147] also highlight the importance of antenna size in photoprotective mechanisms. Light harvesting antennae in plants raised in high light environments are smaller resulting aiding in the photoprotective mechanisms[152,153]. This has been shown to also occur in dinoflagellate species whereby the accessory pigments; peridinin-chl-*a* -protein complex (PCP) and the chl *a*–chl c_2 peridinin protein complex (acpPC), increase their photosynthetic unit size[154]. Under increasing temperature treatments, the coral *A. aspera* exhibited a loss in photosynthetic efficiency, this was accompanied by an upregulation of three acpPC genes which may be involved in the photoprotection of this species[155]. The acpPC gene expression in coral symbionts has not been researched in depth and so at this point cannot be confirmed. However, it has been shown that DD and DT are abundant in the acpPC along with the photosynthetic pigments Chl *a*, Chl c_2, and peridinin[111]. Chlorophyll *a* complexes in two common scleractinian corals *A. millepora* and *P. damicornis* become

disconnected from PSII light harvesting complexes (LHCs) when put under high light stress. This occurs when the corals xanthophyll cycle was inhibited[141]. Corals less susceptible to coral bleaching such as the coral *Pavona decussata* (Dana, 1846) exhibit a greater chlorophyll a disconnection from the LHC[156]. In the presence of the xanthophyll inhibitor, dithiothreitol (DTT), the potential quantum efficiency is lowered. These results indicate that once the xanthophyll cycle has performed the maximum capabilities of photoprotection, changes made to the LHC further aid or promote photoprotective mechanisms. Dissociation of the LHCs has not been studied as extensively as the xanthophyll cycles, although reductions in the electron transport rate and the abundance of D1 proteins in plants are observed when dissociation was inhibited[157].

De-epoxidation increases in some corals during bleaching events[156,158,159], however this is dependent on the symbiont and coral genotypes[167]. A combination of increased heat and light initiated an increase in DT in the xanthophyll pool in five of six tested species of coral[159], exhibiting the variable success of xanthophyll cycling in corals. In addition, the coral *P. asteroides* which are more tolerable to bleaching events showed no increase in DD, DT, or β-carotene[159]. This response, however, is perhaps species specific as another bleaching tolerant species, *P. porites*, did show an increase in xanthophylls under increased heat and light stress[159]. Species which are more susceptible to coral bleaching, such as the coral *A. millepora*, exhibit increased β-carotene levels[156,158] which are known to aid in the protection from reactive oxygen species[160] and is abundant in the core complex of the LHC[154]. This is accompanied by increased xanthophyll cycling with daily irradiance variations[156, 161]. The coral *Goniastrea aspera* (Verrill, 1866) observes a daily cycle of increased fluorescence quenching correlating with an increase in the DT to DD ratio[161]. This has been shown in other coral such as *Acropora cervicornis* (Lamarck, 1816), *Montastrea faveolate* (Ellis & Solander, 1786), and *Montastrea annularis* (Ellis & Solander, 1786)[162]. The xanthophyll ratio and NPQ peaked in all species around midday in conjunction with the highest irradiance levels.

Differences in xanthophyll concentrations on opposite sides of the same colony of *G. aspera*, while receiving the same light regimes, provide evidence of previous acclimation[161]. This acclimation may be due to prolonged high light levels on one side of the colony resulting in the need for protection for a longer period. This could be done by changes made to the LHCs as mentioned above. Acclimation to differing light intensities may also affect the amount of xanthophyll cycling occurring as differing levels of NPQ were observed in these corals at 10:00 hours and 18:00 hours despite the same amount of incident PAR[162]. Winters et al.[163] also observed this in the coral *S. pistilatta* with both studies observing lowered electron transport rate (ETR) and increased NPQ in the afternoon. This could be indicative of persistent photoinhibition and a slow recovery period following peak irradiances at midday. Quick switches in the daily changes of the DD:DT ratio in zooxanthellae is essential in ensuring that light harvesting is efficient and maximised[164]. Epoxidation of DT to DD is inhibited in high-light environments as it is reliant on the proton gradient across the trans-thylakoid

membrane[164,165]. A higher pH gradient affects the DD cycle by limiting the amount of DT epoxidase is being produced, thus slowing down DT epoxidation[165]. However, once NPQ has been established in the symbiont, it has been suggested that the continuation of NPQ is then solely reliant on the abundance of DT and not the proton gradient[164].

Results from Hoegh-Guldberg and Jones[166] suggest that in the corals *P. cylindrica* and *S. pistillata,* NPQ is greater in the afternoon after longer exposure to high light levels and the apparent increase in epoxidase with the increased light. When going from high light to low light, DT epoxidation in diatoms occurs along with NPQ, however when in complete darkness epoxidation ceases[167]. This is due to the availability of NADPH which is an important co-substrate for epoxidase. The slow rate of NPQ in the early morning could be due to epoxidase depletion occurring overnight and the lack of NADPH available. Epoxidase has been shown to bind tightly with the thylakoid membrane during periods of high light which reduces the pH creating the proton gradient[132]. During the night or low light, epoxidase have been shown to move freely within the thylakoid lumen[132]. This is associated with a neutral pH. Slow morning reactions of NPQ to increased light levels show the delayed response of a proton gradient and the binding of epoxidase. Another proposed method of xanthophyll photoprotection is the maintenance of de-epoxidation in dark-adapted corals after a period of stress[158]. This may occur due to a persistent pH gradient after dark acclimation has occurred. While this has been demonstrated with the violaxanthin cycle in plants, there is not enough evidence of DT being stored overnight in corals. However, in diatoms a delayed cessation of epoxidase and continued NPQ is observed for a period after complete darkness, this is attributed to chlororespiration and the subsequent proton gradient created[162,168].

These studies all indicate a wide array of responses among species and reinforce the idea that a range of photoprotective mechanisms are working to prevent photoinhibition and coral bleaching. This is highlighted in a study by Middlebrook et al.[158], whereby corals which were previously stressed and corals which were not previously stressed both exhibited the same level of symbiont loss despite observed differences in photosynthetic productivity, pigments, and the surrounding proteins.

Role of ascorbate

Ascorbate within the lumen is the required substrate for both violaxanthin and diadinoxanthin de-epoxidation, and the concentration of ascorbate is controlled by the lumen pH[169,170]. Ascorbate also aids in preventing the harmful oxygen species such as hydroxide[171]. In the DD cycle little research has been made to determine if the DD de-epoxidase has an affinity for ascorbate. Grouneva et al.[170] was the first study to do so and found that DD de-epoxidase has a strong affinity for ascorbate at high pH levels. Their results also show that when ascorbate levels are high, de-epoxidation can occur at neutral pH levels. Thus, DD epoxidase requires less ascorbate present for de-epoxidation to occur and may aid in quick responses to changes in pH levels. Ascorbate levels can, therefore, influence the de-

epoxidation activity aiding in photoprotection. It is important to note that this study was done on diatoms and not zooxanthellae which may have a different response. In high light ascorbate concentrations may increase over the period of a few days, and vice versa in low light conditions[172]. Under high light levels there is an increase in the conversion of violaxanthin to zeaxanthin, the concentration of ascorbate, and the concentration of xanthophyll cycle pigments[173]. Ascorbate deficient mutants of the rockcress plant *Arabidposis thaliana* (Heynh, 1842) show a decrease in NPQ related to the xanthophyll cycle indicating the importance of ascorbate in NPQ maintenance[172]. However, as the concentration of ascorbate and xanthophyll cycle pigments continue to increase beyond the increased rate of de-epoxidation the authors suggest here that these interactions may only explain part of the increased rate of de-epoxidation[173].

Fluorescence measurements

Chlorophyll fluorescence measuring

Before the use of fluorescence measurements, O_2 and carbon fixation measurements were common in understanding photosynthetic efficiency and productivity. While productivity could be measured, these measurements did not provide information about how the light energy is allocated and its fate within the reaction centres. Fluorescence induction kinetics in dark-adapted leaves was first observed in 1931 by Kautsky and Hirsch[174]. After an initial increase in fluorescence following a dark period, the fluorescence decreased slowly until a steady state was reached. This discovery aided in progressing photosynthesis research through exposing the kinetics of fluorescence and therefore photochemistry as the relaxation of fluorescence is linked with the increase in photochemical quenching and the decrease in non-photochemical quenching. Fluorescence measurement is the result of a photon of light being reemitted due to the inability of the LHCs to absorb that photon. These processes are competitive and so the measurement of one, such as fluorescence, allows the quantification of the other two.

The pulse amplitude modulated fluorometry meter (PAM) allows non-intrusive measurements of photosynthetic properties to determine the levels of stress and damage within an organism through the change in photochemical efficiency (or the quantum yield of PSII). The PAM uses saturation pulses to determine several different fluorescence measurements which represent the state of the PSII reaction centres (Table 1). In a dark-adapted state, we can assume that all reaction centres are fully open and are capable of photochemical quenching, by providing a high intensity saturation pulse of light we can calculate the maximum potential fluorescence whereby all reaction centres are closed. Heat dissipation during the dark-adapted state should be zero or very minimal which allows the calculation of both photochemical quenching and fluorescence emissions. During the light-adapted measurements we can then calculate the number of closed reaction centres resulting in an increase in fluorescence and heat dissipation, and therefore NPQ. Maximum fluorescence in the dark-adapted state (F_m)

represents the maximum potential fluorescence without the inclusion of heat dissipation or photochemical quenching. A reduction in the light adapted F_m (F_m') indicates an increase in photochemical quenching or heat dissipation. A reduction in the dark-adapted minimum fluorescence (F_0) may indicate a reduction in photochemical quenching. These are simplistic views of what is occurring within the organisms and so other parameters are required. Calculation of the number of open and closed reaction centres helps in determining the fate the excitation energy.

Table 1: Summary of commonly used fluorescence parameters during dark adaptation and light adaptation, and their descriptions.

Actinic light	Fluorescence term	Description
Off (darkness)	F	Minimum fluorescence yield
	F_m	Maximum fluorescence yield
	F_v	Variable florescence
	F_v/F_m	Maximum photochemical efficiency
On	F'	Fluorescence yield in the light adapted state
	F_s	Fluorescence yield at steady state
	F_m'	Maximum fluorescence in the light adapted state
	F_0'	Minimum light adapted fluorescence yield
	F_v'	Variable fluorescence in the light adapted state
	NPQ	Non-photochemical quenching
	Y(NO)	Non-regulated non-photochemical quenching
	$\Delta F/F_m$'	Effective photochemical efficiency

Open reaction centres are available to receive and transport electrons through the electron transport chain to be used in photosynthesis. Closed reaction centres are not able to accept any electrons and the transfer of electrons will cease, thereby reducing, or if all reaction centres are closed, stopping photosynthesis. We can gauge the fraction of open reaction centres using the following equation:

$$q_p = F_m' - F_s / F_m' - F_o'$$ [175] [Eq. 5]

As the light intensity increases, the maximum fluorescence (F_m') in the light adapted cells will decrease indicating the closure of some reaction centres. This will result in an increase in heat dissipation and a reduction in photochemical quenching. F_m' will therefore not be as high as the dark-adapted F_m. To determine the level of photochemical quenching occurring the following equation is used;

$$\Phi PSII = F_m' - F_s / F_m'$$ [176] [Eq. 6]

$\Phi PSII$ is also commonly denoted as $\Delta F/F_m'$ or Δ'/F_m' and is often referred to as the yield of effective photochemical efficiency. This equation represents the amount of light energy that is used in photochemistry, and can be used to determine the relative electron transport rate calculated using the absorbed photosynthetic photon flux density (PPFDa);

$$\text{rETR} = \Phi PSII \times PPFDa \times (0.5)^{[177]} \quad \text{[Eq. 7]}$$

Where 0.5 accounts for half of the absorbed photons; 50% used in PSII and 50% used in PSI.

The F_v/F_m ratio which is the yield of maximum photochemical efficiency of the PSII is widely used in determining the health of the coral and is a proxy for $\Phi PSII$. Lowered F_v/F_m values may indicate photoinhibition or stress. This is due to the damage occurring to the PSII occurring at a faster rate than repair can keep up with. In healthy plants this ratio is 0.83[179], and in corals it is thought to be slightly lower than this[179,180]. It is important to ensure that when measuring the dark-adapted fluorescence that the organism is properly dark-adapted to ensure no previous light history impacts the measurements. A 20-minute dark-adaptation is common in corals to ensure all of reaction centres are open[181,182]. However, dark-adapted measurements are traditionally made after a full night of darkness. The use of far-red light aids in opening the reaction centres through activation of the PSI promoting electron flow, many commercial PAMs have this feature[183].

Daily changes in light intensities cause various responses among coral species depending on their photoacclimatory responses and tolerance to high light[184,185]. As discussed, these daily fluctuations are accompanied by NPQ mechanisms to aid in removing the excess excitation energy before it becomes deleterious to the photosystems. F_m' can be lowered by not only heat dissipation, but also photoinhibition, state transitions, and chloroplast movement. These collectively make up the components of NPQ and can be differentiated through their relaxation kinetics. Energy dependent quenching (qE) in the antennae occurs rapidly from seconds to minutes[138], whereas state transitioning (qT), has slower quenching kinetics[186,138]. qT is important in minimizing the potential damage from excitation pressure, such as oxidative damage[187]. State transitioning is the movement of the PSII LHCs from PSII to PSI following overexcitation and the reduction of the plastoquinones[187]. qT reverses when light intensity decreases resulting in lowered excitation pressure and the plastoquinone pool is oxidised[187]. The fluorescence emitted during state transitioning is well defined[e.g.,188]. The transition from state 1 (LHCS associated with PSII) to state 2 (LHCs associated with PSI), occurs when PSII becomes overexcited and the LHCs move to PSI, the fluorescence yield increases due to the overexcitation of PSII and then decreases to a steady state[189]. The opposite occurs when transitioning from state 2 to state 1, when overexcitation of PSI occurs and the LHCs move back to PSII[189]. During state 2 PSII will exhibit a lowered capacity for electron movement while PSI will increase its electron transport shown by the increase (PSI)/ decrease (PSII) in the optical cross section of the photosystems[189]. Reversible photoinhibition (qI) occurs when qE and qT no longer have the capacity to protect the photosystems[190]. Relaxation kinetics for qI take tens of minutes to hours[190]. For this reason, qI is often referred to as photoinactivation instead of photoinhibition. A reduction in F_v is often connected to qI and therefore a reduction in the F_v/F_m ratio is often associated with qI[190]. Recovery from daily midday increased irradiances is shown by

increasing $\Delta F/F_m'$ (the effective quantum yield of fluorescence). If this does not increase as light intensity decreases, it may indicate a more chronic photoinhibition not described by NPQ[191].

Fluorescence measurements and photoinhibition

The relationship between fluorescence, energy dependent quenching, and xanthophyll cycling allows photoinhibition to be measured in coral symbiont photosynthesis studies[130,138]. The F_v/F_m and the $\Delta F/F_m'$ are often used as an indicator of coral health[e.g.,130,192,158]. $\Delta F/F_m'$ declines as irradiance increases[164] and is associated with the decrease in the steady state fluorescence (F_s) and maximum fluorescence in the light (F_m') associated with the de-epoxidation of xanthophylls[158,162]. All responses are dependent upon a species susceptibility and response to stressful conditions. These are shown in changes to xanthophyll cycling and chlorophyll pigments[e.g.,156,162]. Photoinhibition, caused by damage to the PSII unable to be repaired at a fast pace, is shown by a decrease in the F_v/F_m ratio[130,190,161]. For example, over a two-day period corals exposed to increased irradiance in 25 ℃ recovered as the irradiance decline, however, recovery was either inhibited or was minimal in corals exposed to temperatures reaching 31 ℃[156]. The corals *A. millepora* and *P. damicornis* showed a decline in F_v/F_m in response to a combination of light and heat to 0.12 with no recovery and 0.10 with minimal recovery respectively. There was no further reduction in F_v/F_m in the coral *P. decussata* with the increased heat[156]. Significant reductions in chlorophylls *a* and c_2, and peridinin were observed in the corals *A. millepora* and *P. damicornis*, which also exhibited decreased F_v/F_m. This was not observed in the coral *P. decussata*[156] indicating that this species had a greater tolerance to these conditions through maintenance of symbionts or increased concentrations of chlorophyll pigments. In the temperate coral *Plesiastrea versipora* (Lamarck, 1816) a decrease in F_v/F_m followed an increase in heat with no changes to irradiance levels[179]. This was accompanied by a loss in dinoflagellates.

In many studies also looking into the xanthophyll cycle, a decrease in F_m' is accompanied by a decrease in de-epoxidation rates[e.g.,156,130, 58]. Diel xanthophyll cycling is observed with the greatest abundance of diatoxanthin around midday, accompanied with a decline in the $\Delta F/F_m'$[162]. Maximum excitation pressure over PSII, denoted as Q_m, is used to evaluate the photochemical efficiency under maximum daily irradiance observed in the middle of the day. Q_m is calculated as;

$$Q_m = 1 - [\Delta F/Fm'_{\text{at peak sunlight}} / Fv/Fm'_{\text{at dark adaptation}}]$$ [188] [Eq. 8]

As with the F_v/F_m and $\Delta F/F_m'$ ratios, Q_m is useful in understanding the health of the coral by using the photochemical and non-photochemical processes to assess the physiological state of the coral. This metric has been found to be useful in understanding the adaptations of different symbionts to variations in PAR at different water depth. For example, the species *Pavona gigantea* (Verrill, 1869) exhibited smaller changes in Q_m with depth compared to *Pocillopora verrucosa* (Ellis &Solander, 1786), indicating the symbionts of *P. gigantea* are more adapted to the shade and are less tolerable to high light environments[188]. This is a similar response to *Siderastrea sidereal* (Ellis &Solander,

1786), *M. annularis,* and *M. faveolate* which display relatively high Q_m values at 2 and 8 m depth[191]. The species *Porites astreoides* (Lamarck, 1816) displayed constant lowered Q_m at depths of both 2m and 8m compared to the other sampled species indicating a greater number of open reaction centres and potentially less photoinhibition occurring[191]. The corals *P. astreoides* and *P. verrucosa* may therefore be less susceptible to light changes than other species as they are able to efficiently remove excitation pressure from the PSII. Corals adapted to high light also exhibit greater levels of NPQ than low light adapted corals under increased irradiances and diel light cycles which has been linked with state transitioning as cyclic electron flow (CEF) promotes a ΔpH gradient[193,110].

In plants cyclic electron flow has been found to function as a photoprotective mechanism during periods of increased heat and light[194]. Cyclic electron flow works in photoprotection during state transitioning and the promotion of qE through the production of a ΔpH gradient[194,195]. Limited research of cyclic electron flow in coral symbionts has been conducted, however it has also been shown to function as a photoprotective mechanism under heat stress[195]. Without the presence of cyclic electron flow photoinhibition is increased under high light as NPQ, in particular qE, is reduced[194]. Light and heat has been demonstrated in symbiodinium to promote cyclic electron flow with heat tolerant symbiodinium having greater capacity to form cyclic electron flow under heat stress[196]. Takahashi et al.[194] demonstrated that high light on differing temperatures induced NPQ, and with the addition of NH_4Cl, preventing the formation of a proton gradient, all NPQ diminished. When measuring over a natural daily light cycle *A. cervicornis* had increased NPQ despite no significant change in xanthophyll cycling indicating that the main component of this NPQ is not qE[162]. The authors suggest that this could be due to dissociation of LHCs from the reaction centres. These LHCs may not associate with PSI, however, this will still contribute to the increase in the PSII absorption cross section which may increase quenching associated with qT.

In corals exposed to bleaching stress of increased light and heat, NPQ has been shown to transition from favouring qE to favouring qT[110]. The effects of high light conditions, up to 475 μmol photons m^{-2} s^{-1}, without the influence from increased heat, showed that NPQ did not change throughout the experiment done by Hill et al.[110] on the coral *P. damicornis.* An increase in heat, without increased light, up to 32 ℃, resulted in an increase of qE, while qT remained lower. When combined, it took four hours to see a reduction in qE which may be indicative of a reduction in the thylakoid pH gradient. A reduction in qE leads to an increase in excitation energy build up in PSII leading to either qT or qI. The reduction of qE in the coral *P. damicornis* resulted in an increase in qT becoming near equal with qE, around 40%[110]. Increased heat alone in the coral *Turbinaria reniformis* (Bernard, 1896*)*, however, did not alter the electron flow through PSI and PSII, whereas under high light the rETR(I) increased and the rETR(II) did not[193]. This result could be attributed to the occurrence of state transitioning. In this study the results also show that PSII can become damaged under increased heat while PSI does not and remains operative.

As with the cyclic electron flow, the Mehler-ascorbate peroxidase (MAP) pathway, also known as the water–water cycle (WWC), works in dissipating excess energy through NPQ by creating a pH gradient[197]. The MAP pathway is an important electron sink when photosynthesis, and the pH gradient, is limited[198]. This is shown by a decrease in the quantum yield of photosynthesis ($\Phi PSII$)[198]. Electron transport through this system is O_2 dependent which has been shown through MAP suppression in anaerobic conditions[199]. When energy levels exceed the ability of the MAP cycle as an electron sink, a pH gradient is created inducing NPQ[199]. Heat stress of 34 ℃ on the coral *S. pistillata* resulted in a decrease in the $\Phi PSII$ and oxygen evolution, and an increase in NPQ[197]. Electron flow through the MAP cycle is the suggested route of electron flow as photochemical quenching did not significantly decrease with the increase in NPQ and decrease in O_2 evolution[197]. This is supported in their study as the removal of oxygen resulted in the collapse of NPQ[197].

Fluorescence measurements made for Ocean Acidification in corals

The effect of OA on the photosystems of coral is difficult to determine due to the connectivity of calcification and photosynthesis in both coral and symbiont, and due to HCO_3^- being abundant in acidified oceans[e.g.,75]. The two main arguments which may explain how increased pCO_2 affects photosynthesis are; increased metabolic cost or photochemical inhibition like that of bleaching. The available metabolites used in photosynthesis and calcification are intertwined, and as discussed above, HCO_3^- is the main source of DIC used in both processes[45,75]. Light enhanced calcification occurs as increased photosynthesis provides more oxygen which promotes $CaCO_3$ deposition[74]. Therefore, it would be expected that calcification would decrease under acidified conditions if photosynthesis became impaired. Increased heat and light have been shown to alter the function of the photosystems, however not all reefs will experience these changes.

Under a 3-step pH decrease (8.0, 7.6, and 7.4) a decrease on the Fv/Fm ratio on the coral *P. australiensis* was observed which significantly correlated with a decrease in calcification[105]. These corals were maintained at a temperature of 27 ℃ under natural light conditions, therefore these variables should not have influenced the F_v/F_m ratio. The lack of change in chlorophyll content is consistent with the decrease in photosynthesis as supported by Chauvin et al.[200]. Their results suggest a carbon limiting factor in treatments with low pCO_2 in the corals with a comparatively higher abundance of chlorophyll *a*. In this study, however, an increase in net photosynthesis and calcification following an increase in pCO_2 is observed. Along with Iguchi et al.[105], Edmunds[201] also observed a decline in F_v/F_m as well as in the $\Delta F/F_m'$. These results indicate no change in calcification rates or increased energy expenditure supporting the idea that increased pCO_2 has the greatest effect on photochemical efficiency thereby causing a decline in metabolism.

Much research, however, has shown that without the contribution of increased heat, photosynthesis is not affected by acidification. Heat has been shown to negatively affect chlorophyll abundance,

however, under pCO_2 no change is observed[202,103,104]. In the temperate coral *C. caespitosa* four weeks of exposure to elevated temperature caused a decline in $\Delta F/F_m'$[103]. Increased pCO_2 had no effect on this result despite prolonged exposure for one year[103]. This is also shown in the tropical coral species *Acropora digitifera* (Dana, 1846) after a five week experiment[104]. In the coral *Seriatopora caliendrum* (Ehrenberg, 1834) a decline in F_v/F_m and $\Delta F/F_m'$ was observed in high temperature treatments with ambient pCO_2 and increased pCO_2 but not in treatments with ambient temperatures[202]. Increased pCO_2, therefore, did not affect the photosynthetic efficiency. This is supported by Godinot et al.[203] with no influence of pCO_2 on F_v/F_m or ETR, whereas a slight increase in heat (26–29 ℃) caused a small increase in these parameters followed by a significant decrease at 33 ℃. Chlorophyll density in this study[203] was not affected by heat or pCO_2, however at high temperatures when photosynthesis was normalised to chlorophyll, photosynthesis declined.

To support the present studies and to provide further information on how corals will be affected by CO_2 enrichment, the present study is designed to test the effect of CO_2 enrichment on the photochemical efficiency of coral *A. millepora* without the additive influence of temperature.

Methods

Experimental design

Three experimental seawater re-circulation systems were set-up to simulate open ocean conditions in the laboratory by controlling the salinity, temperature, PAR, and seawater carbonate system. The experiment was run three times using three coral fragments each experiment, one coral fragment per experimental system. Nine coral fragments were tested in total. Each experiment ran 16 days, including 7 days acclimation and 9 days of treatment, increasing [H^+] every three days (Fig.1). Seawater pH was established through the injection of CO_2-enriched air bubbled into the system.

Each tank set-up had one piece of *Acropora millepora* (Ehrenberg, 1834), fragment placed directly under the PAM measuring head, under a light, and in the line of water flow from the particle filter. The coral was acclimatised to the experiment tanks using the drip method allowing the coral to slowly adjust to the temperature and water in the tanks[213]. This is done by slowly dripping water from the experimental tanks into the aquarium bag over an hour slowly displacing the aquarium shop water[213]. The coral fragments were then left to acclimate to the seawater and light conditions for 7 days before any pH manipulation occurred (Fig. 1).

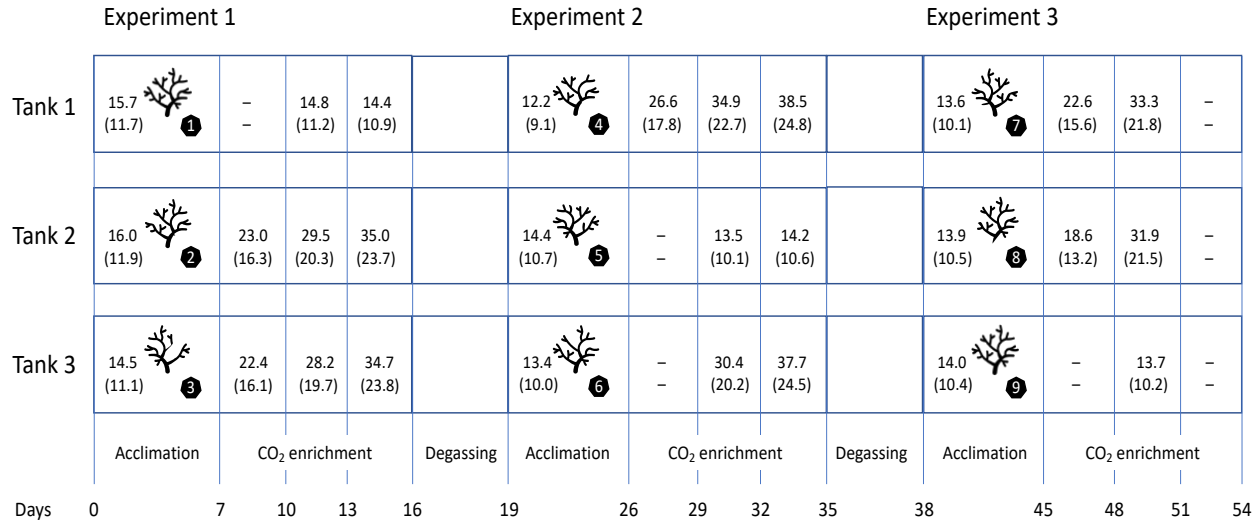

Figure 1. Experimental design and timeline. In each of three 16-day experiments, three coral fragments were tested in separate tanks. Each coral fragments acclimated to tank conditions for 7 days. Following this, the seawater [H^+] in two treatment tank per experiment was raised and then maintained by injection of CO_2 enriched air for three days, three times (transitions from white to blue shades). Numbers, seawater [CO_2] at 25 ℃ (µmol/kg SW); numbers in parenthesis, seawater [H^+] at 25 ℃ (nmol L^{-1}). N-dashes are in place of missing data. A three-day de-gassing period preceded Experiments 2 and 3 allowing the seawater carbonate system to return to an equilibrium with the atmosphere in the laboratory.

The experiment was repeated three times using new coral each time. One tank per experiment remained at 8.0 pH ($[H^+]$ ~ 10.6 nmol L^{-1}) for the entire experiment as a control, while the pH in the remaining two tanks were reduced in three further steps; 7.8 ($[H^+]$ ~ 16.1 nmol L^{-1}), 7.7 ($[H^+]$ ~ 21.1 nmol L^{-1}), and 7.6 ($[H^+]$ ~ 24.3 nmol L^{-1}). Each step remained at that pH for three days. Once the experiment was finished, the CO_2 was shut off and the water was allowed to off-gas naturally over the period of three days before the next experiment began. This was then repeated two more times in the same way for repetition. To minimise the effect of outside influence, such as differences in temperature in the room, the control tank was rotated on each experiment.

Coral

Nine fragments of the coral *Acropora millepora*, approximately 7 cm tall and 4 cm wide, was purchased from an aquarium shop (Reef Aquaria). This branching scleractinian coral species is common in many tropical reefs worldwide. The two large specimens from which these fragments originated were originally collected from the East Coast of Australia. The store maintained these specimens for at least six months in seawater at an average temperature of 26.5 ℃, a salinity of 32, and under a 12 hour constant light at ~80 µmol m^{-2} s^{-1} and 12 hour constant dark regime. Three fragments per experiment were transported from the aquarium shop to the laboratory in the morning of day 1 of acclimation (see Fig. 1). Corals were acclimatised to tank temperatures by submerging the aquarium bags with coral in the experiment tanks for an hour. Acclimation to water conditions was achieved through the drip method as described above[213]. Once fully acclimated to the water, the corals were placed on an aquarium gridded plate under the measuring frame of the PAM and directly under the light. A 1 kg dive weight was placed next to the coral on the aquarium gridded plate to ensure no movement of the coral during testing.

Laboratory setup

Each experimental set-up (Fig. 2) circulated ~450 L of seawater, collected from Okahu Bay, between the main tank (112 × 72 × 60 cm) and an elevated mixing barrel (210 L). Seawater was circulated using a submerged pump (1260 universal pump, Eheim) in the main tank, pumping ~9 L min^{-1} through a water cooler (HC-300A, Hailea) and UV sterilizer (Pond One UV-C 9W, ClearTec) into the mixing barrel from which the seawater returned to the main tank by gravity. A heater (500 W GH Quartz Glass heater, Aqua One) was placed in the floor of the bottom tank. The chiller and heater worked in unison to maintain the water temperature at 25 ± 0.5 ℃. The chiller was set to turn on when the water temperature increased above 25.5 ℃ and switch off at 24.5 ℃. The seawater was also pumped from the main tank through an external particle filter (Professional 4+ 350 Cannister filter, Eheim) into a small plastic container (30 × 20 × 10) raised within the main tank. The overflow from this container returned the seawater into the main tank. The tube returning seawater from the particle

filter was aimed towards a fragment of the coral *A. millepora*, placed inside the raised container to maintain seawater flow across the surface of the coral.

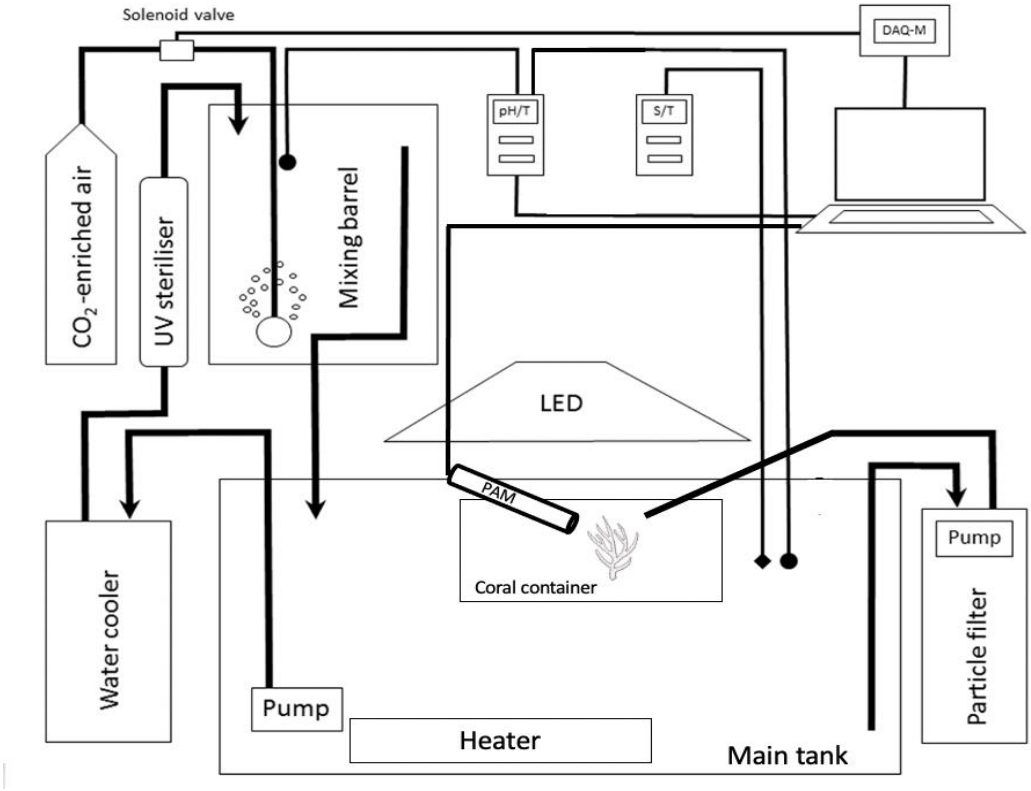

Figure 2. Diagram depiction of one of the three pH controlled experimental setups. CapCtr Software kept the pH of the seawater in the mixing barrel at a setpoint by opening and closing a solenoid valve that controlled the addition of CO_2-enriched air. PAM software controlled the saturation pulses for the induction/ recovery analyses and the saturation pulse analyses. The heater stayed at a constant temperature while the water cooler worked to maintain a stable temperature of 25 ℃. The coral was held in a small container under the LED lights which ran a diel cycle from 0500–1900 h. The output of the particle filter was directed at the coral to allow continuous water flow over the coral tissue, this water in the coral container then overflowed back into the main tank where it circulated through the mixing barrel and particle filter to ensure units were well mixed.

A pulse amplitude modulation fluorometer (Monitoring-PAM aquatic version, Walz GmbH, Germany) was installed in each of the three raised containers with the coral fragment (~7 × 4 cm) placed at a distance (~40 mm) defined by the dimensions of a square measuring frame that was attached to the measuring end (head) of the emitter–detector unit (Fig. 2). A Kessil A80 Tuna Blue LED light, installed above each of the three coral fragments, provided a daily light cycle as follows: darkness from 1900–0500 h, 20 ± 10 µmol m^{-2} s^{-1} from 0500 h, increasing approximately 5 µmol m^{-2} s^{-1} every hour until 1200 h with a maximum PAR of 70 ± 10 µmol m^{-2} s^{-1}, and then decreasing approximately 5 µmol m^{-2} s^{-1} until 1900 h (Appendix 1). The Monitoring-PAM measured the PAR reaching an internal sensor from a reflective surface placed in front of the emitter–detector unit at the distance of the measuring frame. Because the distance between the LED lights and this reflective

surface varied slightly between the three experimental setups, the minimum and maximum PAR varied slightly.

Seawater carbonate system

The pH of the seawater in the mixing barrel of each circulation unit was continuously measured with a SenTix HWD electrode connected to a pH 3310 meter (WTW). These measurements were sent to a computer with CapCtr software (Loligo® Systems ApS) controlling the opening and closing of a solenoid valve when the pH of the seawater in the mixing barrel increased above or decreased below a set point (Appendix 2). The solenoid valve released CO_2-enriched air (5% CO_2, 21% O_2 in nitrogen) from a gas cylinder to a perforated tube in the mixing barrel. The pH electrodes submerged in the seawater of the mixing barrel were calibrated using NIST/DIN pH buffers to test for theoretical Nernstian electrode behaviour, then conditioned in seawater before determining the electrode-specific offset between the potential measured in NIST/DIN pH buffer and that measured in certified seawater reference material (TRIS in synthetic seawater). The electrodes were re-calibrated at the start of each experiment.

Determination of seawater DIC and TA

To determine the seawater dissolved inorganic carbon content and total alkalinity, I collected a one-litre sample from each circulation unit at the start of the incubation period, each night before the pH was reduced, and at the end of the experiment (5 × per set-up per experiment). These samples were preserved by injection of 400 µL mercuric chloride, stored in darkness until sent to the NIWA carbonate chemistry lab at Otago university.

Salinity was maintained at 34.5 ± 0.5 with the addition of distilled water using a reverse osmosis machine. Salinity was measured using a conductivity meter (Knick) and the water was added to the bottom tank manually by slowly pouring it in the back above the pump to ensure adequate missing occurred before reaching the coral.

Pulse amplitude modulated fluorometry

A batch file was created on the PAM software to initiate induction and recovery analyses and saturation pulses (Appendix 3). Pam settings: Actinic light = 65 µmol photon m^{-2} s^{-1}, saturation width = 0.6, Saturation intensity = 1500 µmol photon m^{-2} s^{-1}, gain = 1, measuring light intensity = 190 µmol photon m^{-2} s^{-1},

Induction and recovery analysis

The induction analyses began at 0200 h every day when the coral is adequately dark-adapted. The induction curve was created using a series of 12 saturation pulses, 40 seconds apart with the actinic light on (Width = 0:20, Length = 12, Saturation intensity = 1500 µmol photon m^{-2} s^{-1}, Actinic light = 65 µmol photon m^{-2} s^{-1}). The recovery analysis began immediately after the induction analysis. The

actinic light turned off and a series of 8 saturation pulses occurring every 5 minutes (Width = 0:20, Length = 8, Saturation intensity = 1500 µmol photon m^{-2} s^{-1}). We used the maximum F_v from the first saturation pulse of the induction analysis to detect any effect of CO_2 enrichment on the reaction centres. The F_v of the recovery analysis were averaged to determine how CO_2 enrichment affected the relaxation of fluorescence.

Saturation analysis

A saturation pulse was set off every 30 minutes recording the minimum (F) and maximum fluorescence (F_m) between 0300 and 2400 h. During dark adaptation the minimum fluorescence was measured using the PAM measuring light emitting light at a very low value of <0.15µmol photon m^{-2} s^{-1} to ensure no closure of reaction centers. The saturation pulse reached an intensity of 1500 µmol photon m^{-2} s^{-1}.

Measurements derived from the Saturation pulses:

We derived the maximum photochemical efficiency, F_v/F_m, calculated as

$$Fv/Fm = (F_m–F_o)/F_m \text{ [175]} \quad \text{[Eq. 9]}$$

from the F and F_m taken from the initial saturation pulse at 1900 h. The yield of photochemical quenching $\Phi PSII$, or the effective photochemical efficiency (commonly denoted as $\Delta F/F_m$' or Y(II)), was calculated using the maximum (F_m') and minimum (F') fluorescence yields during light adaptation from saturation pulses (F_m'–F)/F_m' [175]. The maximum photochemical efficiency (F_v/F_m) after dark adaptation (at 1900 h) and the effective yield of photochemical efficiency $\Delta F/F_m$' at midday were used to calculate the maximum excitation pressure (Q_m), calculated as

$$Q_m = (1–\Delta F/F_m'_{\text{at peak PAR}}) / (F_v/F_{m\ \text{at dark adaptation}}) \text{ [189]}. \quad \text{[Eq. 10]}$$

The non-regulated non-photochemical quenching, Y(NO), was calculated by the PAM software following the equation by Genty et al. (1989)

$$Y(NO) = F/F_m. \quad \text{[Eq. 11]}$$

The non-photochemical quenching was derived from the Stern-Volmer relationship:

$$NPQ_{SV} = (F_m/F_m')–1 \text{ [215]}. \quad \text{[Eq. 12]}$$

However, as our NPQ_{SV} values were negative, due to the light adapted maximum fluorescence being higher than the dark-adapted maximum fluorescence, they needed to be corrected for. This correction was done by replacing the F_m value with the max F_m' value:

$$NPQ = (F_m'_{max}/F_m')–1 \text{ [216]} \quad \text{[Eq. 13]}$$

The PAM measures ambient light remitted by a Teflon sheet to a PAR sensor within the monitoring head.

The yield of photochemical quenching, $\Phi PSII$, and the PAR were then used to calculate the relative electron transport rate

$$\text{rETR} = \Phi PSII \times PPFDa \times 0.5 \quad \text{Eq. [14]}$$

The multiplier 0.5 was used because PSII utilises only half of the absorbed photons (50% used in PSII and 50% used in PSI[176].

Measurements were taken continuously, however, we used the data from the last day of each treatment assuming that during this day, conditions in the experimental tanks had been fully established as per the set point. These were day 0, 3, 6, and 9 after acclimation (of 7 days).

Table 2: Used fluorescence parameters including the derivation.

Fluorescence parameter	Symbol	Equation	Reference
Maximum photochemical efficiency	F_v/F_m	$(F_m – F_o) / F_m$	Kitajima and Butler[175]
Effective photochemical efficiency	$\Delta F/F_m'$	$(F_m' – F) / F_m'$	Kitajima and Butler[175]
Excitation pressure	Q_m	$(1 – [\Delta F / F_m'_{\text{at peak PAR}}) / (F_v / F_{m\text{ at dark adaptation}})$	Taylor et al.[189]
Non-regulated non-photochemical quenching	Y(NO)	F / F_m	Genty et al.[214]
Non- photochemical quenching (Stern-volmer relationship)	$NPQS_V$	$NPQ_{SV} = (F_m/F_m')–1$	Bilger and Björkman[215]
Non- photochemical quenching (corrected)	NPQ	$(F_m'_{max} / F_m') – 1$	Serôdio et al.[216]
Relative electron transport rate	rETR	$\Phi PSII \times PPFDa \times 0.5$	Klughammer and Schrieber[176]

Statistical analysis

All statistical analysis were done using R statistical software (version 1.3.959). The Shapiro-Wilk test was used to assess if the data was normally distributed, and homogeneity of variance was tested using Levenes test. The F_v/F_m, $\Delta F/F_m'$, Q_m, and slopes were analysed using a four-factor, nested ANOVA in which individual corals were the random factor nested in tank, treatment, and day of measurement which were fixed factors. The same ANOVAs were then used to analyse the maximum F_v from the induction analysis and the average F_v of the recovery analysis.

We used an Akaike information criterion model selection to determine the best model possible to describe the relationship between the fluorescence parameters, the three tanks, the treatment, and the individual coral fragments. Tank effect was not significant and was removed from the model.

Results

In the following, I will report how experimental CO_2 enrichment affected the carbonate chemistry of the seawater in the three circulation units, and then evaluate the effects of this manipulation on the measured proxies of coral photosynthesis. Following this, I will present evidence for chlororespiratory induced state transitioning of the PSII reaction centres. Because the range of seawater $[H^+]$ observed in this experiment was small, I do not report these as pH but instead as nmol L^{-1}.

Effects of CO_2 enrichment on seawater carbonate chemistry

Control of the carbonate chemistry is presented in Table 3. Dashed lines in the control tanks for experiment one and two represent water samples that were not tested. Water samples were not taken for the last day of experiment three due to Covid restrictions. Across all three experiments the ambient $[H^+]$ was maintained at ~10.6 nmol L^{-1}, increasing to ~16.1 nmol L^{-1}, 21.1 nmol L^{-1}, and ~24.3 nmol L^{-1}. CO_2 enrichment resulted in an increase in $[HCO_3^-]$ from ~1902 µmol kg SW^{-1} in the controls and ambient treatments to ~2144 µmol kg SW^{-1} in the last treatment, whereas the $[CO_3^{2-}]$ decreased from 195 µmol kg SW^{-1} in the controls and ambient treatments to 96 µmol kg SW^{-1} in the last treatment.

Table 3. Properties of ambient (Control) and CO_2-enriched (Treatment) seawater in three Tanks at the start of each of three consecutive experiments, and 3, 6, and 9 days later. Measured and calculated variables (derived for a temperature of 25 °C) are based on analysis of one 2-L seawater sample collected from each Tank on the dates given in the format of day/months. Temp., Temperature (°C); DIC, dissolved inorganic carbon (µmol kg SW^{-1}); TA, total alkalinity (µmol kg SW^{-1}); pH_T, seawater pH (total scale); $[H^+]$, hydrogen ion concentration (nmol L^{-1}); pCO_2, partial pressure of CO_2 (µatm); $[CO_3^{2-}]$, $[HCO_3^-]$, $[CO_2]$, (µmol kg SW^{-1}); Ω_{CA} and Ω_{AR}, calcite and aragonite saturation states, respectively.

Exp 1	Tank 1 (Control)				Tank 2 (Treatment)				Tank 3 (Treatment)			
	27/6	29/6	3/7	6/7	27/6	29/6	3/7	6/7	27/6	29/6	3/7	6/7
Measured parameters												
Temp.	24.7	–	24.9	25.0	24.6	24.6	24.4	24.5	25.5	25.5	25.2	25.2
Salinity	35.0	–	35.0	35.0	35.0	34.6	34.9	34.9	35.0	34.6	34.9	34.9
DIC	2101	–	2080	2072	2106	2154	2203	2234	2066	2126	2178	2204
TA	2344	–	2333	2329	2345	2323	2334	2340	2320	2297	2314	2308
Calculated parameters at 25 °C												
pH_T	7.93	–	7.95	7.96	7.92	7.79	7.69	7.63	7.96	7.79	7.71	7.62
$[H^+]$	11.7	–	11.2	10.9	11.9	16.3	20.3	23.7	11.1	16.1	19.7	23.8
pCO_2	555	–	522	508	565	811	1041	1236	514	790	996	1226
$[CO_2]$	15.7	–	14.8	14.4	16.0	23.0	29.5	35.0	14.5	22.4	28.2	34.7
$[HCO_3^-]$	1909	–	1883	1872	1915	1999	2064	2103	1869	1973	2038	2075
$[CO_3^{2-}]$	177	–	183	185	174	131	110	96	183	131	112	94
Ω_{CA}	4.24	–	4.39	4.45	4.19	3.17	2.64	2.31	4.39	3.16	2.69	2.27
Ω_{AR}	2.8	–	2.9	2.9	2.8	2.1	1.7	1.5	2.9	2.1	1.8	1.5

Exp 2	Tank 1 (Treatment)				Tank 2 (Control)				Tank 3 (Treatment)			
	18/7	21/7	24/7	27/7	18/7	21/7	24/7	27/7	18/7	21/7	24/7	27/7
Measured parameters												
Temp.	24.8	24.9	25.0	24.8	24.6	–	24.8	24.6	25.5	25.5	25.5	25.5
Salinity	34.9	35.2	35.1	35.1	34.9	–	35.1	35.1	34.9	35.0	35.0	35.0
DIC	2155	2284	2331	2346	2118	–	2112	2113	2129	2333	2286	2323
TA	2471	2445	2447	2446	2384	–	2394	2384	2415	2424	2421	2425
Calculated parameters at 25 °C												
pH_T	8.04	7.75	7.64	7.61	7.97	–	7.99	7.98	8.00	–	7.69	7.61
$[H^+]$	9.1	17.8	22.7	24.8	10.7	–	10.1	10.6	10.0	–	20.2	24.5
pCO_2	433	941	1235	1362	508	–	476	501	475	–	1076	1334
$[CO_2]$	12.2	26.6	34.9	38.5	14.4	–	13.5	14.2	13.4	–	30.4	37.7
$[HCO_3^-]$	1915	2128	2191	2210	1911	–	1895	1904	1910	–	2141	2189
$[CO_3^{2-}]$	227	130	105	97	193	–	203	195	206	–	115	97
Ω_{CA}	5.47	3.11	2.51	2.32	4.64	–	4.88	4.68	4.96	–	2.75	2.32
Ω_{AR}	3.61	2.05	1.66	1.53	3.06	–	3.22	3.09	3.27	–	1.81	1.53

Exp 3	Tank 1 (Treatment)				Tank 2 (Treatment)				Tank 3 (Control)			
	9/8	12/8	15/8	–	9/8	12/8	15/8	–	9/8	12/8	15/8	–
Measured parameters												
Temp.	24.7	24.5	25.1	–	25.1	24.5	25.2	–	24.9	–	25.3	–
Salinity	35.0	35.0	34.9	–	34.6	34.6	34.6	–	35.1	–	35.0	–
DIC	2141	2101	2131	–	2222	2186	2124	–	2313	–	2128	–
TA	2426	2373	2407	–	2405	2405	2351	–	2436	–	2409	–
Calculated parameters at 25 °C												
pH_T	8.00	7.81	7.66	–	7.98	7.88	7.67	–	7.98	–	7.99	–
$[H^+]$	10.1	15.6	21.8	–	10.5	13.2	21.5	–	10.4	–	10.2	–
pCO_2	482	798	1176	–	491	655	1128	–	495	–	483	–
$[CO_2]$	13.6	22.6	33.3	–	13.9	18.6	31.9	–	14.0	–	13.7	–
$[HCO_3^-]$	1921	2058	2172	–	1891	2004	2114	–	1918	–	1911	–
$[CO_3^{2-}]$	206	142	108	–	196	163	106	–	199	–	203	–
Ω_{CA}	4.95	3.41	2.59	–	4.71	3.94	2.56	–	4.80	–	4.88	–
Ω_{AR}	3.26	2.25	1.71	–	3.10	2.60	1.69	–	3.16	–	3.22	–

Effects of CO_2 enrichment on photosynthetic performance indicators

A four-factor nested ANOVAs revealed that CO_2 enrichment of the seawater surrounding the coral *A. millepora* did not affect the maximum photochemical efficiency (F_v/F_m), the effective photochemical efficiency ($\Delta F/F_m$'), or the maximum excitation pressure over PSII, Q_m, of the coral symbiont (Table 4, Fig.4). The ratios F_v/F_m and $\Delta F/F_m$' ranged between 0.631 and 0.636, and between 0.564 and 0.580, respectively, and Q_m varied from 0.088 to 0.108 (Table 4).

The Akaike information criterion model indicated that tank should not be included in the analysis for the best model fit (Appendix 4).

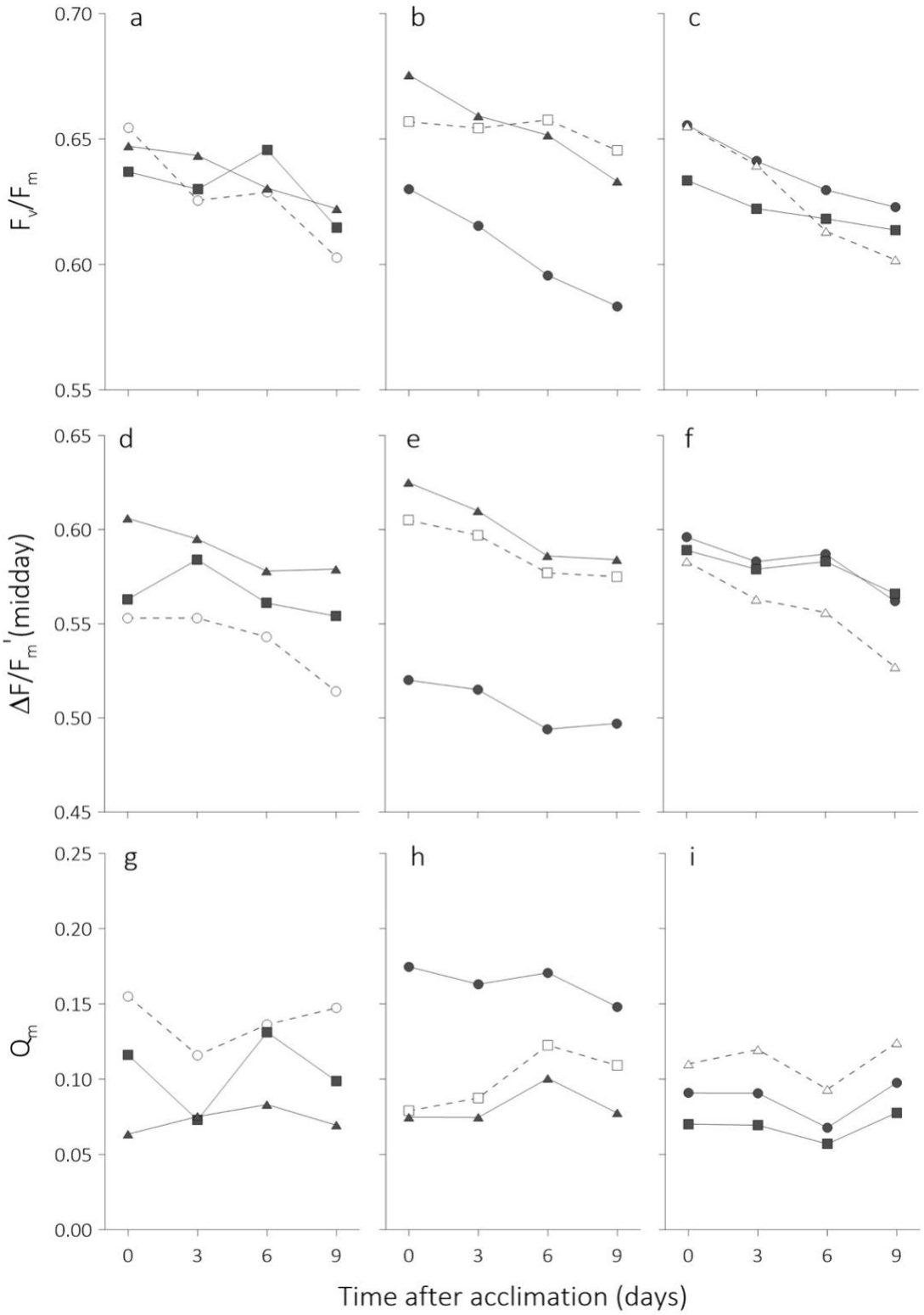

Figure 3. *Acropora millepora*. Time-series of the maximum photochemical efficiency (a, b, c; $F_v/F_m = (F_m–F_0)/F_m$), the midday effective quantum yield (d, e, f; $\Delta F/F_m = (F_m'–F_s)/F_m'$), and the maximum excitation pressure (g, h, i; $Q_m = 1–$ [$\Delta F/F_m$' at midday/ F_v/F_m peak dark adaptation]) of nine coral fragments, one placed in each of three seawater circulation units (Circles, Unit 1; squares, Unit 2; triangles, Unit 3) in each of three consecutive experiments (three panels). In each experiment, the seawater in two units (filled symbols) was gradually enriched with CO_2 (Treatment) to increase the [H^+] from ~10.6 (day 0), to ~16.1 (day 3), to ~21.1 (day 6), to ~24.3 nmol L^{-1} (day 9). The seawater [H^+] in the third unit (open symbols) remained at ~10.6 nmol L^{-1} over the duration of the experiment (Control). Note that the maximum and minimum fluorescence, F_m and F_0, were measured at 1900 hours. The maximum midday fluorescence, F_m', and the steady state fluorescence, F_s, were measured at the 1200 hours at peak irradiance (between ~51 and 84 µmol m^{-2} s^{-1}).

Table 4. Results of the nested ANOVA testing the maximum photochemical efficiency (F_v/F_m), the midday effective photochemical efficiency ($\Delta F/F_m'$), and the maximum excitation pressure of PSII (Qm) including the least square means. Model description: treatment, and day were set as fixed factors, and coral individuals were set as the random factor. AIC, Akaike information criterion; SE, standard error; DF, degrees of freedom; Lsmean, Least square means; Lower CL, lower confidence limits; Upper CL, upper confidence limits.

Variable	Treatment	Estimates	SE	DF	p-value	
F_v/F_m (AIC = -143.0868)						
	Intercept	0.6494440	0.005805436	21	0.0000	
	pH 7.8	0.0020038	0.008424640	21	0.8143	
	pH 7.7	0.0019395	0.008424640	21	0.8202	
	pH 7.6	0.0048859	0.008424640	21	0.5681	
	Day 3	-0.0140472	0.007055794	21	0.0597	
	Day 6	-0.0206611	0.007055794	21	0.0080	
	Day 9	-0.0371678	0.007055794	21	0.0000	
	Treatment	Lsmean	SE	DF	Lower CL	Upper CL
	pH 8.1	0.631	0.00615	8	0.617	0.646
	pH 7.8	0.633	0.00807	8	0.615	0.652
	pH 7.7	0.633	0.00807	8	0.615	0.652
	pH 7.6	0.636	0.00807	8	0.618	0.655
$\Delta F/F_m'$ (AIC = -136.8972)						
	Intercept	0.5822222	0.010059886	21	0.0000	
	pH 7.8	0.0040465	0.008121268	21	0.6235	
	pH 7.7	0.0035465	0.008121268	21	0.6668	
	pH 7.6	0.0157132	0.008121268	21	0.0666	
	Day 3	-0.0094755	0.006674052	21	0.1704	
	Day 6	-0.0218088	0.006674052	21	0.0037	
	Day 9	-0.0418088	0.006674052	21	0.0000	
	Treatment	Lsmean	SE	Df	Lower CL	Upper CL
	pH 8.1	0.564	0.00103	8	0.540	0.588
	pH 7.8	0.568	0.01044	8	0.542	0.594
	pH 7.7	0.567	0.01044	8	0.541	0.594
	pH 7.6	0.580	0.01044	8	0.553	0.606
Q_m (AIC = -108.4108)						
	Intercept	0.10378550	0.01126535	21	0.0000	
	pH 7.8	-0.01936993	0.01503727	21	0.2117	
	pH 7.7	-0.00299961	0.01503727	21	0.8438	
	pH 7.6	-0.00404595	0.01503727	21	0.7905	
	Day 3	-0.00451270	0.01253178	21	0.7224	
	Day 6	0.00515269	0.01253178	21	0.6851	
	Day 9	0.01465221	0.01253178	21	0.2554	
	Treatment	Lsmean	SE	DF	Lower CL	Upper CL
	pH 8.1	0.1076	0.0119	8	0.0802	0.135
	pH 7.8	0.1036	0.0150	8	0.0689	0.138
	pH 7.7	0.1046	0.0150	8	0.0700	0.139
	pH 7.6	0.0882	0.0150	8	0.0536	0.123

Temporal trends in the ratios F_v/F_m and $\Delta F/F_m'$

Inspection of Figure 3a and 3b revealed a gradual reduction in the maximum photochemical efficiency (F_v/F_m) and effective photochemical efficiency ($\Delta F/F_m'$) over the course of the 16 day experiment and independently of [H^+] treatment (Fig. 3). That is, this gradual reduction was not caused by CO_2 enrichment or increasing [H^+], but observed in both control and treatment tanks (Table 4). The gradual reduction of the maximum photochemical efficiency (F_v/F_m) produced a significant reduction on day 6 and 9 of the three experiments (Table 4). In contrast to the ratios F_v/F_m and $\Delta F/F_m'$, Q_m did not decrease over the course of the experiments (Fig. 3).

The relationship between rETR and PAR was linear, which suggests that the coral did not reach light saturation during the day (Fig. 4). The slope of this linear regressions, which is a measure of the response of the coral symbiont to increasing PAR, decreased over the course of the experiment (Fig. 5). Such decrease was observed in all tanks, that is, there was no evidence for an effect of CO_2 enrichment or seawater [H^+] on the rETR/PAR relationship (Fig. 5). Note, however, that in Experiment 1 and 3 this slope decreased faster in the Control than in the two Treatments, but this difference was not confirmed in Experiment 2.

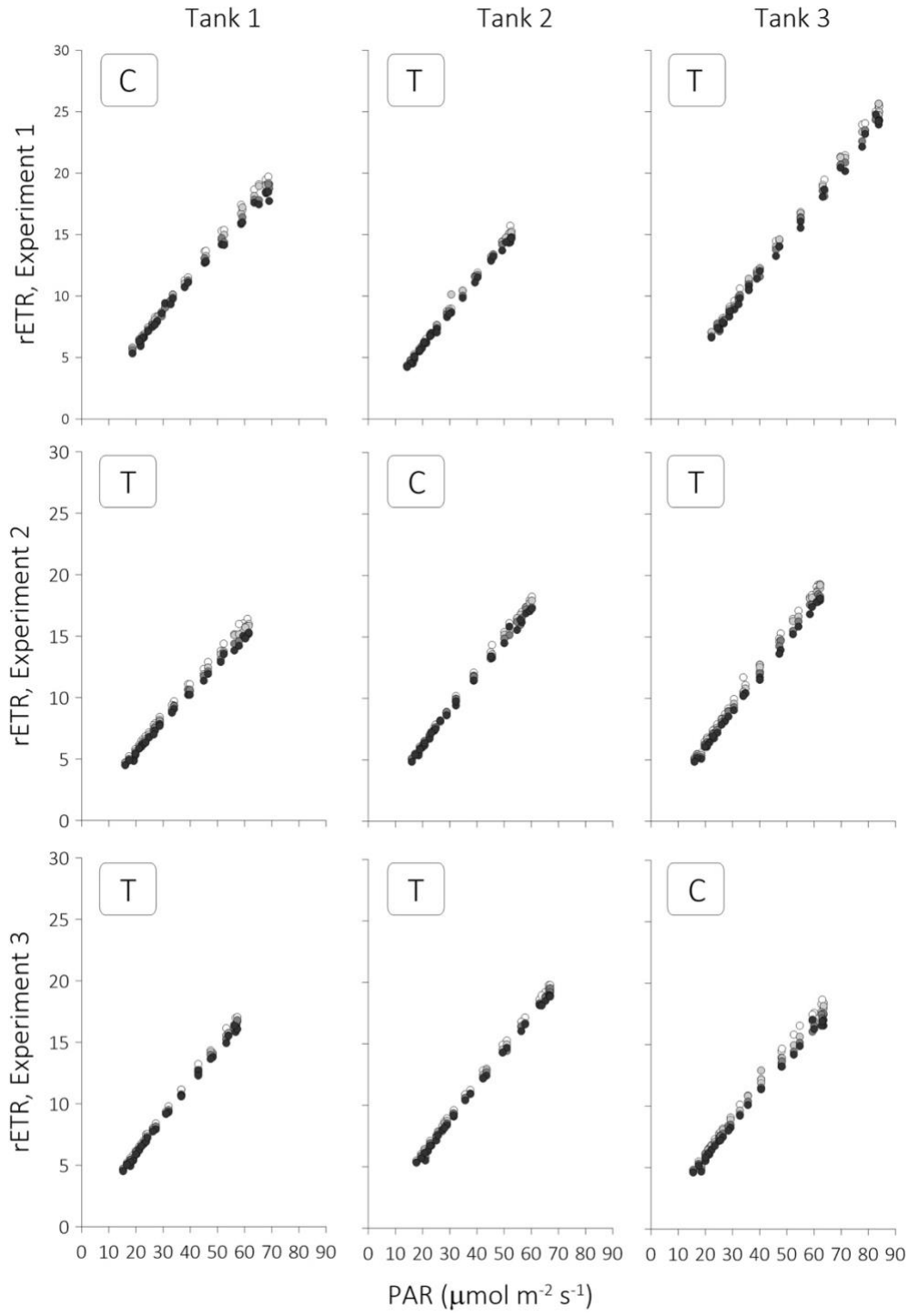

Figure 4. *Acropora millepora*. Relative electron transport rate (rETR) as a function of the incident photosynthetically active radiation (PAR, µmol m^{-2} s^{-1}) measured immediately after (day 0, open symbols), and three (grey symbols), six (dark grey symbols) and nine days (black symbols) after acclimation of nine coral fragments, one placed in each of three experimental units (Tank 1, 2, 3) for each of three consecutive experiments. The framed letters C and T refer to Control and Treatment units. In the Treatment units, the seawater was gradually enriched with CO_2 to increase the $[H^+]$ from ~10.6 (day 0), to ~16.1 (day 3), to ~21.1 (day 6), to ~24.3 nmol L^{-1} (day 9). The seawater $[H^+]$ in the Control unit remained at ~10.6 nmol L^{-1} over the duration of the experiment. rETR = $-\Delta F/F_m' \times 0.5 \times$ PAR.

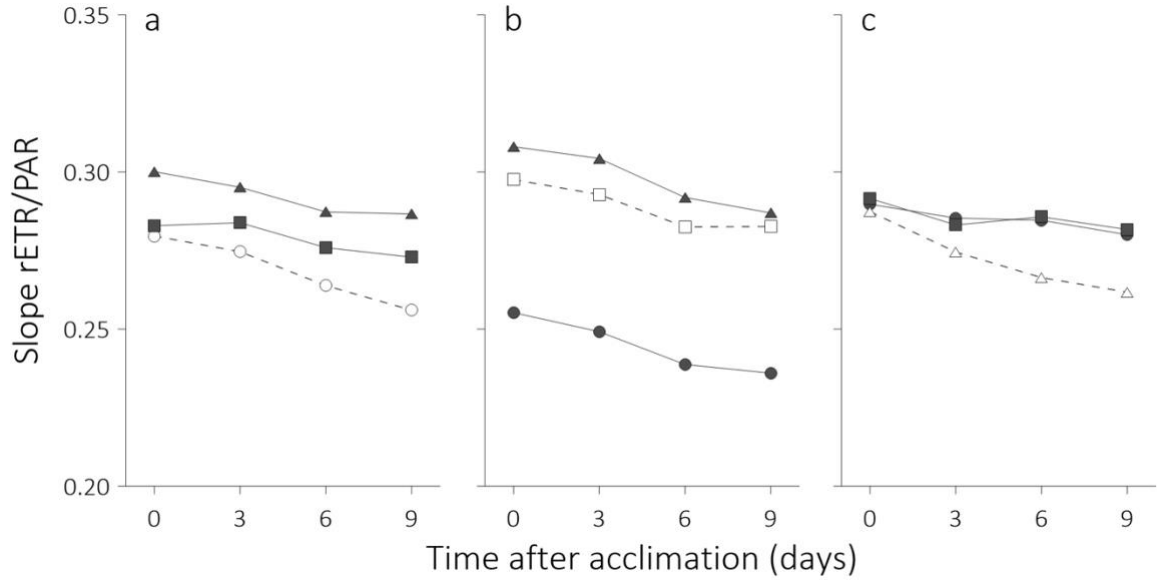

Figure 5. *Acropora millepora.* Time-series of the slope of the linear regression of relative electron transport rate (rETR) versus incident photosynthetically active radiation (PAR, µmol m^{-2} s^{-1}) shown in Figure 2. The rETR was measured immediately after (0 days), and three, six and nine days after acclimation of nine coral fragments, one placed in each of three experimental units (Circles, Unit 1; squares, Unit 2; triangles, Unit 3) for each of three consecutive experiments (a, b, c). In each experiment, the seawater in two units (filled symbols) was gradually enriched with CO_2 (Treatment) to increase the $[H^+]$ from ~10.6 (day 0), to ~16.1 (day 3), to ~21.1 (day 6), to ~24.3 nmol L^{-1} (day 9). The seawater $[H^+]$ in the third unit (open symbols) remained at ~10.6 nmol L^{-1} over the duration of the experiment (Control).

Photosynthesis induction and recovery: time-series measurements

The variable fluorescence F_v, measured at the beginning of each nocturnal induction analysis, was not affected by CO_2 enrichment or time (Table 5, Fig. 6). Furthermore, there was no evidence for an effect of CO_2 enrichment on the recovery of F_v during darkness following a period of light (Fig. 6).

A reduction in F_v following the onset of actinic light is observed with a reduction in F_m' and F due to closures of reaction centres. The induction and recovery were accompanied by positive Non Photochemical quenching (NPQ) values (data not shown), which increased steadily under conditions of actinic light and then decreased slightly at the end of the induction period under actinic light indicating the induction of the Calvin cycle. During the recovery period the NPQ decreased as F_m increased. F remained steady throughout the recovery period.

Table 5: Results of the nested ANOVA testing the maximum variable fluorescence during the induction analysis and the average maximum variable fluorescence during the recovery analysis, including the least square means. Model description: treatment and day were set as the fixed factors, and coral individuals were set as the random factor. AIC, Akaike information criterion; SE, standard error; DF, degrees of freedom; Lsmean, Least square means; Lower CL, lower confidence limits; Upper CL, upper confidence limits.

Variable	Treatment	Estimates	SE	DF	p-value	
Maximum variable fluorescence during induction analysis (AIC = 350.6269)						
	Intercept	679.7778	68.50259	21	0.0000	
	pH 7.8	-30.4632	31.14689	21	0.3392	
	pH 7.7	-29.6299	31.14689	21	0.3523	
	pH 7.6	-53.7965	31.14689	21	0.988	
	Day 3	-13.3579	25.48111	21	0.6056	
	Day 6	-38.6912	25.48111	21	0.1438	
	Day 9	-18.3579	25.48111	21	0.4792	
	Treatment	Lsmean	SE	DF	Lower CL	Upper CL
	pH 8.1	662	69.1	6	503	821
	pH 7.8	632	71.4	6	467	796
	pH 7.7	633	71.4	6	468	797
	pH 7.6	608	71.4	6	444	773
Average Maximum variable fluorescence during recovery analysis (AIC = 286.7392)						
	Intercept	358.9858	25.347942	21	0.0000	
	pH 7.8	6.1140	9.944923	21	0.5453	
	pH 7.7	14.8576	9.944923	21	0.1501	
	pH 7.6	9.7294	9.944923	21	0.3390	
	Day 3	-23.6942	8.131763	21	0.0083	
	Day 6	-36.6430	8.131763	21	0.0002	
	Day 9	-48.4635	8.131763	21	0.0000	
	Treatment	Lsmean	SE	Df	Lower CL	Upper CL
	pH 8.1	332	25.5	8	273	391
	pH 7.8	338	26.2	8	278	398
	pH 7.7	347	26.2	8	286	407
	pH 7.6	342	26.2	8	281	402

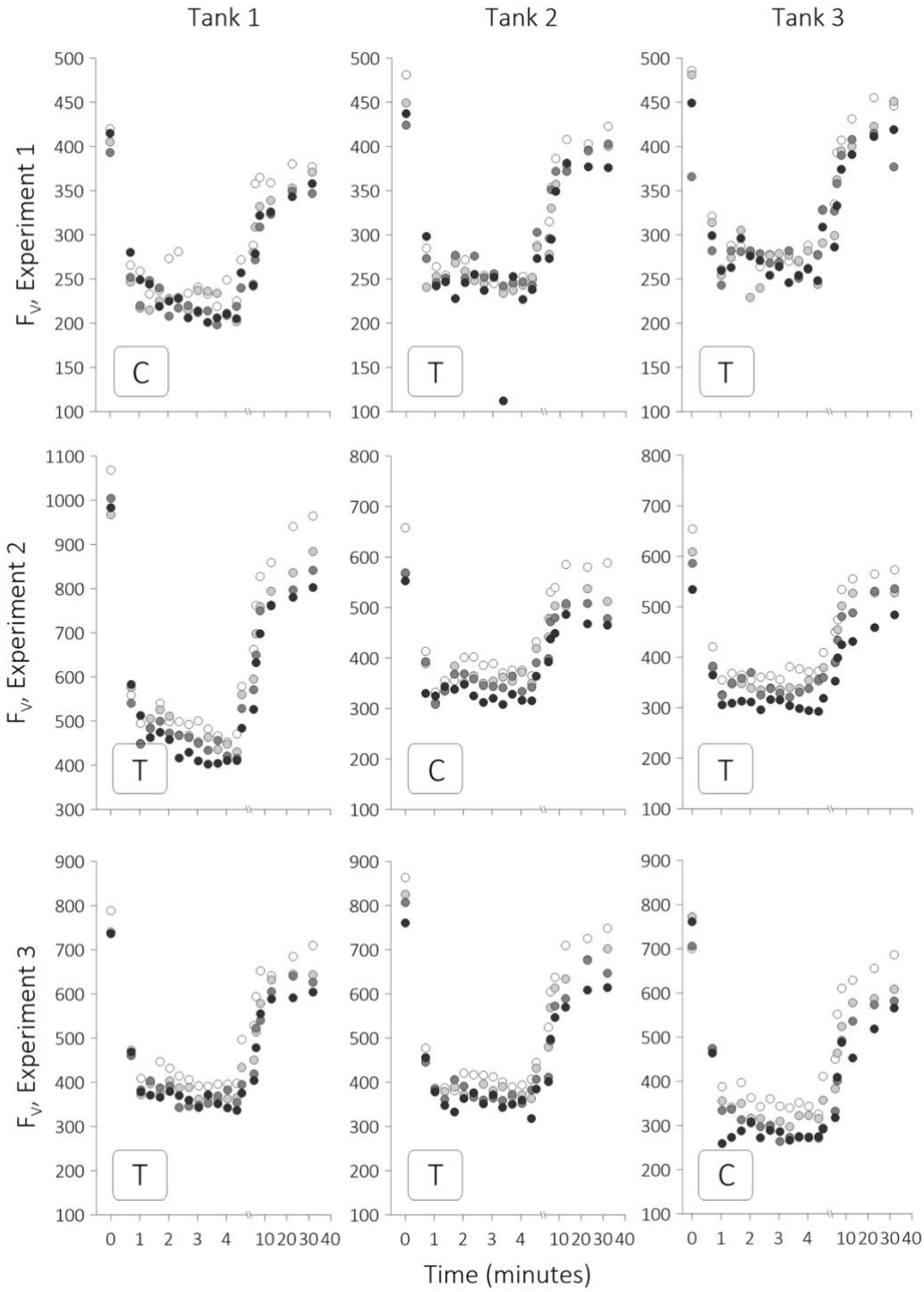

Figure 6. *Acropora millepora*. Variable fluorescence ($F_v = F_m – F_0$) during induction and recovery analyses immediately after (open symbols), and three (grey symbols), six (dark grey symbols), and nine days (black symbols) after acclimation of nine dark-adapted coral fragments, one placed in each experimental units (Tank 1, 2, 3) for each consecutive experiments. The framed letters C and T refer to Control and Treatment units. In the Treatment units, the seawater was gradually enriched with CO_2 to increase the $[H^+]$ from ~10.6 (open symbols, day 0), to ~16.1 (grey symbols, day 3), to ~21.1 (dark grey symbols, day 6), to ~24.3 nmol L^{-1} (black symbols, day 9). The seawater $[H^+]$ in the Control unit remained at ~10.6 nmol L^{-1} over the duration of the experiment. Note differences in the scale of the y-axis.

Relationship between PAR and photochemical yields

The $\Delta F/F_m$' decreased with increasing PAR typically from ~ 0.65 to 0.55 (Fig. 7). The quantum yield of nonphotochemical quenching (NPQ, corrected) showed no clear pattern with increasing PAR, however, experiment 2 tank 1 showed an increase in NPQ with increasing irradiances (Fig. 8). The quantum yield of non-regulated non-photochemical quenching (Y(NO)) did not change with increasing irradiances and remained high between ~0.4 and 0.5 (Fig. 9).

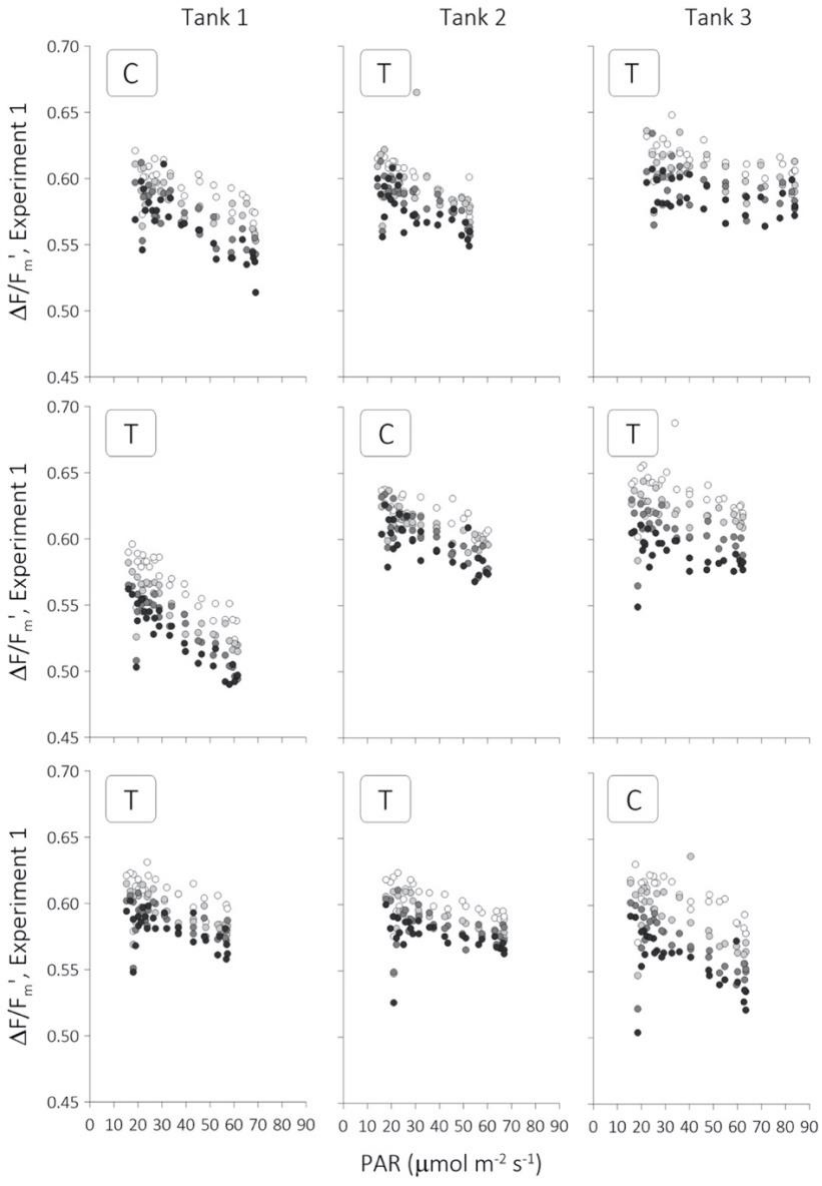

Figure 7. *Acropora millepora.* The effective quantum yield ($\Delta F/F_m' = F_m'–F_s)/F_m'$ as a function of incident photosynthetically active radiation (PAR, µmol m^{-2} s^{-1}) measured immediately after (day 0, open symbols), and three (grey symbols), six (dark grey symbols) and nine days (black symbols) after acclimation of nine coral fragments, one placed in each of three experimental units (Tank 1, 2, 3) for each of three consecutive experiments. The framed letters C and T refer to Control and Treatment units. In the Treatment units, the seawater was gradually enriched with CO_2 to increase the $[H^+]$ from ~10.6 (day 0), to ~16.1 (day 3), to ~21.1 (day 6), to ~24.3 nmol L^{-1} (day 9). The seawater $[H^+]$ in the Control unit remained at 10 nmol L^{-1} over the duration of the experiment.

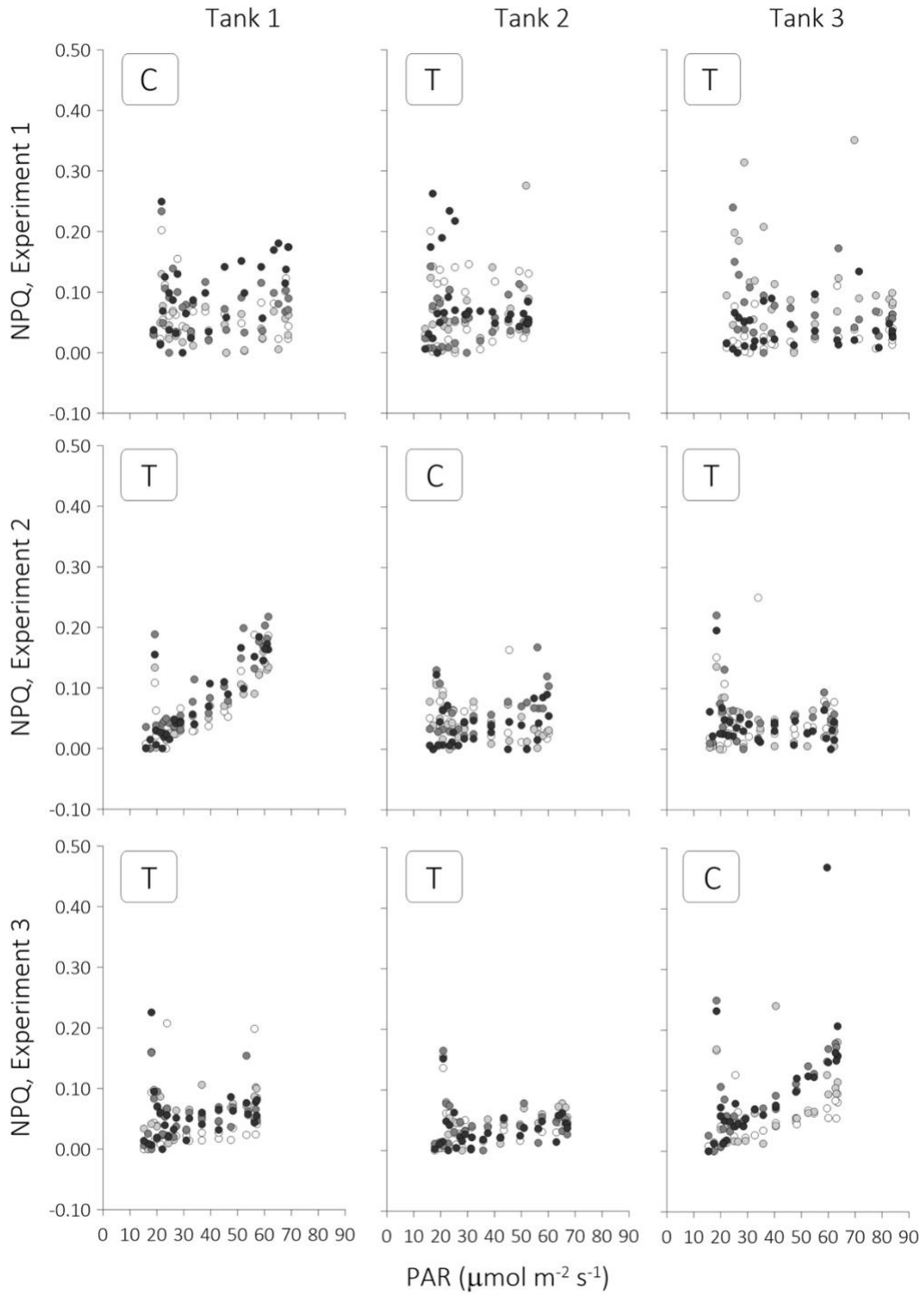

Figure 8. *Acropora millepora*. Non-photochemical quenching (NPQ = $F_m'_{max}/F_m'$) – 1) as a function of incident photosynthetically active radiation (PAR, µmol m^{-2} s^{-1}) measured immediately after (day 0, open symbols), and three (grey symbols), six (dark grey symbols) and nine days (black symbols) after acclimation of nine coral fragments, one placed in each of three experimental units (Tank 1, 2, 3) for each of three consecutive experiments. The framed letters C and T refer to Control and Treatment units. In the Treatment units, the seawater was gradually enriched with CO_2 to increase the $[H^+]$ from ~10.6 (day 0), to ~16.1 (day 3), to ~21.1 (day 6), to ~24.3 nmol L^{-1} (day 9). The seawater $[H^+]$ in the Control unit remained at 10 nmol L^{-1} over the duration of the experiment.

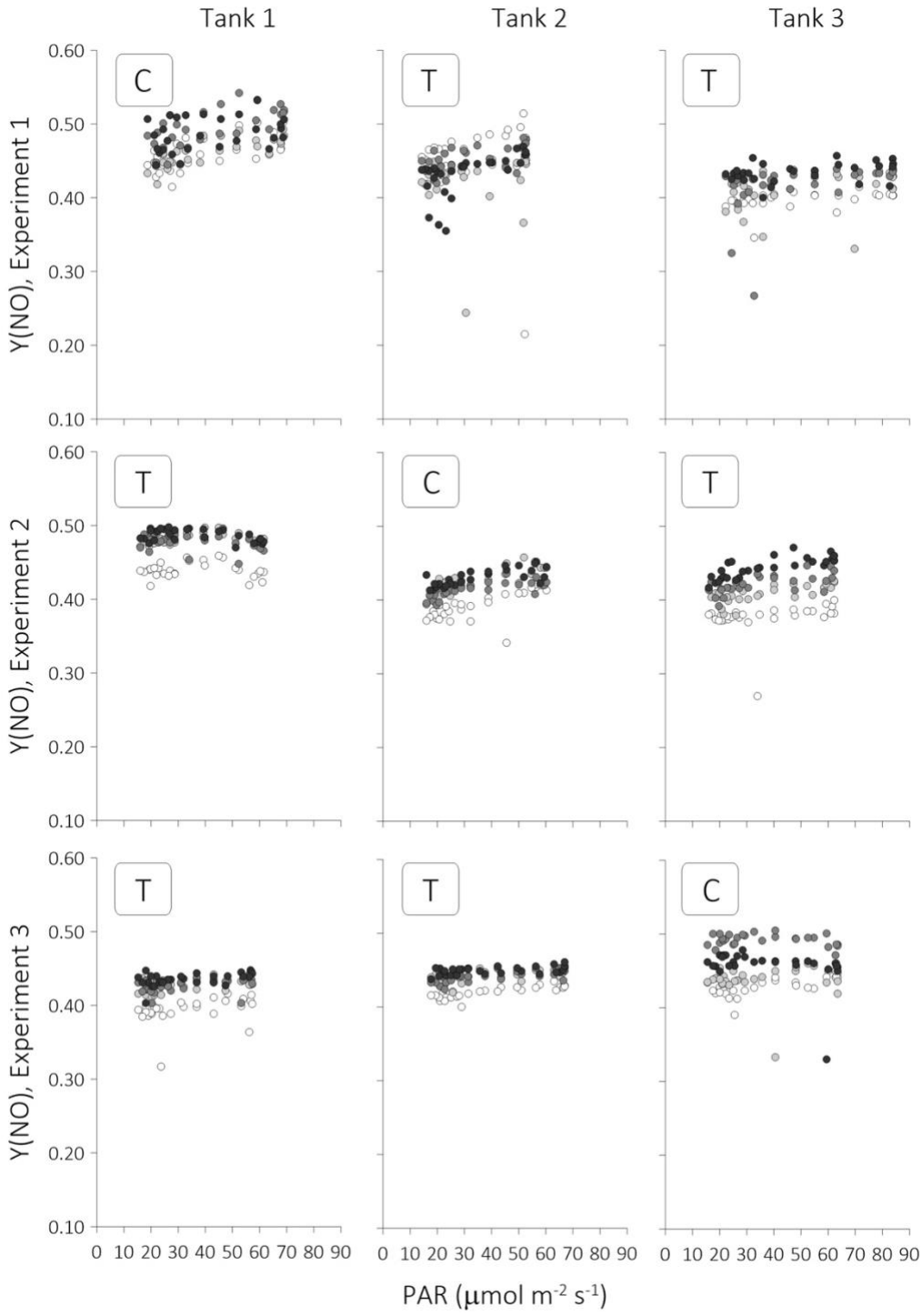

Figure 9. *Acropora millepora.* Non-regulated non-photochemical quenching (Y(NO) = F/F_m) as a function of incident photosynthetically active radiation (PAR, µmol m^{-2} s^{-1}) measured immediately after (day 0, open symbols), and three (grey symbols), six (dark grey symbols) and nine days (black symbols) after acclimation of nine coral fragments, one placed in each of three experimental units (Tank 1, 2, 3) for each of three consecutive experiments. The framed letters C and T refer to Control and Treatment units. In the Treatment units, the seawater was gradually enriched with CO_2 to increase the $[H^+]$ from ~10.6 (day 0), to ~16.1 (day 3), to ~21.1 (day 6), to ~24.3 nmol L^{-1} (day 9). The seawater $[H^+]$ in the Control unit remained at ~10.6 nmol L^{-1} over the duration of the experiment.

Chlororespiration and state transitioning

The F_m during dark adapted periods leading to the calculation of negative NPQ yields. A sharp increase in the F_v/F_m within the first 30 mins of extremely low-light to no light at 1900 hours followed by a gradual decrease in F_v/F_m to 0500 h. A sharp increase in F_v/F_m with the low-light induction at 0500 h was observed indicating the presence of an alternate electron chain, chlororespiration (Figs 10 and 11). An increase in NPQ throughout the night, observed before the induction and recovery analysis, is characteristic of state transitioning.

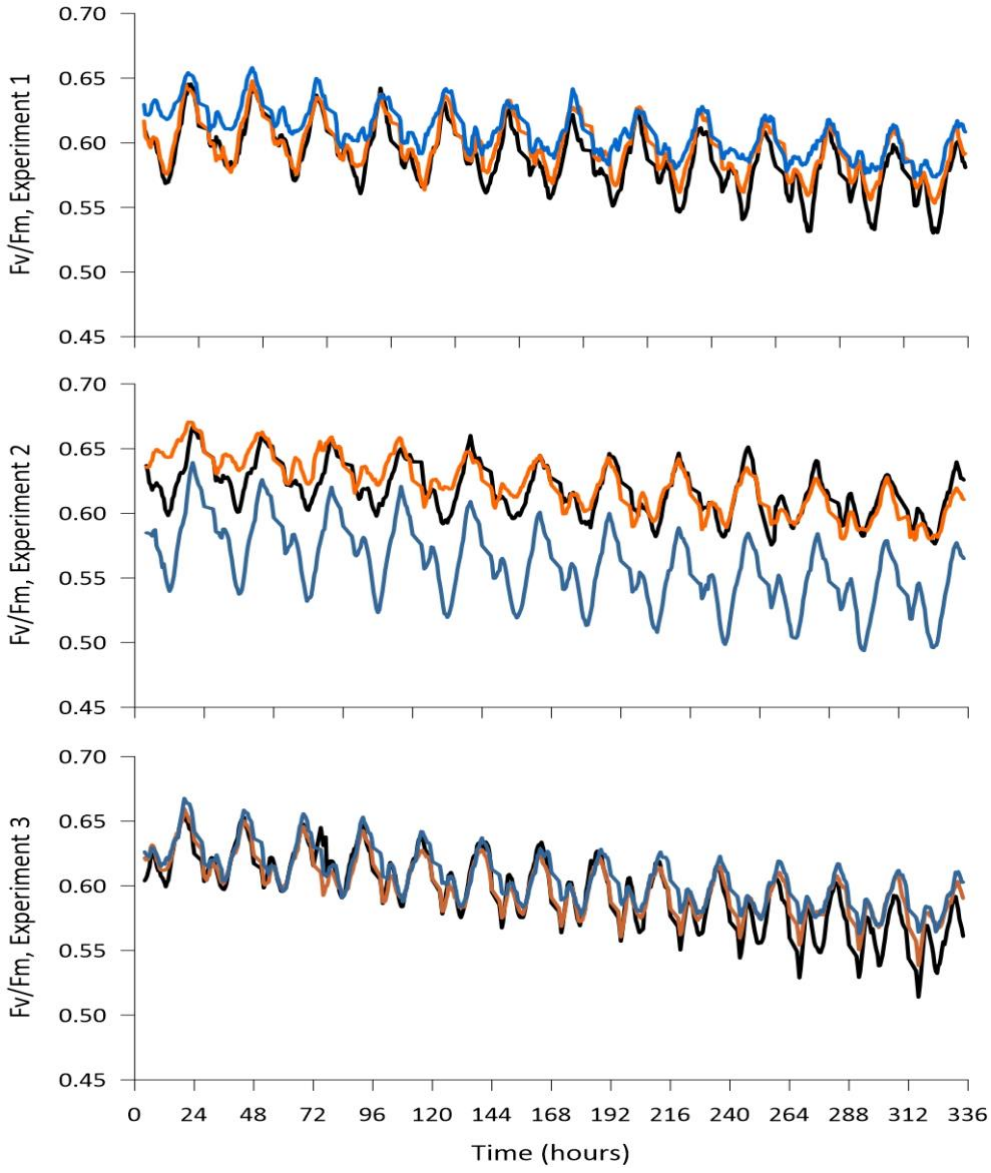

Figure 10. *Acropora millepora*. Diel variations in the photochemical efficiency (F_v/F_m for dark adapted hours, and $\Delta F/F_m$' for light adapted hours) derived from 30-minute interval saturation pulse analyses of nine coral fragments, one placed in each of three experimental units (blue, black, orange) for each of three consecutive experiments (a, b, c). Daily induction and recovery analyses caused gaps in time series from midnight to 0300 h.

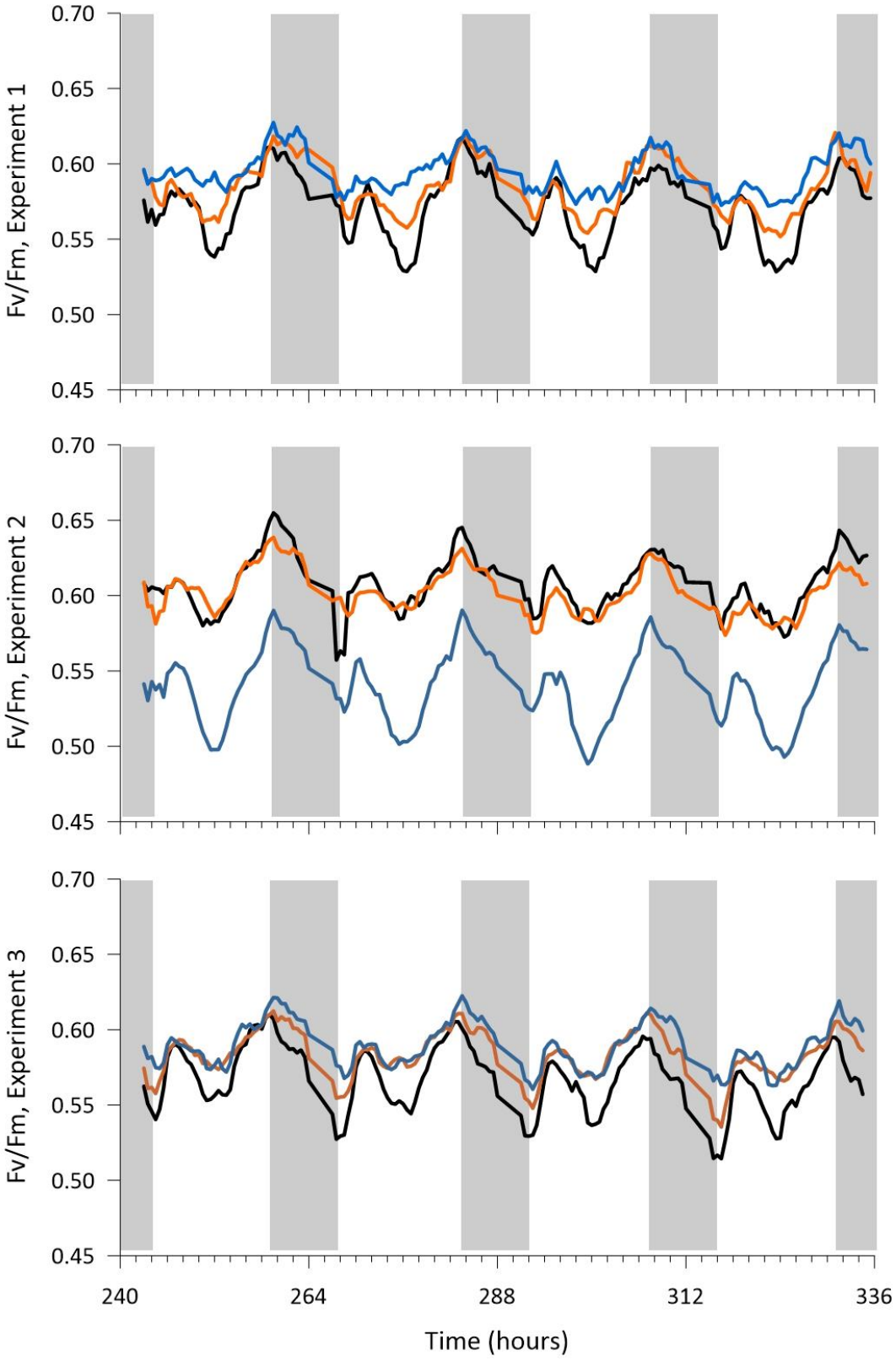

Figure 11: *Acropora millepora*. Last four days of diel variations in the photochemical efficiency (F_v/F_m for dark adapted hours, and $\Delta F/F_m$' for light adapted hours) derived from 30-minute interval saturation pulse analyses of nine coral fragments, one placed in each of three experimental units (blue, black, orange) for each of three consecutive experiments (a, b, c). Daily induction and recovery analyses caused gaps in time series from midnight to 0300 h.

Discussion

Influence of CO_2 enrichment on the photosynthetic properties

CO_2 enrichment did not influence the photochemical efficiency of *Acropora millepora* (Ehrenberg, 1834) (Fig. 3 a, b, Table 4). The maximum (F_v/F_m) and effective ($\Delta F/F_m$') photochemical efficiencies ranged between 0.631 and 0.636, and 0.564 and 0.580, respectively; similar values were reported by Kuanui et al.[218] and Hill and Takahashi[219]. This result agrees with studies of other coral species showing little to no effect under conditions of CO_2 enrichment[e.g.,103,220,203,221]. Godinot et al.[203], for example, observed no change in the F_v/F_m ratio and the electron transport rate (ETR) across three CO_2 treatments (378, 903, and 2039 µatm) in the coral *Stylophora pistillata* (Esper, 1792). Similarly, Takahashi and Kurihara[103] failed to show any change in the F_v/F_m ratio in the coral *Acropora digitifera* (Dana, 1846) maintained at seawater pCO_2 of 343, 744, and 2142 µatm for a five-week period. Across all three treatments, the F_v/F_m ratio remained around 0.70 indicating that no stress was exerted on these corals. Noonan and Fabricus[220], however, demonstrated an increase in the ratio F_v/F_m from 0.53 to 0.63 after 21 days exposure of the coral *Stylophora hystrix* (Dana, 1846) to a seawater pCO_2 of ~780 µatm, indicating that CO_2 enrichment enhanced the photochemical efficiency in this species. The coral *A. millepora* in the same study, however, did not respond to CO_2 enrichment[220].

In my study, the excitation pressure over the PSII (Q_m) remained between 0.088 and 0.107 across all treatments of CO_2 enrichment (Fig. 3c). Q_m values can range from 0 to 1; values close to zero indicate that few reaction centres are closed and that there is little to no damage of the reaction centres due to photoinhibition[188]. Considering that CO_2 enrichment did not affect the ratios F_v/F_m and $\Delta F/F_m$', we expected low Q_m values and this is consistent with previous studies showing either no change or a decrease in Q_m in response to CO_2 enrichment[222,223]. For example, Crawley et al.[223] observed a decrease in Q_m from 0.322 to 0.262 in the coral *Acropora formosa* (Dana, 1846) when exposed to a pCO_2 of ~600 µatm. At a pCO_2 of ~1160 µatm, Q_m increased, however, still remaining below that of the Control (0.301). Jiang et al.[222], on the other hand, demonstrated that in the coral *Pocillopora damicornis* (Linnaeus, 1758) CO_2 enrichment increased the ratio $\Delta F/F_m$' and decreased Q_m. The ratio F_v/F_m, however, was not affected by CO_2 enrichment pCO_2. As this change in Q_m is due to a change in the ratio $\Delta F/F_m$' and not the ratio F_v/F_m, chronic photoinhibition is unlikely to affect the coral symbiont long term.

The corals used in my experiment were low light acclimated in the aquarium shop for at least six months in a daily regime of 12 hours constant light (80 µmol quanta m^{-2} s^{-1}) followed by 12 hours darkness. In the research laboratory they were exposed to the sub-saturating diel light regime shown in Figure 5. This is a reduction from 80 µmol quanta m^{-2} s^{-1} to ~ 31–49 µmol quanta m^{-2} s^{-1}. DiPerna et al.[184] and Kuanui et al.[218] showed that *A. millepora* tolerates low-light conditions[184,218], therefore

the coral used in my experiment should not be affected by low-light levels given that they have adequate time to acclimate. A reduction in F_v/F_m and $\Delta F/F_m$' over time was observed (Fig. 3 a, b), which may have been a response to the change in the light regime. This is supported by Di Perna et al.[184] who demonstrated that *A. millepora* can take up to 20 days to acclimate to low light conditions, determined by the stabilisation of the F_v/F_m ratio. However, the reduction in F_v/F_m and $\Delta F/F_m$' over time (Fig. 3 a, b) could have been due to a measuring artifact as the PAM measures in one spot and there may have been internal changes such as symbiont movement occurring during the experiment resulting in a change on the absorbed PAR.

The relationship between rETR and PAR was linear in my experiment, which suggests that the coral did not reach light saturation during the day (Fig. 4). The F_v/F_m values did not reach a stable state during the acclimation period (data not shown), which would indicate full acclimation to the light conditions. Our results indicate no difference in rETR between CO_2 enriched and control tanks (Figs 4 and 5). The photosynthetic response of the coral to CO_2 enrichment, however, may depend on the intensity of the available PAR[e.g.,80]. Under sub-saturating light conditions CO_2 enrichment can enhance photosynthesis as it does under high irradiances, however the response is muted[80]. In CO_2 enriched water the corals *Acropora horrida* (Dana, 1846) and *Porites cylindrica* (Dana, 1846) increased their gross photosynthesis by 60 and 20%, respectively, under saturating light conditions. Photosynthesis only increased by 15 and 10%, however, under sub-saturating light conditions[15]. Low light treatments resulted in a small increase in F_v/F_m and were not affected by increased pCO_2 in the coral *Acropora cervicornis* (Lamarck, 1816)[224]. Electron transport rates were enhanced in the corals *S. hystrix* and *A. millepora* in sub-saturating light and CO_2 enrichment[220]. CO_2 enrichment has been shown to affect symbiont acclimation to low light, for example, an increase in photochemical efficiency observed by Noonan and Fabricus[220] in the coral *S. pistillata* was accompanied by an increase in symbiont pigment concentration at higher pCO_2. Symbiont concentration in the two corals *S. pistillata* and *Porites* sp. decreased with increasing pCO_2 (pH 8.09 to 7.49 and 7.19), while the concentration of chlorophyll per cell at pH 7.19 was significantly increased (31% increase *S. pistillata* and 23% in *Porites* sp.)[225]. In contrast to this, Vogel et al.[226] found no change in chlorophyll *a* content under increased pCO_2 or under low light resulting in an overall negative impact of low light on the photosynthetic efficiency[226]. The chlorophyll composition did not increase in response to CO_2 enrichment the corals *S. pistillata*[203], *Pocillopora acuta* (Lamarck, 1816)[227], *Seriatopora caliendrum* (Ehrenberg, 1834)[221].

The shape of the induction and recovery curves shown in Figure 6 resemble that observed in low-light adapted corals by others showing efficient use of the low light levels[181,228]. Once the actinic light was switched off the F_v values gradually recovered almost reaching pre-light exposure values at the start of the induction analysis (Fig. 6). The induction and recovery were accompanied by positive non-photochemical quenching values (NPQ), which increased steadily under conditions of actinic

light and then decreased slightly at the end of the induction period indicating the onset of the Calvin cycle. This response did not change after CO_2 enrichment. Vogel et al.[226] also did not observe an effect of CO_2 enrichment at low light on the photosynthesis of *A. millepora*. In Figure 6 we can see a slight decrease in the slope of the recovery curve with time indicating the presence of a mechanism lowering the rate of recovery after light exposure. There is no evidence to suggest that this is due to CO_2 enrichment, however, as it is also occurring in the control tanks (Table 5).

Diffusive boundary layer

I observed marked lower values in the ratios F_v/F_m and $\Delta F/F_m$', and a higher value of Q_m in one coral fragment compared to the other fragments (Fig. 3 b, e, h). This fragment had a different morphology and was sampled on a flat tissue surface, while all other fragments were sampled at the tip of a pointed branch typical to the morphology of this species. The ratios F_v/F_m and the $\Delta F/F_m$' of this individual coral fragment were lower than those of all other fragments. Q_m values, on the other hand, were higher than those of all other fragments. These differences could be due to the higher concentration of zooxanthellae near the surface of the coral, or perhaps due to differences in the exposure of the coral surface to seawater flow altering the thickness of the diffusive boundary layer. As the flat part of this coral fragment was near the base of the fragment, it may have been less exposed to turbulent flow than the pointy tips of the coral branches but in the absence of flow measurements, this remains speculative. Reduced water flow can negatively affect photosynthesis as demonstrated by Dennison and Barnes[229] who showed that photosynthesis in the coral *A. formosa* was ~25% less in still water than in moving water. The diffusive boundary layer separates the coral tissue from the surrounding seawater and controls the exchange of solutes such as oxygen between the coral tissues and the surrounding seawater[230]. Under low flow velocities, the diffusive boundary layer becomes thicker, which limits solute exchange leading, under conditions of light, to a decrease in tissue $[H^+]$, and an increase in tissue $[O_2]$. This can affect the rate of photosynthesis, calcification, and respiration and how a coral responds to CO_2 enrichment[231,232,233]. During periods of light, tissue $[O_2]$ and $[H^+]$ increases and decreases, respectively, because of the production of O_2 and removal of inorganic carbon by photosynthesis. As the distance for the diffusion of both solutes across the diffusive boundary layer increases, the rate of exchange decreases, and hence O_2 accumulates in the tissue and the supply of H^+ from the surrounding seawater decreases[231]. In the dark the presence of a thicker diffusive boundary layer will slow down the rate of O_2 diffusion across the diffusive boundary layer resulting in a reduced $[O_2]$ and a higher $[H^+]$ within the tissues[231].

In our flat coral fragment the low photosynthetic rates may have occurred due to a thicker diffusive boundary layer with lowered flow causing a reduction in the solute exchange. Likewise, the response of the flatter coral fragment in our study may have been caused by a reduction in chlorophyll content per zooxanthellae or perhaps by the acclimation period of this fragment due to its different morphology. This was shown in the coral *A. digitifera* whereby a decrease in water flow resulted in a

decrease in F_v/F_m and a significant decrease in chlorophyll content per zooxanthellae[234]. A decrease in F_v/F_m with reduced water flow was also observed in the corals *P. damicornis*, *S. pistillata*, and again in *A. digitifera* in a study by Nakamura and Yamasaki[235]. However, they found variable magnitudes of responses among species including no significant response to flow in the corals *Pavona decussata* (Dana, 1846) and *Isopora palifera* (Lamarck, 1816). The authors suggest that this response may be due to the acclimation ability of each species to the water flow conditions. These studies and our own highlight the need to take the diffusive boundary layer thickness and water velocity into account when measuring photosynthesis or calcification.

Analysis of the F_v/F_m, $\Delta F/F_m$', and Q_m without the data collected from the flat coral fragment was done to ensure this outlier did not mask any potential effect of CO_2 enrichment in the analysis. Removing the flat coral fragment from our analysis does not change the outcome of the statistical analysis, supporting the conclusion that CO_2 enrichment had no effect on the photochemical efficiency of *A. millepora* (Appendix 5).

Regulated and non-regulated non-photochemical quenching, NPQ & Y(NO)

I observed that the ratio $\Delta F/F_m$' decreased from ~0.65 to 0.55 as PAR increased from ~20 to 60 µmol photons m^{-2} s^{-1} (Fig. 7). This indicates that the coral is far from saturation. When all reaction centres are closed, no transfer of electrons can occur, and the coral is considered saturated with light[236]. In Figure 4 rETR is increasing with PAR, if the coral was saturated the rETR would no longer increase with increasing PAR. Likewise, with increasing PAR, NPQ should increase and the ratio $\Delta F/F_m$' should decrease[163]. While the PAR increases, the ratio $\Delta F/F_m$' does decrease (Fig. 7), however the NPQ does not appear to increase (Fig. 8) indicating the corals capacity to efficiently move this level of electrons through photochemical pathways. If the $\Delta F/F_m$' slope in Figure 7 were to steepen it would indicate that the reaction centres are closing at a rapid pace, in which case the NPQ should increase. At high irradiances an increase in NPQ indicates that the organism has the capacity to protect itself from potentially damaging energy levels through safe dissipation of that energy as heat or fluorescence[176].

The yield of non-regulated non photochemical quenching (Y(NO)) levels in our experiment remain around 0.4 and 0.5 at all irradiances (Fig. 9). The higher Y(NO) values are caused by the decreasing F_m and increasing F during the night. This is also shown in the declining F_v/F_m ratio. These results are consistent with the results presented by Hoogenboom et al.[193] in which corals adapted to low light exhibited lower levels of NPQ, and higher levels of Y(NO) when exposed to high irradiances. If NPQ does not increase, then Y(NO) increases indicating that the organism does not have the capacity to protect itself leading to photodamage[176]. In plants a typical Y(NO) remains around 0.2[176]; in corals, Y(NO) has not been extensively reported on, however, as with the F_v/F_m ratio being slightly lower than in plants we could expect the Y(NO) in corals to be slightly higher. Similar to our results,

Schrameyer et al.[237] reported that Y(NO) levels of their corals at the start of the experiment ranged between 0.21 and 0.43, and in Hoogenboom et al.[193], the Y(NO) ranged between 0.4 and 0.6 in low light and between 0.5 and 0.6 in high light.

Chlororespiration

The analysis of the saturation pulse time-series revealed that the F_v/F_m ratio was highest just before the onset of darkness, around 1900 h while the coral remained under very low light (~20–0 μmol photons m^{-2} s^{-1}) (Figs 10 and 11). Once the light was off, we would expect this ratio to increase, however, we noticed a decrease in this ratio during the following 10 hours of darkness including the first hours of low light (0500 h, ~20 μmol photons m^{-2} s^{-1}). The induction and recovery analysis, performed at 0200 h, also showed that the maximum dark adapted fluorescence (F_m) was not as high as the F_m measured at 1900 h, the start of the dark period. NPQ is calculated using the maximum fluorescence during the dark adapted state (F_m), divided by the maximum fluorescence in the light adapted state (F_m')[215]. This calculation works under the assumption that the F_m does not change over time. The overnight decrease in F_m, however, led to the calculation of negative NPQ values as the daytime F_m' became higher than the dark-adapted F_m as the night progressed. Therefore, the NPQ values need to be corrected[15] (see Methods).

The main part of NPQ is the energy dependent quenching, which is activated by a $[H^+]$ gradient across the thylakoid membrane ($\Delta[H^+]$)[130,131]. Carotenoids, such as diadinoxanthin and diatoxanthin, aid in the protection of corals during periods of intense light, and act as light harvesting pigments during periods of low light[134]. Diadinoxanthin will go through a $[H^+]$ dependent reaction known as de-epoxidation forming diatoxanthin[141]. De-epoxidation is often shown in the fluorescence output as a decrease in F_m'[e.g.,156,130,158]. Diel xanthophyll cycling is observed with the greatest abundance of diatoxanthin between mid-morning and mid-afternoon, accompanied with a reduced $\Delta F/F_m'$[162]. Jakob et al.[238] and Jakob et al.[168] found that diatoxanthin in diatoms can form under darkness which increases NPQ and decreases the F_m value below the value of F_m'. Because the xanthophyll cycle is controlled by the trans-thylakoid $\Delta[H^+]$[129], there must be mechanisms in the dark that develops this gradient.

One way that a $[H^+]$ gradient can be formed in the dark is by the movement of electrons through an alternative respiratory pathway known as chlororespiration. Chlororespiration is defined as an alternative electron transport chain, often referred to as the respiratory transport chain, and involves the cyclic electron transport around PSI promoting ATP production[239]. Chlororespiration requires oxygen and darkness or very low light[240]. However, Shashar et al.[84] and Kühl et al.[231] have shown that coral tissue can become hypoxic within minutes of darkness, reducing the likelihood of chlororespiration. Because of this chlororespiration in corals has been questioned[e.g.,241,242]. Jakob et al.[238] and Jakob et al.[168] have shown that the diatoxanthin cycle can be induced by even a small

chlororespiratory proton gradient in the dark. Chlororespiration may therefore be able to produce a proton gradient large enough to induce diatoxanthin formation before the coral tissue becomes hypoxic. Branching corals which typically have thinner diffusive boundary layers may be able to take up oxygen at a higher rate from the surrounding seawater slowing down the onset of hypoxic conditions in the dark[242].

In Figure 11 we can see an increase in the ratio F_v/F_m between 1830 and 1900 h every evening due to the onset of dark adaptation, increasing the F_m, with a light level between ~20–0 µmol photons m^{-2} s^{-1}. When the limited oxygen in the dark has been used up with chlororespiration the electron sink is no longer available and a buildup of electrons within the electron transport chain occurs, causing a reduction of the plastoquinones in the dark rather than the expected oxidation[241]. The light levels that the coral received within the 30 minutes before 1900 h were low enough to induce the reduction of plastoquinone through chlororespiration causing the transition from State 1 to State 2. This transition is indicated by the sharp increase in fluorescence shown in Figure 11, due to the overexcitation of PSII followed by a gradual decrease as PSI quenches the fluorescence[189]. These changes in fluorescence are caused by a reduction in the absorption cross section available for PSII (ability of light harvesting by PSII), which occurs when light harvesting complexes (LHCs) are connected to PSI while in State 2[162]. This state transition is associated with an uncharacteristic increase in NPQ during dark periods.

The increase in F_v/F_m between 1830 and 1900 h is followed by a gradual decrease in F_v/F_m until dawn at which point the ratio F_v/F_m increases sharply, presumably due to the oxidation of PSI and the transition back to State 1 (Fig. 11). Hoegh-Guldberg and Jones[166] found similar findings to our results in the coral *P. cylindrica* an increase in the dark adapted F_v/F_m ratio after dawn with the light level under 100 µmol photons m^{-2} s^{-1}. They gave no explanation for this, however in a later paper by Jones and Hoegh-Guldberg[241], they found that in the corals *Montipora digitata* (Dana, 1846) and *S. pistillata* the F_v/F_m ratio initially rose under darkness and then began to decrease after four hours of complete darkness. Once low light was introduced this F_v/F_m ratio sharply increased. This slow reduction in F_v/F_m followed by a dawn increase was also observed by Hill and Ralph[242] in multiple scleractinian corals including *Acropora nobilis* (Dana, 1846).

The overnight decrease in F_v/F_m in my study is interrupted by the induction and recovery analyses between 0200 and 0230 h (Fig. 6). In the induction analysis the second saturation pulse results in a higher F_m value than the initial saturation pulse. This could indicate the occurrence of plastoquinones in the reduced state, State 2, before the onset of actinic light for the induction analysis[241]. The subsequent decrease in F_m values under conditions of actinic light then indicates that the coral transitioned back to State 1 caused by increased pressure around PSII[241].

Conclusion

My aim was to identify the effects of CO_2 enrichment on the photochemical efficiency of the symbionts of the coral *A. millepora*. Using a combination of chlorophyll fluorescence measurements and statistical analysis, I have failed to demonstrate an effect of CO_2 enrichment on *A. millepora* at an ambient temperature of ~25 ℃ adding to the existing evidence that CO_2 enrichment does not influence the ratios F_v/F_m, $\Delta F/F_m$', and Q_m. My results indicate that the ratios F_v/F_m and $\Delta F/F_m$' were declining over time due to possible continued symbiont acclimation to the experimental light regime or symbiont movement, and not due to CO_2 enrichment. The linear relationship between rETR and PAR and the low Q_m values indicate that the coral was adapted to low-light conditions. The transition of the coral from 80 µmol m^{-2} s^{-1} constant over 12 hours (aquarium shop) to a more realistic diel light cycle (research laboratory) overall exposed the coral to less light (from 80 to ~ 31 – 49 µmol m^{-2} s^{-1}) and may indicate a stress exerted on the coral resulting in a gradual decrease of F_v/F_m and $\Delta F/F_m$'. Acclimating our coral for a longer period to these laboratory light conditions may have stabilised these values. Our analysis support previously published results that without the inclusion of heat as a stressor pCO_2 enrichment may not influence the photochemical efficiency[e.g.,103,220,203,221].

The overnight decrease in F_v/F_m and sharp increase at the onset of low irradiance at the start of the day. indicate an alternative respiratory pathway, chlororespiration, and the induction of a NPQ pathway, state transitioning. The induction analysis supports this with evidence of state transitioning. Chlororespiration has implications for the accurate interpretation of chlorophyll fluorescence. Chlororespiration and state transitioning were not induced due to CO_2 enrichment as the trends discussed also occurred in the control tanks. Additional analysis of the chlorophyll pigment concentrations and symbiont genotypes would give more information on the acclimation to the light conditions. Future studies using a greater irradiance and the inclusion of heat as a stressor would give additional insight into how this species will respond to future environmental conditions.

References

1. Hoegh-Guldberg O, Mumby PJ, Hooten AJ, Steneck RS, Greenfield P, Gomez E, Harvell CD, Sale PF, Edwards AJ, Caldeira K, Knowlton N (2007) Coral reefs under rapid climate change and ocean acidification. Science 318(5857):1737-1742.
2. Sale PF (1977) Maintenance of high diversity in coral reef fish communities. The American Naturalist 111(978):337-359.
3. Komyakova V, Munday PL, Jones GP (2013) Relative importance of coral cover, habitat complexity and diversity in determining the structure of reef fish communities. PLoS One 8(12):e83178.
4. Chave KE, Smith SV, Roy KJ (1972) Carbonate production by coral reefs. Marine Geology 12(2):123-140.
5. Hoegh-Guldberg O (1999) Climate change, coral bleaching and the future of the world's coral reefs. Marine and Freshwater Research 50(8):839-866.
6. Muscatine L (1990) The role of symbiotic algae in carbon and energy flux in reef corals. Coral Reefs 25(1.29):75-87.
7. Muscatine L, Falkowski PG, Porter JW, Dubinsky Z (1984) Fate of photosynthetic fixed carbon in light and shade adapted colonies of the symbiotic coral *Stylophora pistillata*. Proceedings of the Royal Society of London. Series B. Biological Sciences 222(1227):181-202.
8. Van Oppen MJ, Medina M (2020) Coral evolutionary responses symbioses. Philosophical Transactions of the Royal Society B 375(1808):20190591.
9. Ralph PJ, Gademann R, Larkum AW (2001) Zooxanthellae expelled from bleached corals at 38℃ are photosynthetically competent. Marine Ecology Progress Series 220:163-168.
10. Stimson J, Sakai K, Sembali H (2002) Interspecific comparison of the symbiotic relationship in corals with high and low rates of bleaching-induced mortality. Coral Reefs 21(4):409-421.
11. Ansell AD, Gibson RN, Barnes M, Press UC (1998) Coral/seaweed competition and the control of reef community structure within and between latitudes. Oceanography and Marine Biology 36:65-96.
12. Lapointe BE (1999) Simultaneous top-down and bottom-up forces control macroalgal blooms on corals reefs (Reply to the comment by Hughes et al.). Limnology and Oceanography 44(6):1586-1592.
13. Sabine CL, Feely RA, Gruber N, Key RM, Lee K, Bullister JL, Wanninkhof R, Wong CS, Wallace DW, Tilbrook B, Millero FJ (2004) The oceanic sink for anthropogenic CO_2. Science 305(5682):367-371.
14. IPCC (2014) Climate Change 2014: Synthesis Report. Contribution of Working Groups I, II and III to the Fifth Assessment Report of the Intergovernmental Panel on Climate. IPCC, Geneva, Switzerland.
15. Doney SC, Fabry VJ, Feely RA, Kleypas JA (2009) Ocean Acidification: The Other CO_2 Problem. ASLO Web Lectures 3(1):1-59.
16. Morse JW, Arvidson RS (2002) The dissolution kinetics of major sedimentary carbonate minerals. Earth-Science Reviews 58(1-2):51-84.
17. Kitano Y, Kanamori N, Tokuyama A (1969) Effects of organic matter on solubilities and crystal form of carbonates. American Zoologist 9(3):681-688.
18. Falini G, Albeck S, Weiner S, Addadi L (1996) Control of aragonite or calcite polymorphism by mollusk shell macromolecules. Science 271(5245):67-69.

19. Berner RA (1975) The role of magnesium in the crystal growth of calcite and aragonite from seawater. Geochimica et Cosmochimica Acta 39(4):489-504.

20. Jiang LQ, Feeley RA, Carter BR, Greeley DJ, Gledhill DK, Arzayus KM (2015) Climatological distribution of aragonite saturation state in the global oceans. Global Biogeochemical Cycles 29(10): 1656-1673.

21. Barker S, Higgins JA, Elderfield H (2003) The future of the carbon cycle: review, calcification response, ballast, and feedback on atmospheric CO_2. Philosophical Transactions of the Royal Society of London. Series A: Mathematical, Physical and Engineering Sciences 361(1810):1977-1999.

22. Zhang H, Cao L (2018) Simulated effects of interactions between ocean acidification, marine organism calcification, and organic carbon export on ocean carbon and oxygen cycles. Science China Earth Sciences 61(6): 804-822.

23. Sarma VV, Ono T, Saino T (2002) Increase of total alkalinity due to shoaling of aragonite saturation horizon in the Pacific and Indian Oceans: Influence of anthropogenic carbon inputs. Geophysical Research Letters 29(20):32-1.

24. Ben-Yaakov S, Ruth E, Kaplan IR (1974) Carbonate compensation depth: relation to carbonate solubility in ocean waters. Science 184(4149):982-984.

25. Li YH, Yakahashi T, Broecker WS (1969) Degree of saturation of $CaCO_3$ in the oceans. Journal of Geophysical Research 74(23):5507-5525.

26. Feely RA, Sabine CL, Hernandez-Ayon JM, Ianson D, Hales B (2008) Evidence for upwelling of corrosive "acidified" water onto the continental shelf. Science 320(5882):1490-1492.

27. Cooper TF, De'Ath G, Fabricius KE, Lough JM (2008) Declining coral calcification in massive Porites in two nearshore regions of the northern Great Barrier Reef. Global Change Biology 14(3):529-538.

28. Marubini F, Atkinson MJ (1999) Effects if lowered pH and elevated nitrate on coral calcification. Marine Ecology Progress Series 188:117-121.

29. Kleypas JA, McManus JW, Menez LA (1999) Environmental limits to coral reef development: where do we draw the line? American Zoologist 39(1):146-159.

30. Silverman J, Lazar B, Erez J (2007) Effect of aragonite saturation, temperature, and nutrients on the community calcification rate if a coral reef. Journal of Geophysical Research: Oceans 112(C5).

31. Zheng MD, Cao L (2014) Simulation of global ocean acidification and chemical habitats of shallow-and cold-water coral reefs. Advances in Climate Change Research 5(4):189-196.

32. Kleypas JA, Buddemeier RW, Archer D, Gattuso JP, Langdon C, Opdyke BN (1999) Geochemical consequences of increased atmospheric carbon dioxide on coral reefs. Science 284(5411):118-120.

33. Andersson AJ, Kuffiner IB, Mackenzie FT, Jokiel PL, Rodgers KS, Tan A (2009) Net loss of $CaCO_3$ from a subtropical calcifying community due to seawater acidification: mecocosm-scale experimental evidence. Biogeosciences 6(8):1811-1823.

34. Crook ED, Cohen AL, Rebolledo-Vieyra M, Hernandez L, Paytan A (2013) Reduced calcification and lack of acclimatization by coral colonies growing in areas of persistent natural acidification. Proceedings of the National Academy of Science 110(27):11044-11049.

35. Shamberger KEF, Feely RA, Sabine CL, Atkinson MJ, DeCarlo EH, Mackenzie FT, Drupp PS, Butterfield DA (2011) Calcification and organic production on a Hawaiian coral reef. Marine Chemistry 127(1-4):64-75.

36. McMahon A, Santos IR, Cyronak T, Eyre BD (2013) Hysteresis between coral reef calcification and the seawater aragonite saturation state. Geophysical Research Letters 40(17):4675-4679.

37. Form AU, Riebesell U (2012) Acclimation to ocean acidification during long-term CO_2 exposure in the cold-water coral *Lophelia pertusa*. Climate Change Biology 18(3):843-853.

38. Dandan SS, Falter JL, Lowe RJ, McCulloch MT (2015) Resilience of coral calcification to extreme temperature variations in the Kimberley region, northwest Australia. Coral Reefs 34(4):1151-1163.

39. Howells EJ, Beltran VH, Larsen NW, Bay LK, Willis BL, Van Oppen MJH (2012) Coral thermal tolerance shaped by local adaptation of photosymbionts. Nature Climate Change 2(2):116-120.

40. Waldbusser GC, Hales B, Langdon CJ, Haley BA, Schrader P, Brunner EL, Gray MW, Miller CA, Gimenez I (2015) Saturation-state sensitivity of marine bivalve larvae to ocean acidification. Nature Climate Change 5(3):273-280.

41. Gagnon AC, Adkins JF, Erez J (2012) Seawater transport during coral biomineralization. Earth and Planetary Science Letters 329:150-161.

42. Tabutté E, Tambutté S, Segnonds N, Zoccola D, Venn A, Erez J, Allemand D (2012) Calcein labelling and electrophysiology: insights on coral tissue permeability and calcification. Proceedings of the Royal Society B: Biological Sciences 279(1726):19-27.

43. Tambutté E, Allemand D, Mueller ER, Jaubert JE (1996) A compartmental approach to the mechanism of calcification in hermatypic corals. The Journal of Experimental Biology 199(5):1029-1041.

44. Zoccola D, Tambutté E, Sénégas-Balas F, Michiels JF, Faila JP, Jaubert J, Allemand D (1999) Cloning of a calcium channel α1 subunit from the reef-building coral, *Stylophora pistillata*. Gene 227(2):157-167.

45. Bertucci A, Tambutté E, Tambutté S, Allemand D, Zoccola D (2010) Symbiosis-dependent gene expression in coral-dinoflagellate association: cloning and characterization of a P-type H^+-ATPase gene. Proceedings of the Royal Society B: Biological Sciences 277(1678):87-95.

46. Furla P, Galgani I, Durand I, Allemand D (2000) Sources and mechanisms of inorganic carbon transport for coral calcification and photosynthesis. Journal of Experimental Biology 203(22): 3445-3457.

47. Comeau S, Carpenter RC, Edmunds PJ (2013) Coral reef calcifiers buffer their response to ocean acidification using both bicarbonate and carbonate. Proceedings of the Royal Society B: Biological Sciences 280(1753):20122374.

48. McCulloch M, Falter J, Trotter J, Montagna P (2012) Coral resilience to ocean acidification and global warming through pH-upregulation. Nature Climate Change 2(8):623-627.

49. Venn A, Tabutté E, Holcomb M, Allemand D, Tabutté S (2011) Live tissue imaging shows reef corals elevate pH under their calcifying tissue relative to seawater. PloS One 6(5):e20013.

50. Ries JB, Cohen AL, McCorkle DC (2010) A nonlinear calcification response to CO_2-induced ocean acidification by the coral *Oculina arbuscula*. Coral Reefs 29(3):661-674.

51. Ross CL, Falter JL, McCulloch MT (2017) Active modulation of the calcifying fluid carbonate chemistry (δ 11 B, B/Ca) and seasonally invariant coral calcification at sub-tropical limits. Scientific Reports 7(1):1-11.

52. Georgiou L, Falter J, Trotter J, Kline DI, Holcomb M, Dove SG, Hoegh-Guldberg O, McCulloch M (2015) pH homeostasis during coral calcification in a free ocean CO_2

enrichment (FOCE) experiment, Heron Island reef flat, Great Barrier Reef. Proceedings of the National Academy of Sciences 112(43):13219-13224.

53. Holcomb M, Venn AA, Tambutté E, Tambutté S, Allemand D, Trotter J, McCulloch M (2014) Coral calcification fluid pH dictates response to ocean acidification. Scientific Reports 4(1):1-4.

54. McCulloch MT, D'Olivo JP, Falter J, Holcomb M, Trotter JA (2017) Coral calcification in a changing world and the interactive dynamics of pH and DIC upregulation. Nature Communication 8(1):1-8.

55. Hemming NG, Guilderson TP, Fairbanks RG (1998) Seasonal variations in the boron isotopic composition of coral: A productivity signal? Global Biogeochemical Cycles 12(4):581-586.

56. Reynaud S, Hemminng NG, Juillet-Leclerc A, Gattuso JP (2004) Effect of pCO_2 and temperature on the boron isotopic composition of the zooxanthellae coral *Acropora* sp. Coral Reefs 23(4):539-546.

57. Wall M, Fietzke J, Schmidt GM, Fink A, Hofmann LC, De Beer D, Fabricus KE (2016) Internal pH regulation facilities in situ long-term acclimation of massive corals to end-of-century carbon dioxide conditions. Scientific reports 6(1):1-7.

58. Allison N, Finch AA (2010) δ11B, Sr, Mg and B in a modern Portites coral: the relationship between calcification site pH and skeletal chemistry. Geochimica et Cosmochimica Acta 74(6):1790-1800.

59. Venn AA, Tambutté E, Holcomb M, Laurent J, Allemand D, Tambutté S (2013) Impact of seawater acidification on pH at the tissue-skeleton interface and calcification in reef corals. Proceedings of the National Academy of Sciences 110(5):1634-1639.

60. Huang H, Yuan XC, Cai WJ, Zhang CL, Li X, Liu S (2014) Positive and negative responses of coral calcification to elevated pCO_2: case studies of two coral species and the implications of their responses. Marine Ecology Progress Series 502:145-146.

61. Jury CP, Whitehead RF, Szmant AM (2010) Effects of variations in carbonate chemistry on calcification rates of *Madracis auretenra* (=*Madracis mirabilis* sensu Wells, 1973): bicarbonate concentrations best predict calcification rates. Global Change Biology 16(5):1632-1644.

62. Marubini F, Thake B (1999) Bicarbonate addition promotes coral growth. Limnology and Oceanography 44(3):716-20.

63. Schneider K, Erez J (2006) The effect of carbonate chemistry on calcification and photosynthesis in the hermatypic coral *Acropora eurystoma*. Limnology and Oceanography 51(3):1284-1293.

64. Marubini F, Ferrier-Pages C, Furla P, Allemand D (2008) Coral calcification responds to seawater acidification: a working hypothesis towards physiological mechanism. Coral Reefs 27(3):491-499.

65. Herfort L, Thake B, Taubner I (2008) Bicarbonate stimulation of calcification and photosynthesis in two hermatypic corals. Journal of Phycology 44(1):91-98.

66. de Putron SJ, McCorkle DC, Cohen AL, Dillon AB (2011) The impact of seawater saturation state and bicarbonate ion concentration on calcification by new recruits of two Atlantic corals. Coral Reefs 30(2):321-328.

67. Jokiel PL (2013) Coral reef calcification: carbonate, bicarbonate and proton flux under conditions of increasing ocean acidification. Proceedings of the Royal Society B: Biological Sciences 280(1764):20130031

68. Jokiel PL (2011a) Ocean acidification and the control of reef coral calcification by boundary layer limitation of proton flux. Bulletin of Marine Science 87(3):639-657.

69. Comeau S, Cornwall CE, DeCarlo TM, Krieger E, McCulloch MT (2018) Similar controls on calcification under ocean acidification across unrelated coral reef taxa. Global Change Biology 24(10):4857-4868.

70. Enns T (1967) Facilitation by carbonic anhydrase of carbon dioxide transport. Science 155(3758):44-47.

71. Moya A, Tambutté S, Bertucci A, Tambutté E, Lotto S, Vullo D, Supuran CT, Allemand D, Zoccola D (2008) Carbonic anhydrase in the scleractinian coral *Stylophora pistillata*: characterization, localization, and role in biomineralisation. Journal of Biological Chemistry 283(37):25475-25484.

72. Bertucci A, Tambutté S, Supuran CT, Allemand D, Zoccola D (2011) A new coral carbonic anhydrase in *Stylophora pistillata*. Marine Biotechnology 13(5):992-1002.

73. Al-Horani FA, Al-Moghrabi SM, De Beer D (2003) The mechanism of calcification and its relation to photosynthesis and respiration in the scleractinian coral *Galaxea fascicularis*. Marine Biology 142(3):419-426.

74. Goreau TF (1959) The physiology of skeleton formation in corals. I. A method for measuring the rate of calcium deposition by corals under different conditions. The Biological Bulletin 116(1):59-75.

75. Jokiel PL (2011b) The reef coral two compartment proton flux model: A new approach relating tissue-level physiological processes to gross corrallum morphology. Journal of Experimental Marine Biology and Ecology 409(1-2):1-12.

76. Rinkevich B, Loya Y (1984) Does light enhance calcification in hermatypic corals? Marine Biology 80(1):1-6.

77. Mass T, Genin A, Shavit U, Grinstein M, Tchernov D (2010) Flow enhances photosynthesis in marine benthic autotrophs by increasing the efflux of oxygen from the organism to the water. Proceedings of the National Academy of Sciences 107(6):2527-2531.

78. Colombo-Pallotta MF, Rodríguez-Román A, Iglesias-Prieto R (2010) Calcification in bleached and unbleached *Montastraea faveolata*: evaluating the role of oxygen and glycerol. Coral Reefs 29(4):899-907.

79. Galli G, Solidoro C (2018) ATP supply may contribute to light-enhanced calcification in corals more than abiotic mechanisms. Frontiers in Marine Science 5:68.

80. Suggett DJ, Dong LF, Lawson T, Lawrenz E, Torres L, Smith DJ (2013) Light availability determines susceptibility of reef building corals to ocean acidification. Coral reefs 32(2):327-337.

81. Zoccola D, Ganot P, Bertucci A, Caminit-Segonds N, Techer N, Voolstra CR, Aranda M, Tambutté E, Allemand D, Casey JR, Tambutté S. (2015) Bicarbonate transporters in corals point towards a key step in the evolution of cnidarian calcification. Scientific Reports 5(1):1-1.

82. Erez J (1978) Vital effect on stable-isotope composition seen in foraminifera and coral skeletons. Nature 273(5659):199-202.

83. Fang LS, Chen YW, Chen CS (1989) Why does the white tip of stony coral grow so fast without zooxanthellae? Marine Biology 103(3):359-363.

84. Shashar N, Cohen Y, Loya Y (1993) Extreme diel fluctuations of oxygen in diffusive boundary layers surrounding stony corals. The Biological Bulletin 185(3):455-461.

85. Venti A, Andersson A, Langdon C (2014) Multiple driving factors explain spatial and temporal variability in coral calcification rates on the Bermuda platform. Coral Reefs 33(4):979-997.

86. Langdon C, Atkinson MJ (2005) Effect of elevated pCO_2 on photosynthesis and calcification of corals and interaction with seasonal change in temperature/irradiance and nutrient enrichment. Journal of Geophysical Research: Oceans 110(C9).

87. Kaniewska P, Campbell PR, Kline DI, Rodriguez-Lanetty M, Miller DJ, Dove S, Hoegh-Guldberg O (2012) Major cellular and physiological impacts of ocean acidification on a reef building coral. PloS one 7(4):e34659.

88. Towle EK, Carlton R, Langdon C, Manzello DP (2015a) In-situ measurement of metabolic status in three coral species from the Florida Reef Tract. Regional Studies in Marine Science 2:145-153.

89. Grottoli AG, Rodrigues LJ, Palardy JE (2006) Heterotrophic plasticity and resilience in bleached corals. Nature 440(7088):1186-1189.

90. Rodrigues LJ, Grottoli AG (2007) Energy reserves and metabolism as indicators of coral recovery from bleaching. Limnology and Oceanography 52(5):1874-1882.

91. Towle EK, Enochs IC, Langdon C (2015b) Threatened Caribbean Coral is able to mitigate to adverse effects of ocean acidification on calcification by increasing feeding rate. PLoS One 10(9):e0139398.

92. Teece MA, Estes B, Gelsleichter E, Lirman D (2011) Heterotrophic and autotrophic assimilation of fatty acids by two scleractinian corals, *Montastrea faveolata* and *Porites astreoides*. Limnology and Oceanography 56(4):1285-1296.

93. Rocker MM, Noonan S, Humphrey C, Moya A, Willis BL, Bay LK (2015) Expression of calcification and metabolism-related genes in response to elevated pCO_2 and temperature in the reef-building coral *Acropora millepora*. Marine Genomics 24:313-318

94. Moya A, Huisman L, Ball EE, Hayward DC, Grasso LC, Chua CM, Woo HN, Gattuso JP, Foret S, Miller DJ (2012) Whole transcriptome analysis of the coral *Acropora millepora* reveals complex responses to CO_2-driven acidification during the initiation of calcification. Molecular Ecology 21(10):2440-2454.

95. Ogawa D, Bobeszko T, Ainsworth T, Leggat W (2013) The combined effects of temperatures and CO_2 lead to altered gene expression in *Acropora aspera*. Coral Reefs 32(4):895-907.

96. Carreiro-Silva M, Cerqueira T, Godinho A, Caetano M, Santos RS, Bettencourt R (2014) Molecular mechanisms underlying the physiological responses of the cold-water coral *Desmophyllum dianthus* to ocean acidification. Coral Reefs 33(2):465-476.

97. Rowan R, Whitney SM, Fowler A, Yellowlees D (1996) Rubisco in marine symbiotic dinoflagellates: form II enzymes in eukaryotic oxygenic phototrophs encoded by a nuclear multigene family. The Plant Cell 8(3):539-553.

98. Tabita FR (1988) Molecular and cellular regulation of autotrophic carbon dioxide fixation in microorganisms. Microbiological Reviews 52(2):155-189.

99. Timm S, Florian A, Fernie AR, Bauwe H (2016) The regulatory interplay between photorespiration and photosynthesis. Journal of Experimental Botany 67(10):2923-2929

100. Comeau S, Edmunds PJ, Spindel NB, Carpenter RC (2014) Diel pCO_2 oscillations modulate the response of the coral *Acropora hyacinthus* to ocean acidification. Marine Ecology Progress Series 501:99-111.

101. Leggat W, Badger MR, Yellowlees D (1999) Evidence for an inorganic carbon-concentrating mechanism in the symbiotic dinoflagellate Symbiodinium sp. Plant Physiology 121(4):1247-1255.

102. Leggat W, Marendy EM, Baillie B, Whitney SM, Ludwig M, Badger MR, Yellowlees D (2002) Dinoflagellate symbiosis: strategies and adaptations for the acquisition and fixation of inorganic carbon. Functional Plant Biology 29(3):309-322.

103. Takahashi A, Kurihara H (2013) Ocean acidification does not affect the physiology of the tropical *Acropora digitifera* during a 5-week experiment. Coral Reefs 32(1):305-314.

104. Rodolfo-Metalpa R, Martin S, Ferrier-Pagès C, Gattuso JP (2010) Response of the temperate coral *Cladocora caespitosa* to mid- and long-term exposure to pCO_2 and temperature levels predicted for the year 2100 AD. Biogeosciences 7(1):289-300.

105. Iguchi A, Ozaki S, Nakamura T, Inoue M, Tanaka Y, Suzuki A, Kawahata H, Sakai K (2012) Effects of acidified seawater on coral calcification and symbiotic algae on the massive coral *Porites australiensis*. Marine Environmental Research 73:32-36.

106. Langdon C, Broecker WS, Hammond DE, Glenn E, Fitzsimmons K, Nelson SG, Peng TH, Hajdas I, Bonani G (2003) Effect of elevated pCO_2 on the community metabolism of an experimental coral reef. Global Biogeochemical Cycles 17(1).

107. Müller P, Li XP, Niyogi KK (2001) Non-photochemical quenching. A response to excess light energy. Plant Physiology 125(4):1558-1566

108. Schrieber US, Schliwa U, Bilger W (1986) Continuous recording of photochemical and non-photochemical chlorophyll fluorescence quenching with a new type of modulation fluorometer. Photosynthesis Research 10(1):51-62.

109. Li X, Huang H, Lian J, Huang L, Dong J (2009) Effects of the multiple stressors high temperature and reduced salinity on the photosynthesis of the hermatypic coral *Galaxea fascicularis*. Acta Ecologica Sinica 29(3):155-159.

110. Hill R, Frankart C, Ralph PJ (2005) Impact of bleaching conditions on the components of non-photochemical quenching in the zooxanthellae of a coral. Journal of Experimental Marine Biology and Ecology 322(1):83-92.

111. Iglesias-Prieto R, Govind NS, Trench RK (1993) Isolation and characterization of three membrane bound chlorophyll-protein complexes from four dinoflagellate species. Philosophical Transactions of the Royal Society of London. Series B: Biological Sciences 340(1294):381-392.

112. Renger G, Renger T (2008) Photosystem II: The machinery of photosynthetic water splitting. Photosynthesis Research 98(1):53-80.

113. Gorbunov MY, Kolber ZS, Lesser MP, Falkowski PG (2001) Photosynthesis and photoprotection in symbiotic corals. Limnology and Oceanography 46(1):75-85.

114. Styring S, Virgin I, Ehrenberg A, Andersson B (1990) Strong light photoinhibition of electrotransport in Photosystem II. Impairment of the function of the first quinone acceptor, Q_A. Biochimica et Biophysica Acta (BBA)-Bioenergetics 1015(2):269-278.

115. Setlík I, Allakhverdiev SI, Nedbal L, Setlíková E, Klimov VV (1990) Three types of Photosystem II photoinactivation: I. Damaging processes on the acceptor side. Photosynthetic Research 23(1):39-48.

116. Nedbal L, Masojídek J, Komenda J, Prášil O, Setlík I (1990) Three types of Photosystem II photoinactivation: Slow processes. Photosynthetic Research 24(1):89-97.

117. Arntz B, Trebst A (1986) On the role of the Q_B protein of PSII in photoinhibition. FEBS Letters 194(1):43-49.

118. Powles SB (1984) Photoinhibition of photosynthesis induced by visible light. Annual review of Plant Physiology 35(1):15-44.

119. Andersson B, Barber J (1996) Mechanisms of photodamage and protein degradation during photoinhibition of photosystem II. In Photosynthesis and the Environment 101-121.

120. Rintamäki E, Kettunen R, Aro EM (1996) Differential D1 dephosphorylation in functional and photodamaged photosystem II centers: dephosphorylation is a prerequisite for degradation of damaged D1. Journal of Biological Chemistry 271(25):14870-14875.

121. Keren N, Gong H, Ohad I (1995) Oscillations of reaction center II – D1 protein degradation in vivo induced by repetitive light flashes. Correlation between the level of RCII-Q_B- and protein degradation in low light. Journal of Biological Chemistry 270(2):806-14.

122. Aro EM, Kettunen R, Tyystjärvi E (1992) ATP and light regulate D1 protein modification and degradation Role of D1* in photoinhibition. FEBS Letters 297(1-2):29-33.

123. Tyystjarvi E, Ali-Yrkkö K, Kettunen R, Aro EM (1992) Slow degradation of the D1 protein is related to the susceptibility of low-light-grown pumpkin plants to photoinhibition. Plant Physiology 100(3):1310-1317.

124. Hill R, Brown CM, DeZeeuw K, Campbell DA, Ralph PJ (2011) Increased rate if D1 repair in coral symbionts during bleaching is insufficient to counter accelerated photo-inactivation. Limnology and Oceanography 56(1):139-146.

125. Takahashi S, Whitney SM, Badger MR (2009) Different thermal sensitivity of the repair of the photodamaged photosynthetic machinery in cultured Symbiodinium species. Proceedings of the National Academy of Sciences 106(9):3237-3242.

126. Maor-Landaw K, Karako-Lampert S, Ben-Asher HW, Goffredo S, Falini G, Dubinsky Z, Levy O (2014) Gene expression profiles during short-term heat stress in red sea coral *Stylophora pistillata*. Global Change Biology 20(10):3026-3035.

127. Wong JM, Johnson KM, Kelly MW, Hofmann GE (2018) Transcriptomics reveal transgenerational effects in purple sea urchin embryos: adult acclimation to upwelling conditions alters the response of their progeny to differential pCO_2 levels. Molecular Ecology 27(5):1120-1137.

128. Griffiths JS, Pan TC, Kelly MW (2019) Differential responses to ocean acidification between populations of *Balanophylia elegans* corals from high and low upwelling environments. Molecular Ecology 28(11):2712-2730.

129. Ruban AV, Johnson MP, Duffy CD (2012) The photoprotective molecular switch in the photosystem II antenna. Biochimica et Biophysica Acta (BBA)-Bioenergetics 1817(1):167-181.

130. Demmig B, Winter K, Krüger A, Czygan FC (1987) Photoinhibition and zeaxanthin formation in intact leaves: a possible role of the xanthophyll cycle in the dissipation of excess light energy. Plant Physiology 84(2):218-224.

131. Wraight CA, Crofts AR (1970) Energy-dependent quenching of chlorophyll a fluorescence in isolated chloroplasts. European Journal of Biochemistry 17(2):319-327.

132. Hager A, Holocher K (1994) Localization of the xanthophyll-cycle enzyme violaxanthin de-epoxidase within the thylakoid lumen and abolition of its mobility by a (light-dependent) pH decrease. Planta 192(4):581-589.

133. Pfündel EE, Dilley RA (2003) The pH dependence of violaxanthin deepoxidation in isolated pea chloroplasts. Plant Physiology 101(1):65-71.

134. Frank HA, Cua A, Chynwat V, Young A, Gosztola D, Wasielewski MR (1996) The lifetimes and energies of the first excited singlet states of diadinoxanthin and diatoxanthin: the role of those molecules in excess energy dissipation in algae. Biochimica et Biophysica Acta (BBA)-Bioenergetics. 1277(3):243-252.

135. Frank HA, Cogdell RJ (1996) Caretenoids in photosynthesis. Photochemistry and Photobiology 63(3):257-264.

136. Jahns P, Latowski D, Strzalka K (2009) Mechanism and regulation of the violaxanthin cycle: the role of antenna proteins and membrane lipids. Biochimica et Biophysica Acta (BBA)-Bioenergetics 1787(1):3-14.

137. Demmig-Adams B, Gilmore AM, Iii WW (1996) In vivo functions of carotenoids in higher plants. The FASEB Journal 10(4):403-412.

138. Demmig-Adams B, Winter K, Kriger A, Czygan FC (1989) Light response of CO_2 assimilation, dissipation of excess excitation energy, and zeaxanthin content of sun and shade leaves. Plant Physiology 90(3):881-886.

139. Jahns P, Miehe B (1996) Kinetic correlation of recovery from photoinhibition and zeaxanthin epoxidation. Planta 198(2):202-210.

140. Hartel H, Lokstein H, Grimm B, Rank B (1996) Kinetic studies on xanthophyll cycle in barley leaves (influence of antenna size and relations to nonphotochemical chlorophyll fluorescence quenching). Plant Physiology 110(2):471-482.

141. Olaizola M, Yamamoto HY (1994) Short-term response of the diadinoxanthin cycle and fluorescence yield to high irradiance in *Chaetoceros muelleri (Bacillariophyceae)*. Journal of Phycology 30(4):606-612.

142. Ruban AV, Young A, Horton P (1994) Modulation of chlorophyll fluorescence quenching in isolated light harvesting complex of photosystem II. Biochimica et Biophysica Acta (BBA)-Bioenergetics 1186(1-2):123-127.

143. Niyogi KK, Shih C, Chow WS, Pogson BJ, DellaPenna D, Björkman O (2001) Photoprotection in a zeaxanthin-and lutein-deficient double mutant of *Arabidopsis*. Photosynthesis Research 67(1):139-145.

144. Bilger W, Heber U, Schreiber U (1988) Kinetic relationship between energy-dependent fluorescence quenching, light scattering, chlorophyll luminescence and proton pumping in intact leaves. Zeitschrift für Naturforschung C 43(11-12):877-887.

145. Pfündel EE, Renganathan M, Gilmore AM, Yamamoto HY, Dilley RA (1994) Intrathylakoid pH in isolated pea chloroplasts as probed by violaxanthin deepoxidation. Plant Physiology 106(4):1647-1658.

146. Noctor G, Rees D, Young A, Horton P (1991) The relationship between zeaxanthin, energy-dependent quenching of chlorophyll fluorescence, and trans-thylakoid pH gradient in isolated chloroplasts. Biochimica et Biophysica Acta (BBA)-Bioenergetics 1057(3):320-330.

147. Zulfugarov IS, Ham OK, Mishra SR, Kim JY, Nath K, Koo HY, Kim HS, Moon YH, An G, Lee CH (2007) Dependence of reaction centre-type energy-dependent quenching on photosystem II antenna size. Biochimica et Biophysica Acta (BBA)-Bioenergetics 1767(6):773-780.

148. Sylak-Glassman E.J, Malnoë A, De Re E, Brooks MD, Fischer AL, Niyogi KK, Fleming GR (2014) Distinct roles of the photosystem II protein PsbS and zeaxanthin in the regulation of light harvesting in plants revealed by fluorescence lifetime snapshots. Proceedings of the National Academy of Sciences 111(49):17498-17503.

149. Finazzi G, Johnsom GN, Dallosto L, Joliot P, Wollman FA, Bassi R (2004) A zeaxanthin-independent nonphotochemical quenching mechanism localized in the photosystem II core complex. Proceedings of the National Academy of Sciences 101(33):12375-12380.

150. Hennige SJ, Suggett DJ, Warner ME, McDougall KE, Smith DJ (2009) Photobiology of Symbiodinium revisited: bio-physical and bio-optical signatures. Coral Reefs 28(1):179-195.

151. Guglieli G, Lavaud J, Rousseau B, Etienne AL, Houmard J, Ruban AV (2005) The light-harvesting antenna of the diatom *Phaeodactylum tricornutum*: Evidence for a diadinoxanthin-binding subcomplex. The FEBS Journal 272(17):4339-4348.

152. Baroli I, Melis A (1998) Photoinhibitory damage is modulated by the rate of photosynthesis and by the photosystem II light-harvesting chlorophyll antenna size. Plant 205(2):288-296.

153. Park Il Y, Chow WS, Anderson JM (1997) Antenna size dependency of photoinactivation of photosystem II in light-acclimated pea leaves. Plant Physiology 115(1):151-157.

154. Iglesias-Prieto R, Trench RK (1997) Acclimation and adaptation to irradiance in symbiotic dinoflagellates. II. Response of chlorophyll-protein complexes to different photon-flux densities. Marine Biology 130(1):23-33.

155. Gierz SL, Gordon BR, Leggat W (2016) Integral light-harvesting complex expression in Symbiodinium within the coral *Acropora aspera* under thermal stress. Scientific Reports 6(1):1-10.

156. Hill R, Larkum AW, Prášil O, Kramer M, Szabó M, Kumar V, Ralph PJ (2012) Light-induced dissociation of antenna complexes in the symbionts of scleractinian corals correlates with sensitivity to coral bleaching. Coral Reefs 31(4):963-975.

157. Zhang HB, Xu DQ (2003) Role of light-harvesting complex 2 dissociation in protecting the photosystem 2 reaction centres against photodamage in soybean leaves and thylakoids. Photosynthetica 41(3):383-391.

158. Middlebrook R, Anthony KR, Hoegh-Guldberg O, Dove S (2012) Thermal priming affects symbiont photosynthesis but does not alter bleaching susceptibility in *Acropora millepora*. Journal of Experimental Biology and Ecology 432:64-72.

159. Venn AA, Wilson MA, Trapido-Rosenthal HG, Keely BJ, Douglas AE (2006) The impact of coral bleaching on the pigment profile of the symbiotic alga, *Symbiodinium*. Plant, Cell & Environment 29(12):2133-2142.

160. Burton GW (1989) Antioxidant action of carotenoids. The Journal of Nutrition 119(1):109-111.

161. Brown BE, Ambarsari I, Warner ME, Fitt WK, Dunne RP, Gibb SW, Cummings DG (1999) Diurnal changes in photochemical efficiency and xanthophyll concentrations in shallow water reef corals: evidence for photoinhibition and photoprotection. Coral Reefs 18(2):99-105.

162. Warner ME, Berry-Lowe S (2006) Differential xanthophyll cycling and photochemical activity in symbiotic dinoflagellates in multiple locations of three species of Caribbean coral. Journal of Experimental Marine Biology and Ecology 339(1):86-95.

163. Winters G, Loya Y, Röttgers R, Beer S (2003) Photoinhibition in shallow-water colonies of the coral *Stylophora pistillata* as measured in situ. Limnology and Oceanography 48(4):1388-1393.

164. Goss R, Pinto EA, Wilhelm C, Richter M (2006) The importance of a highly active and ΔpH-regulated diatoxanthin epoxidase for the regulation of the PSII antennae function in diadinoxanthin cycle containing algae. Journal of Plant Physiology 163(10):1008-1021.

165. Mewes H, Richter M (2002) Supplementary ultraviolet-B radiation induces a rapid reversal of the diadinoxanthin cycle in the strong light-exposed diatom *Phaeodactylum tricornutum*. Plant Physiology 130(3):1527-1535.

166. Hoegh-Guldberg O, Jones RJ (1999) Photoinhibition and photoprotection in symbiotic dinoflagellates from reef-building corals. Marine Ecology Progress Series 183:73-86.

167. Grouneva I, Jakob T, Wilhelm C, Goss R (2009) The regulation of xanthophyll cycle activity and of non-photochemical fluorescence quenching by two alternative electron flows in the diatoms *Phaeodactylum tricornutum* and *Cyclotella meneghiniana*. Biochemica et Biophysica Acta (BBA)-Bioenergetics 1787(7):929-938.

168. Jakob T, Goss R, Wilhelm C (1999) Activation of diadinoxanthin de-epoxidase due to a chlororespiratory proton gradient in the dark in the diatom *Phaeodactylum tricornutum*. Plant Biology 1(1):76-82.

169. Gest N, Gautier H, Stevens R (2013) Ascorbate as seen through plant evolution: the rise of a successful molecule? Journal of Experimental Botany 64(1):33-35.

170. Grouneva I, Jakob T, Wilhelm C, Goss R (2006) Influence of ascorbate and pH on the activity of the diatom xanthophyll cycle-enzyme diadinoxanthin de-epoxidase. Physiologia Plantarum 126(2):205-211.

171. Lesser MP, Shick JM (1989) Photoadaptation and defenses against oxygen toxicity in zooxanthellae from natural populations of symbiotic cnidarians. Journal of Experimental Marine Biology and Ecology 134(2):129-141.

172. Smirnoff N (2000) Ascorbate biosynthesis and function in photoprotection. Philosophical transactions of the Royal Society of London. Series B: Biological Sciences 355(1402):1455-1464.

173. Eskling M, Åkerlund HE (1998) Changes in the quantities of violaxanthin de-epoxidase, xanthophylls and ascorbate in spinach upon shift from low to high light. Photosynthesis research 57(1):41-50.

174. Kautsky H, Hirsch A (1931) New attempts at carbonic acid assimilation. Naturwissenschaften 19(48):964-964.

175. Kitajima MB, Butler WL (1975). Quenching of chlorophyll fluorescence and primary photochemistry in chloroplasts by dibromothymoquinone. Biochimica et Biophysica Acta (BBA)-Bioenergetics 376(1):105-115.

176. Klughammer C, Schreiber U (2008) Complimentary PSII quantum yields calculated from simple fluorescence parameters measured by PAM fluorometry and the Saturation Pulse method. PAM application notes 1(2):201-247.

177. Baker NR, Oxborough K, Lawson T, Morison JI (2001) High resolution imaging of photosynthetic activities of tissues, cells and chloroplasts in leaves. Journal of Experimental Botany 52(356):615-621.

178. Björkman O, Demmig B (1987) Photon yield of O_2 evolution and chlorophyll fluorescence characteristics at 77K among vascular plants of diverse origins. Planta 170(4):489-504.

179. Jones RJ, Ward S, Amri AY, Hoegh-Guldberg O (2000) Changes in quantum efficiency of Photosystem II of symbiotic dinoflagellates of corals after heat stress, and of bleached corals sampled after the 1998 Great Barrier Reef mass bleaching event. Marine and Freshwater Research 51(1):63-71.

180. Warner ME, Fitt WK, Schmidt GW (1996) The effects of elevated temperature on the photosynthetic efficiency of zooxanthellae in-hospite from four different species of reef coral: a novel approach. Plant, Cell & Environment 19(3):291-299.

181. Ralph P, Gademann R, Larkum A, Kühl M (2002) Spatial heterogeneity in active chlorophyll fluorescence and PSII activity of coral tissues. Marine Biology 141(4):639-646.

182. Winter AP, Chaloub RM Duarte GA (2016) Photosynthetic responses of corals *Mussismilia hartii* (Verrill, 1987) from turbid waters to changes on temperature and presences/ absence of light. Brazilian Journal of Oceanography 64(3):203-216.

183. Stirbet A, Riznichenko GY, Rubin AB (2014) Modeling chlorophyll a fluorescence transient: relation to photosynthesis. Biochemistry (Moscow) 79(4):291-323.

184. DiPerna S, Hoogenboom M, Noonan S, Fabricius K (2018) Effects of variability in the daily light integrals on the photophysiology of the corals *Pachyseris speciose* and *Acropora millepora*. PloS One 13(9):e0203882.

185. Langlois LA, Hoogenboom MO (2014) Capacity for short-term physiological acclimation to light does not control the lower depth distributions of branching corals. Marine Ecology Progress Series 508:149-162.

186. Bonaventura C, Myers J (1969) Fluorescence and oxygen evolution from *Chlorella pyrenoidosa*. Biochemica et Biophysica Acta (BBA)-Bioenergetics 189(3):366-383.

187. Bellafiore S, Barneche F, Peltier G, Rochaix JD (2005) State transitions and light adaptation require chloroplast thylakoid protein kinase STN7. Nature 433(7028):892-895.

188. Iglesias-Prieto R, Beltran VH, Lajeunesse TC, Reyes-Bonilla H, Thome PE (2004) Different algal symbionts explain the vertical distribution of dominant reef corals in the eastern Pacific. Proceedings of the Royal Society of London. Series B: Biological Sciences 271(1549):1757-1763.

189. Taylor CR, Van Leperen W, Harbinson J (2019) Demonstration of a relationship between state transitions and photosynthetic efficiency in a higher plant. Biochemical Journal 476(21):3295-3312.

190. Krause GH (1988) Photoinhibition of photosynthesis. An evaluation of damaging and protective mechanisms. Physiologia Plantarum 74(3):566-574.

191. Warner ME, LaJeunesse TC, Robison JD, Thur RM (2006) The ecological distribution and comparative photobiology of symbiotic dinoflagellates from reef corals in Belize: potential implications for coral bleaching. Limnology and Oceanography 51(4):1887-1897.

192. Siefermann D, Yamamoto HY (1975) Properties of NADPH and oxygen-dependent zeaxanthin epoxidation in isolated chloroplasts: a transmembrane model for the violaxanthin cycle. Archives of Biochemistry and Biophysics 171(1):70-77.

193. Hoogenboom MO, Campbell DA, Beraud E, DeZeeuw K, Ferrier-Pages C (2012) Effects of light, food availability and temperature stress on the function of photosystem II and photosystem I of coral symbionts. PloS one 7(1):e30167.

194. Takahashi S, Milward SE, Fan DY, Chow WS, Badger MR (2009) How does cyclic electron flow alleviate photoinhibiion in Arabidopsis? Plant Physiology 149(3):1560-1567.

195. Cornic G, Bukhov NG, Wiese C, Bligny R, Heber U (2000) Flexible coupling between light-dependent electron and vectorial proton transport in illuminated leaves of C3 plants. Role of photosystem I-dependent proton pumping. Planta 210(3):468-477.

196. Aihara Y, Takahashi S, Minagawa J (2016) Heat induction of cyclic electron flow around photosystem I in the symbiotic dinoflagellate Symbiodinium. Plant Physiology 171(1):522-529.

197. Jones RJ, Hoegh-Guldberg O, Larkum AW, Schreiber U (1998) Temperature-induced bleaching of corals begins with impairment of the CO_2 fixation mechanism in zooxanthellae. Plant, Cell & Environment 21(12):1219-1230.

198. Miyake C, Shinzaki Y, Nishioka M, Horiguchi S, Tomizawa KI (2006) Photoinactivation of ascorbate peroxidase in isolated tobacco chloroplasts: *Galdieria partita* APX maintains the electron flux through the water-water cycle in transplastomic tobacco plants. Plant and Cell Physiology 47(2):200-210.

199. Neubauer C, Schrieber U (1989) Photochemical and non-photochemical quenching of chlorophyll fluorescence induced by hydrogen peroxide. Zeitschrift für Naturforschung C 44(3-4):262-270.

200. Chauvin A, Denis V, Cuet P (2011) Is the response of coral calcification to seawater acidification related to nutrient loading? Coral Reefs 30(4):911.

201. Edmunds PJ (2012) Effect of pCO_2 on the growth, respiration, and photophysiology of massive Porites spp. in Moorea, French Polynesia. Marine Biology 159(10):2149-2160.

202. Wall CB, Fan TY, Edmunds PJ (2014) Ocean acidification has no effect on thermal bleaching in the coral *Seriatopora caliendrum*. Coral Reefs 33(1):119-130.

203. Godinot C, Houlbreque F, Grover R, Ferrier-Pages C (2011) Coral uptake of inorganic phosphorous and nitrogen negatively affected by simultaneous changes in temperature and pH. PLoS One 6(9):e25024.

204. Kavousi J, Parkinson JE, Nakamura T (2016) Combined ocean acidification and low temperature stressors cause coral mortality. Coral Reefs 35(3):903-907.

205. Kemp DW, Oakley CA, Thornhill DJ, Newcomb LA, Schmidt GW, Fitt WK (2011) Catastrophic mortality on inshore coral reefs of the Florida Keys due to severe low-temperature stress. Global Change Biology 17(11):3468-3477.

206. Roth MS, Goericke R, Deheyn DD (2012) Cold induces acute stress but hear is ultimately more deleterious for the reef-building coral *Acropora yongei*. Scientific Reports 2(1):1-5.

207. Routaboul JM, Fischer SF, Browse J (2000) Trienoic fatty acids are required to maintain chloroplast function at low temperatures. Plant Physiology 124(4):1697-1705.

208. Seeman J, Sawall Y, Auel H, Richter C (2013) The use of lipids and fatty acids to measure the trophic plasticity of the coral *Stylopohora subseriata*. Lipids 48(3):275-286.

209. Sawall Y, Teichberg MC, Seeman J, Litaay M, Jompa J, Richter C (2011) Nutritional status and metabolism of the coral *Stylophora subseriata* along a eutrophication gradient in Spermonde Archipelago (Indonesia). Coral Reefs 30(3):841-853.

210. Silverman J, Lazar B, Erez J (2007) community metabolism of a coral reef exposed to naturally varying dissolved inorganic nutrient loads. Biogeochemistry 84(1):67-82.

211. Schoepf V, Grottoli AG, Warner ME, Cai WJ, Melman TF, Hoadley KD, Pettay DT, Hu X, Li Q, Xu H, Wang Y (2013) Coral energy reserves and calcification in a high-CO_2 world at two temperatures. PLoS One 8(10):e75049.

212. Grinblat M, Fine M, Tikochinski Y, Loya Y (2018) Stylophora pistillata in the Red Sea demonstrate higher GFP fluorescence under ocean acidification conditioned. Coral Reefs 37(1):309-320.

213. Bartlett TC (2013) Small scale experimental systems for coral research: Considerations, planning, and recommendations. NOAA Technical Memorandum NOS NCCOS 165 and CRCP 18:68.

214. Genty B, Briantais JM, Baker NR (1989) "The relationship between the quantum yield of photosynthetic electron transport and quenching of chlorophyll fluorescence. Biochimica et Biophysica Acta (BBA)-General Subjects, 990(1):87-92.

215. Bilger W, Björkman O (1990) Role of xanthophyll cycle in photoprotection elucidated by measurements of light-induced absorbance changes, fluorescence and photosynthesis in leaves of *Hedera canariensis*. Photosynthesis Research 25(3):173-85.

216. Serôdio J, Vieira S, Cruz S, and Coelho H (2006) Rapid light-response curves of chlorophyll fluorescence in microalgae: relationship to steady-state light curves and non-photochemical quenching in benthic diatom-dominated assemblages. Photosynthesis Research 90(1):29-43.

217. Suggett DJ, Prášil O, Borowitzka (2010) Chlorophyll a fluorescence in aquatic sciences: methods and applications. (Vol 4) Dordrecht: Springer.

218. Kuanui P, Chavanich S, Viyakarn V, Omori M, Fujita T, Lin C (2020) Effect of light intensity on survival and photosynthetic efficiency of cultured corals of different ages. Estuarine, Coastal and Shelf Science 235:106515

219. Hill R, Takahashi S (2014) Photosystem II recovery in the presence and absence of chloroplast protein repair un the symbionts of corals exposed to bleaching conditions. Coral Reefs 33(4):1101-11.

220. Noonan SH, Fabricus KE (2016) Ocean acidification affects productivity but not the severity of thermal bleaching in some tropical corals. ICES Journal of Marine Science 73(3):715-26.

221. Wall CB, Fan TY, Edmunds PJ (2014) Ocean acidification has no effect on thermal bleaching in the coral *Seriotopora caliendrum*. Coral Reefs 33(1):119-30.

222. Jiang L, Guo YJ, Zhang YY, McCook LJ, Yuan XC, Lei XM, Zhou GW, Guo ML, Cai L, Lian JS (2019) Diurnally fluctuating pCO_2 modifies the physiological responses of coral recruits under ocean acidification. Frontiers in Physiology 9:1952.

223. Crawley A, Kline DI, Dunn S, Anthony KE, Dove S (2010) The effect of ocean acidification on symbiont photorespiration and productivity in *Acropora formosa*. Global Change Biology 16(2):851-863.

224. Enochs I C, Derek P, Manzello D P, Carlton R, Schopmeyer S, Van Hooidonk R, Lirman D (2014) Effects of light and elevated pCO_2 on the growth and photochemical efficiency of *Acropora cervicornis*. Coral Reefs 33(2):477-85.

225. Krief S, Hendy EJ, Fine M, Yam R, Meibom A, Foster GL, Shemesh A (2010) Physiological and isotopic responses of scleractinian corals to ocean acidification. Geochimica et Cosmochimica Acta 74(17):4988-5001.

226. Vogel N, Meyer FW, Wild C, Uthicke S (2015) Decreased light availability can amplify negative impacts of ocean acidification on calcifying coral reef organisms. Marine Ecology Progress Series 521:49-61.

227. Mason RA, Wall CB, Cunning R, Dove S, Gates RD (2020) High light alongside elevated pCO_2 alleviates thermal depression of photosynthesis in a hard coral (*Pocillopora acuta*). Journal of Experimental Biology 223(20):jeb223198.

228. Ralph PJ, Gademann R (2005) Rapid light curves: a powerful tool to assess photosynthetic activity. Aquatic Botany 82(3):222-37.

229. Dennison WC, Barnes DJ (1988) Effect of water motion on coral photosynthesis and calcification. Journal of Experimental Marine Biology and Ecology. 115(1):67-77.

230. Shashar N, Kinane S, Jokiel PL, Patterson MR (1996) Hydrochemical boundary layers over a coral reef. Journal of Experimental Marine Biology and Ecology 199(1):17-28.

231. Kühl M, Cohen Y, Dalsgaard T, Jørgensen BB, Revsbech NP (1995) Microenvironment and photosynthesis of zooxanthellae in scleractinian corals studied with microsensors for O2, pH and light. Marine Ecology-Progress Series 117(1-3):159-72.

232. Chan N, Wangpraseurt D, Kühl M, Connolly SR (2016) Flow and coral morphology control surface pH: implications for the effects of ocean acidification. Frontiers in Marine Science 3:10.

233. Osinga R, Derksen-Hooijberg M, Wijgerde T, Verreth JA (2017) Interactive effects of oxygen, carbon dioxide and flow on photosynthesis and respiration in the scleractinian coral *Galaxea fascicularis*. Journal of Experimental Biology, 220(12):2236-2242.

234. Nakamura T, Van Woesik R, Yamasaki H (2005) Photoinhibition of photosynthesis is reduced by water flow in the reef-building coral *Acropora digitifera*. Marine Ecology Progress Series 301:109-18.

235. Nakamura T, Yamasaki H (2013) Differential influence of water-flow on photoinhibition of photosynthesis in endosymbiotic algae among shallow-inhabiting scleractinian coral, *Galaxea*. Journal of Coral Reef Studies 15(Supplement):160-65.

236. Maxwell K, Johnson GN (2000) Chlorophyll fluorescence- a practical guide. Journal of Experimental Botany 51(345):659-68.

237. Schrameyer V, Krämer W, Hill R, Jeans J, Larkum AW, Bischof K, Campbell DA, Ralph PJ (2016) Under high light stress two Indo-Pacific coral species display differential photodamage and photo repair dynamics. Marine Biology 163(8):1-13.

238. Jakob T, Goss R, Wilhelm C (2001) Unusual pH-dependence of diadinoxanthin de-epoxidase activation causes chlororespiratory induced accumulation of diatoxanthin in the diatom *Phaeodactylum tricornutum*. Journal of Plant Physiology 158(3):383-90.

239. Rumeau D, Peltier G, Cournac L (2007) Chlororespiration and cyclic electron flow around PSI during photosynthesis and plant stress response. Plant Cell & Environment 30(9):1041-51.

240. Bennoun P (1994) Chlororespiration revisited: mitochondrial-plastid interactions in Chlamydomonas. Biochimica et Biophysica Acta (BBA)-Bioenergetics 1186(1-2):59-66.

241. Jones RJ, Hoegh-Guldberg O (2001) Diurnal changes in the photochemical efficiency of the symbiotic dinoflagellates (*Dinophyceae*) of corals: photoprotection, photoinactivation and the relationship to coral bleaching. Plant, Cell & Environment 24(1):89-99.

242. Hill R, Ralph PJ (2008) Dark-induced reduction of the plastoquinone pool in zooxanthellae of scleractinian corals and implications for measurements of chlorophyll a fluorescence. Symbiosis 46(1):45-56.

Appendix

Table A1. Incident photosynthetically active radiation (PAR, μmol m^{-2} s^{-1}) cycles each coral was exposed to between 0400 and 1900 h. Between 1900 and 0430 h corals were in complete darkness (0 μmol m^{-2} s^{-1}). PAR recorded from the PAM measuring ambient light remitted by a Teflon sheet to a PAR sensor within the monitoring head.

Experiment 1

	Experiment 1			Experiment 2			Experiment 3		
Time	Tank 1	Tank 2	Tank 3	Tank 1	Tank 2	Tank 3	Tank 1	Tank 2	Tank 3
4:30:21	0	0	0	0	0	0	0	0	0
5:00:21	21.75	16.25	25.25	19.25	18.5	18.5	18	21	18.5
5:30:21	23	17	26.75	19.75	19.75	20.5	19	22	20
6:00:21	24.5	18.75	28.75	22	20.75	21.5	20.25	23.25	21.5
6:30:21	26	19.75	30.75	22.75	22.5	23.25	21.25	25	22.25
7:00:21	27.75	21.25	32.75	24.75	24.25	24.5	23	27.25	25
7:30:21	30.75	23.25	36	27	26.5	27.25	23.75	29	26.5
8:00:20	33.5	25.25	40	28.75	28.75	30.5	27.25	31.5	29.25
8:30:21	38	29	46	34	32.25	34.75	32	37.5	35.75
9:00:20	45.25	30.5	55	39.25	38.75	40	36.75	43.5	40.5
9:30:20	51.5	40.25	63.75	46.5	45.5	47.75	43	51	48
10:00:20	58.75	45.25	71.5	52.25	52	54.25	48.25	57.75	54.75
10:30:21	63.5	49.25	77.75	56.25	56.5	58.5	53.25	63	60
11:00:21	68	52.33	82.75	61	56	61.5	56.75	65.25	63.5
11:30:21	67.75	52.75	83.75	59.5	58	62.25	57	66.5	63.5
12:00:21	69	51.75	84	61.5	59.5	61	57.25	67	62.75
12:30:21	68.75	52.5	83.75	60.25	60.25	62.25	56.25	67	63
13:00:20	65.25	50.75	78.75	58	54.75	59.25	54	63.75	59.5
13:30:20	59.25	46	69.75	51.25	50	52.25	47.5	56.25	52.5
14:00:20	52.5	39.25	63.25	45	45	47.25	43	49.5	48.25
14:30:20	45.75	34.75	55	39.75	38.75	40	36.75	42.25	40.5
15:00:21	39.25	29.75	47.25	33.25	32.25	34	31	35.75	32.75
15:30:20	32.75	25.25	39	28.75	28.75	28.5	24.25	28	25.5
16:00:21	29.5	22.75	36	26.5	24.75	26	22	25.75	23.5
16:30:21	27	20.5	32.25	23.5	23.25	22.75	20	22.75	21
17:00:20	24.5	18.75	29	21.25	20.75	20.75	18	20.75	20
17:30:20	22.25	17	26.25	19.75	19	19.75	16.75	19.5	17.5
18:00:20	21.25	15.5	24.5	17.5	17.25	17	15.25	17.75	15.5
18:30:20	18.75	14.25	22.25	16	16	16	0	0	0
19:00:20	0	0	0	0	0	0	0	0	0

Table A2. Set point pH values for the treatments using the Cap ctrl system which controlled the opening and closing of the solenoid valve when the pH of the seawater in the mixing barrel increased above or decreased below the treatment setpoints. The cap ctrl system was turned off during acclimation and again during degassing to allow pH to return to an ambient level.

	Day	Task	Set points		
Experiment 1			Tank 1	Tank 2	Tank 3
	20/06/21	Acclimate	8.060	8.060	8.060
	21/06/21	Acclimate	8.060	8.060	8.060
	22/06/21	Acclimate	8.060	8.060	8.060
	23/06/21	Acclimate	8.060	8.060	8.060
	24/06/21	Acclimate	8.060	8.060	8.060
	25/06/21	Acclimate	8.060	8.060	8.060
	26/06/21	Acclimate	8.060	8.060	8.060
	27/06/21	Treatment	8.060	7.861	7.861
	28/06/21	Treatment	8.060	7.861	7.861
	29/06/21	Treatment	8.060	7.861	7.861
	30/06/21	Treatment	8.060	7.755	7.755
	1/07/21	Treatment	8.060	7.755	7.755
	2/07/21	Treatment	8.060	7.755	7.755
	3/07/21	Treatment	8.060	7.671	7.671
	4/07/21	Treatment	8.060	7.671	7.671
	5/07/21	Treatment	8.060	7.671	7.671
	6/07/21	Degassing	8.060	8.060	8.060
	7/07/21	Degassing	8.060	8.060	8.060

Appendix 2 continued.

	Date	Task	Target pH		
Experiment 2			Tank 1	Tank 2	Tank 3
	12/07/21	Acclimate	8.060	8.060	8.060
	13/07/21	Acclimate	8.060	8.060	8.060
	14/07/21	Acclimate	8.060	8.060	8.060
	15/07/21	Acclimate	8.060	8.060	8.060
	16/07/21	Acclimate	8.060	8.060	8.060
	17/07/21	Acclimate	8.060	8.060	8.060
	18/07/21	Acclimate	8.060	8.060	8.060
	19/07/21	Treatment	7.861	8.060	7.861
	20/07/21	Treatment	7.861	8.060	7.861
	21/07/21	Treatment	7.861	8.060	7.861
	22/07/21	Treatment	7.755	8.060	7.755
	23/07/21	Treatment	7.755	8.060	7.755
	24/07/21	Treatment	7.755	8.060	7.755
	25/07/21	Treatment	7.671	8.060	7.671
	26/07/21	Treatment	7.671	8.060	7.671
	27/07/21	Treatment	7.671	8.060	7.671
	28/07/21	Degassing	8.060	8.060	8.060
	29/07/21	Degassing	8.060	8.060	8.060

	Date	Task	Target pH

Experiment 3			Tank 1	Tank 2	Tank 3
	3/08/21	Acclimate	8.060	8.060	8.060
	4/08/21	Acclimate	8.060	8.060	8.060
	5/08/21	Acclimate	8.060	8.060	8.060
	6/08/21	Acclimate	8.060	8.060	8.060
	7/08/21	Acclimate	8.060	8.060	8.060
	8/08/21	Acclimate	8.060	8.060	8.060
	9/08/21	Acclimate	8.060	8.060	8.060
	10/08/21	Treatment	7.861	7.861	8.060
	11/08/21	Treatment	7.861	7.861	8.060
	12/08/21	Treatment	7.861	7.861	8.060
	13/08/21	Treatment	7.755	7.755	8.060
	14/08/21	Treatment	7.755	7.755	8.060
	15/08/21	Treatment	7.755	7.755	8.060
	16/08/21	Treatment	7.671	7.671	8.060
	17/08/21	Treatment	7.671	7.671	8.060
	18/08/21	Treatment	7.671	7.671	8.060
	19/08/21	Degassing	8.06	8.06	8.06
	20/08/21	Degassing	8.06	8.06	8.06

Table A3. The batch file code and description created on the PAM software to initiate induction and recovery analyses and saturation pulses.

Set time	Analysis	Code	Description
02:00:00	Induction and recovery analysis	while 1	Start block repeating indefinitely
		timeswitch	Time based cycle
		case 2:00:00	
		$M = 1	Measuring light on
		$ROP = 1	Record online on
		delay 20	Pause for specified number of seconds
		$ICR = 1	Induction plus recovery
		wait $ICR = 0	Wait until ICR completed
		$ROP = 0	Record online off
		$M = 0	Measuring light off
		endcase	
03:00:00	Saturation pulse analysis	case from 3:00:00 to 24:00:00 step 30:00	
		$M = 1	Measuring light on
		$ROP = 1	Record online on
		delay 20	Wait 20 seconds
		$S = 1	Start saturation pulse
		wait $S = 0	Wait until S completed
		$ROP = 0	Record online off
		$M = 0	Measuring light off
		endcase	
		endtimeswitch	
24:00:00		wend	

Table A4. Results of the nested ANOVA testing the maximum photochemical efficiency (F_v/F_m), the midday effective photochemical efficiency ($\Delta F/F_m'$), and the maximum excitation pressure of PSII (Qm) including the least square means. Model description: treatment, day, and tank were set as fixed factors, and coral individuals were set as the random factor. AIC, Akaike information criterion; SE, standard error; DF, degrees of freedom; Lsmean, Least square means; Lower CL, lower confidence limits; Upper CL, upper confidence limits.

Variable	Treatment	Estimates	SE	DF	p-value	
Fv/Fm (AIC = -126.6742)						
	Intercept	0.6402444	0.009603205	21	0.0000	
	pH 7.8	0.0021145	0.008454331	21	0.8049	
	pH 7.7	0.0020501	0.008454331	21	0.8108	
	pH 7.6	0.0049965	0.008454331	21	0.5608	
	Day 3	-0.0141209	0.007071531	21	0.0590	
	Day 6	-0.0207349	0.007071531	21	0.0080	
	Day 9	-0.0372416	0.007071531	21	0.0000	
	Tank 3	0.0120016	0.013067648	6	0.3938	
	Tank 4	0.0155972	0.013067648	6	0.2777	
	Treatment	Lsmean	SE	DF	Lower CL	Upper CL
	pH 8.1	0.631	0.00628	6	0.616	0.647
	pH 7.8	0.634	0.00818	6	0.614	0.654
	pH 7.7	0.633	0.00818	6	0.613	0.653
	pH 7.6	0.636	0.00818	6	0.616	0.656
$\Delta F/F_m'$ (AIC = -124.7572)						
	(Intercept)	0.5574722	0.015246283	21	0.0000	
	pH 7.8	0.0040986	0.008079873	21	0.6173	
	pH 7.7	0.0035986	0.008079873	21	0.6606	
	pH7.6	0.0157653	0.008079873	21	0.0645	
	Day 3	-0.0095102	0.006650965	21	0.1675	
	Day 6	-0.0218435	0.006650965	21	0.0035	
	Day 9	-0.0418435	0.006650965	21	0.0000	
	Tank 3	0.0346667	0.021295146	6	0.1547	
	Tank 4	0.0395833	0.021295146	6	0.1124	
	Treatment	Lsmean	SE	Df	Lower CL	Upper CL
	pH 8.1	0.564	0.00928	6	0.541	0.587
	pH 7.8	0.568	0.01044	6	0.542	0.594
	pH 7.7	0.568	0.01044	6	0.542	0.593
	pH 7.6	0.580	0.01044	6	0.554	0.605
Q_m (AIC = -70.34747)						
	Intercept	0.12998461	0.1900031	21	0.5014	
	pH 7.8	0.00240248	0.0146694	21	0.8715	
	pH 7.7	0.00020058	0.0146694	21	0.9892	
	pH 7.6	-0.01476643	0.0146694	21	0.3256	
	Day 3	-0.00712757	0.0119795	21	0.5582	
	Day 6	0.00253782	0.0119795	21	0.8343	
	Day 9	0.01203734	0.0119795	21	0.3264	
	Tank 3	0.28165891	0.2686381	6	0.3348	
	Tank 4	-0.04096808	0.2686381	6	0.8838	
	Treatment	Lsmean	SE	DF	Lower CL	Upper CL
	pH 8.1	0.212	0.011	6	-0.0567	0.481
	pH 7.8	0.214	0.011	6	-0.0551	0.484
	pH 7.7	0.212	0.011	6	-0.0573	0.482
	pH 7.6	0.197	0.011	6	-0.0722	0.467

Table A5. Results of the nested ANOVA testing the maximum photochemical efficiency (F_v/F_m) and the effective photochemical efficiency ($\Delta F/F_m$') with the flat coral fragment removed from analysis. Model description: Treatment and day were set as the fixed factors, and coral individuals were set as the random factor. SE, standard error; DF, degrees of freedom.

Variable	Treatment	Estimates	SE	DF	p-value
F_v/F_m					
	Intercept	0.6518718	0.005216198	18	0.0000
	pH 7.8	0.0029903	0.008409265	18	0.7263
	pH 7.7	0.0055178	0.008409265	18	0.5200
	pH 7.6	0.0082190	0.008409265	18	0.3413
	Day 3	-0.0143297	0.006929630	18	0.0533
	Day 6	-0.0209436	0.006929630	18	0.0073
	Day 9	-0.0374503	0.006929630	18	0.0000
$\Delta F/F_m$'					
	Intercept	0.5900000	0.006868843	18	0.0000
	pH 7.8	0.0068455	0.008535936	18	0.4330
	pH 7.7	0.0079788	0.008535936	18	0.3623
	pH 7.6	0.0179788	0.008535936	18	0.0495
	Day 3	-0.0112784	0.006888337	18	0.1189
	Day 6	-0.0236118	0.006888337	18	0.0030
	Day 9	-0.0436118	0.006888337	18	0.0000